SUBCORTICAL MODULATORY SYSTEMS. MECHANISM OF BEHAVIORAL STATE CONTROL

Outline

1) **Arousal Concepts**
2) **Brain Electrical Activity During Waking and Sleep States**
3) **Mechanism of Arousal: Initial Studies**
4) **The Brainstem Reticular Formation**
5) **‘Diffuse’ Corticopetal Systems**

   a) locus coeruleus-cortical projection

   b) raphe-cortical projectione

   c) histamin system of the tuberomammillary nucleus

   d) orexin system of the lateral hypothalamus

   e) basal forebrain cholinergic corticopetal system

   f) basal forebrain neurons receive input from other ascending modulatory systems

Outline (cont)

6) Sleep-wake control system of the ventral forebrain and their links to the ascending arousal system of the brainstem

7) Thalamo-cortical loops in NREM oscillations and their control by brainstem cholinergic input

8) REM sleep

9) The homeostatic process of sleep-wake control

10) Sleep-wake control and circadian entrainment

DEVELOPMENT OF AROUSAL CONCEPTS

- **Waking** is a complex state. It is characterized by: 1) Perceptions that are influenced by external and internal sensory input; 2) Capacity of directing attention and accessing memory faithful to recent history; 3) Readjustment of posture, array of motor output; 4) Emotions that are focused to percepts and thoughts .(Hobson and Pace-Schott, 2002)

- **1930s**: wakefulness is maintained by afferent input to the brain and sleep ensues when that input is removed, as in the 'cerveau isole' cat, or falls below a certain critical level, as in normal sleeping (Bremer, Deafferentation theory)

- **1950s**: the brain actively controls its own state by the ascending reticular activating system (Magoun-Moruzzi).

- **1965s**- the concept of an undifferentiated reticular formation is gradually replaced by the description of transmitter-specific cell groups in the brainstem, the basal forebrain and the hypothalamus that send widely branching axons to the cortex and other parts of the brain.

- **1980s**- thalamo-cortical oscillations; neuromodulators trigger intrinsically generated oscillatory pattern in cooperating cortical cells. Arousal is a switch from slow to fast oscillatory pattern (Steriade, McCormick, Llinas, Singer, Buzsaki).

- **1990s**- The subjective experience of various states can tentatively be linked to the accompanying systematic changes in balance between various neuromodulators. The characteristic imaging data in various states are likely to relate to the shifts in regional metabolism and blood flow that are orchestrated by the these neuromodulators.

- **2003** Arousal provides the motivational force that activates behavior (Pfaff)

Behavioral states in humans

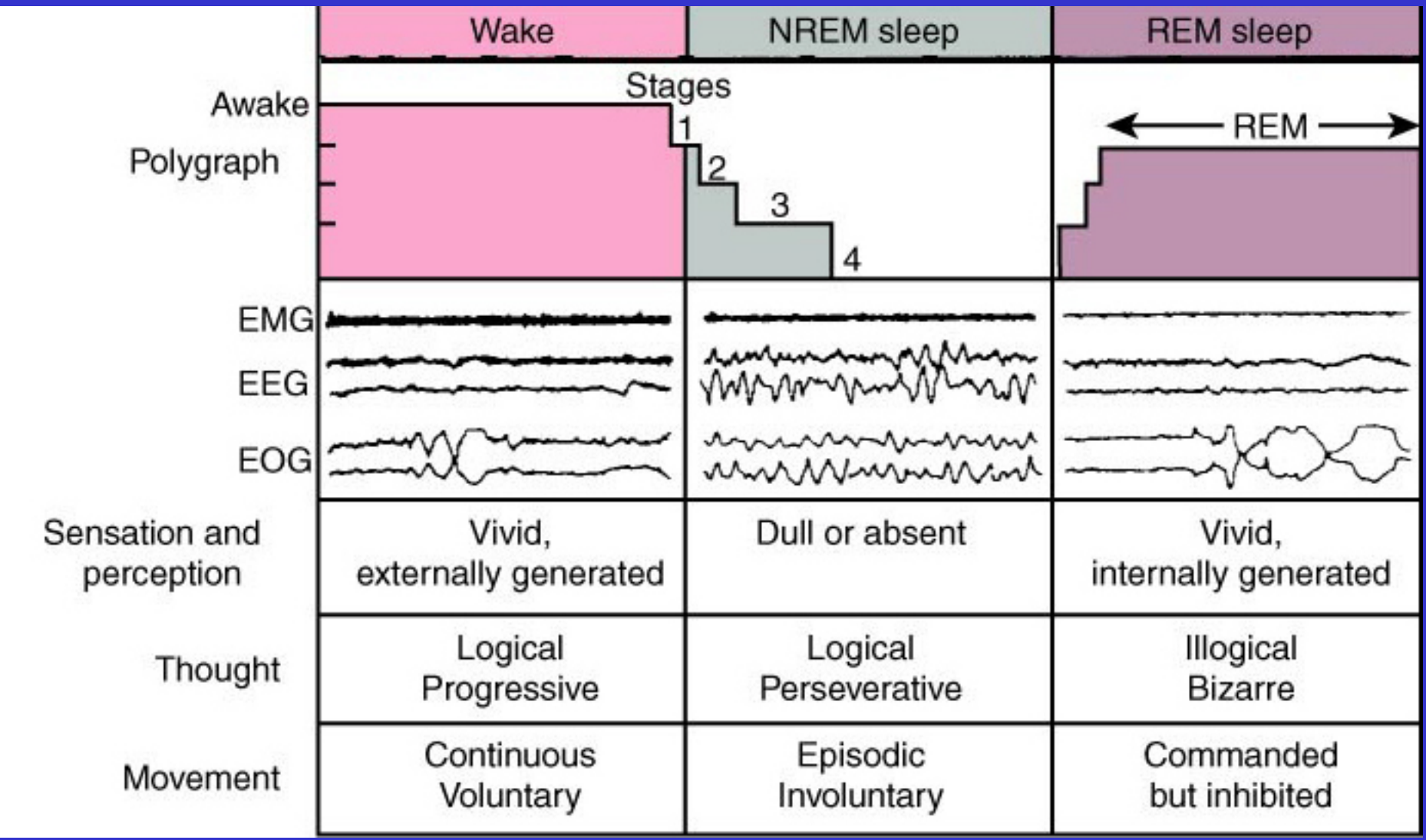

Hobson and Pace-Schott, 2003

•**Arousal** is a complex state. It is characterized by: 1) switch from slow to fast oscillatory pattern in thalamo-cortical circuits; 2)increased discharge in neurons of the 'diffuse' corticopteal' systems. Arousal is a fundamental change of operation from the storage mode to information-processing mode, including perceptions influenced by external and internal sensory input; capacity of directing attention, accessing memory faithful to recent history; array of motor output; and emotions that are focused to percepts and thoughts.

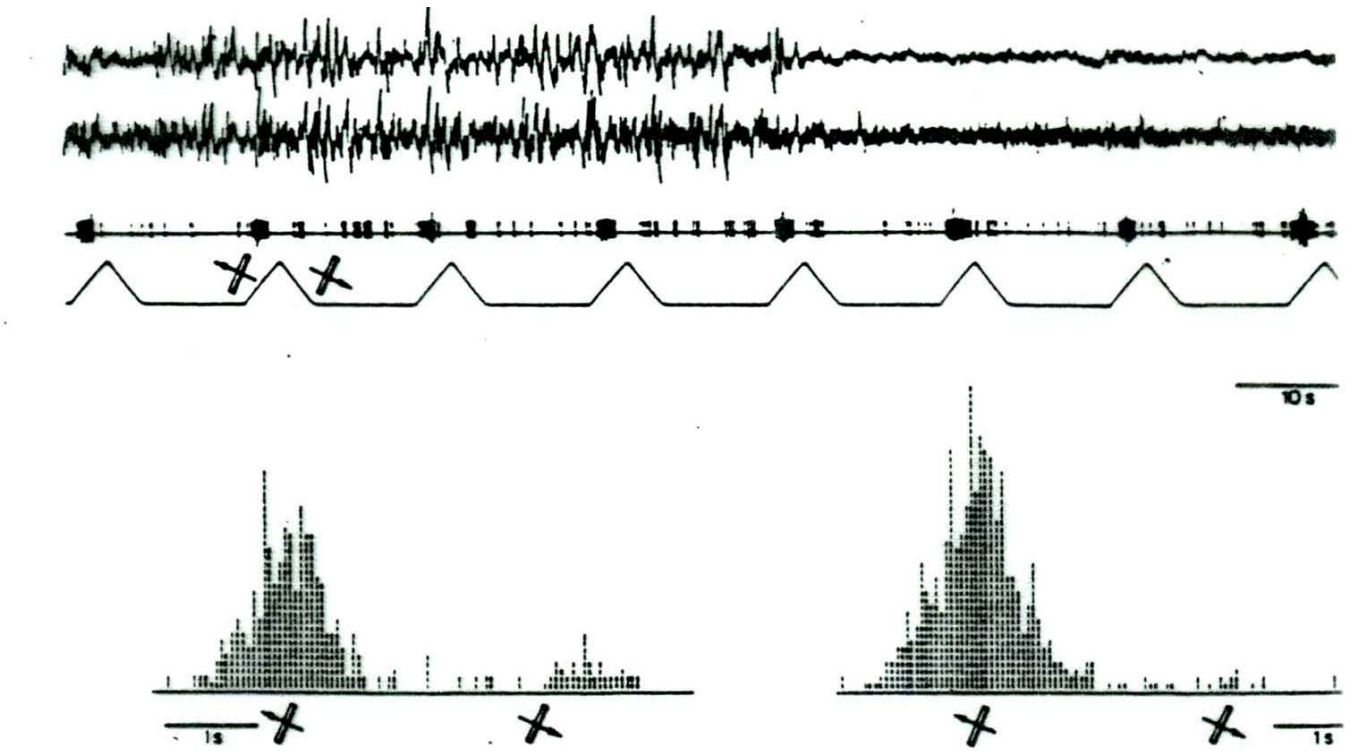

Effects of arousal (noise) from SWS on response selectivity of a cell in LII of the striate cortex. Arousal results in a moderate increase in the response to movement and a virtual elimination of the response to rightward movement (Livingston and Hubel, 1981).

Stages of sleep form cyclical pattern

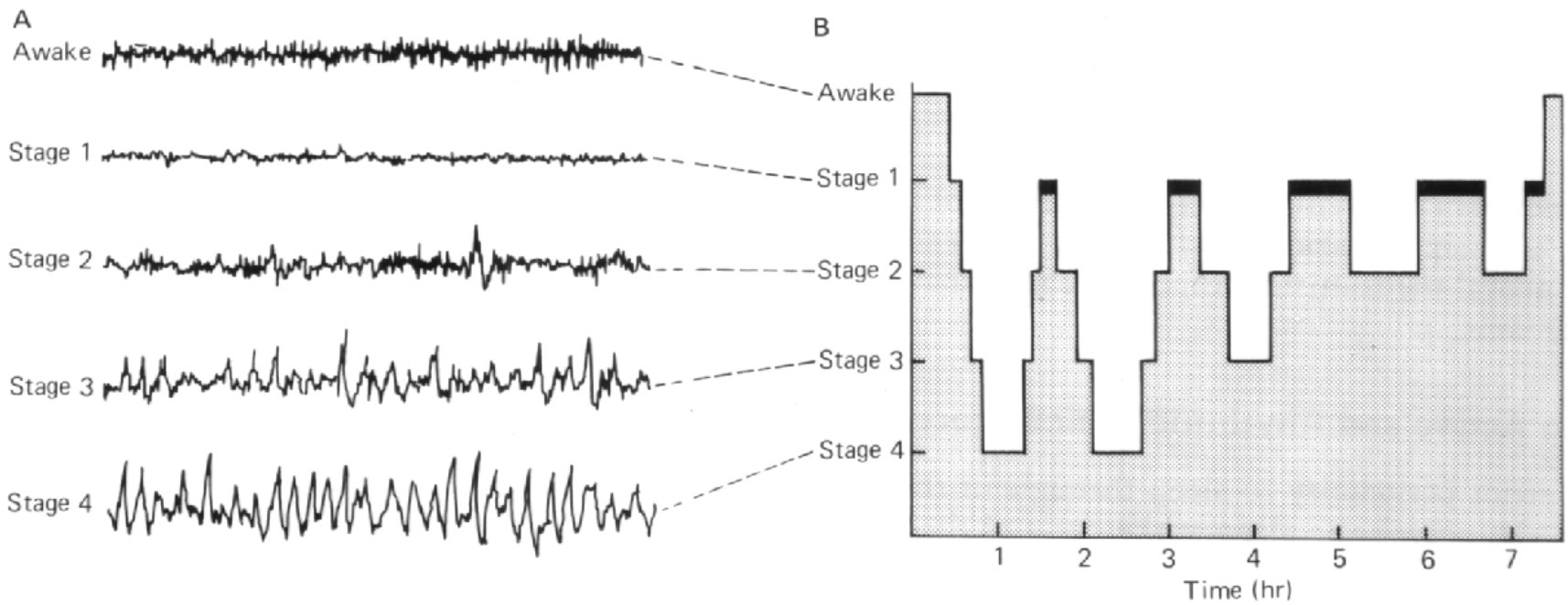

A: EEG recordings during different stages of wakefulness and sleep. B:A typical pattern of sleep in a young adult. REM: black bars (Kandell et al., 1991)

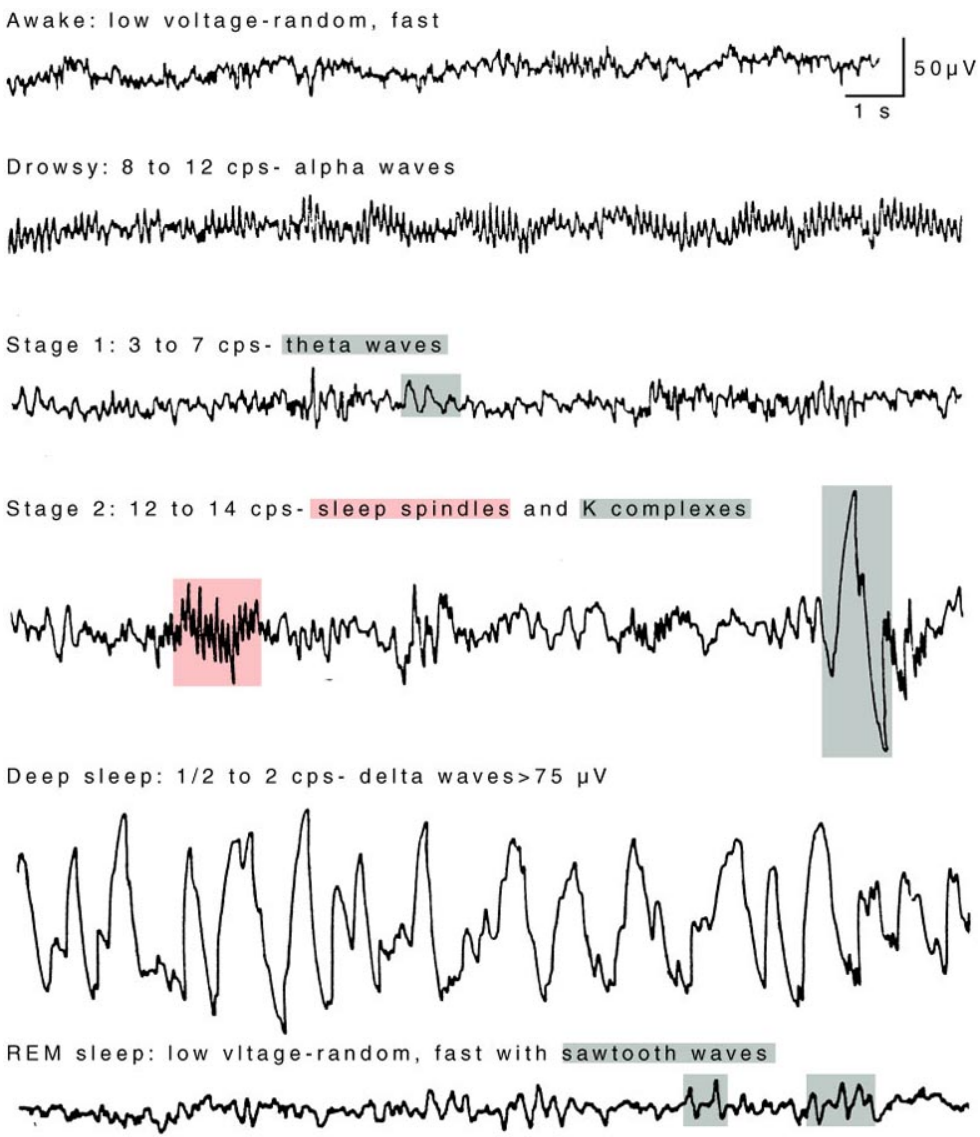

Physiological changes in a volunteer during various sleep states in a typical 8-hr sleep period

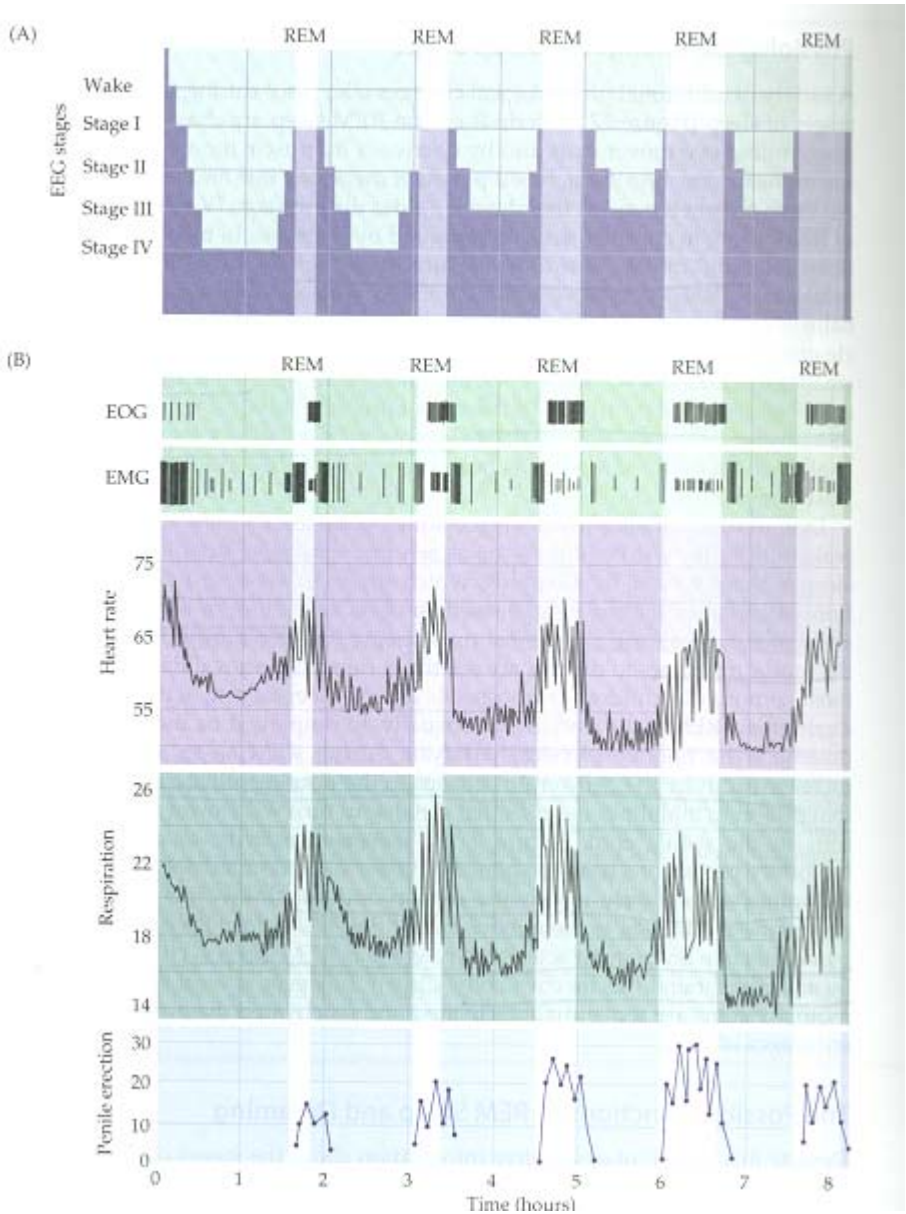

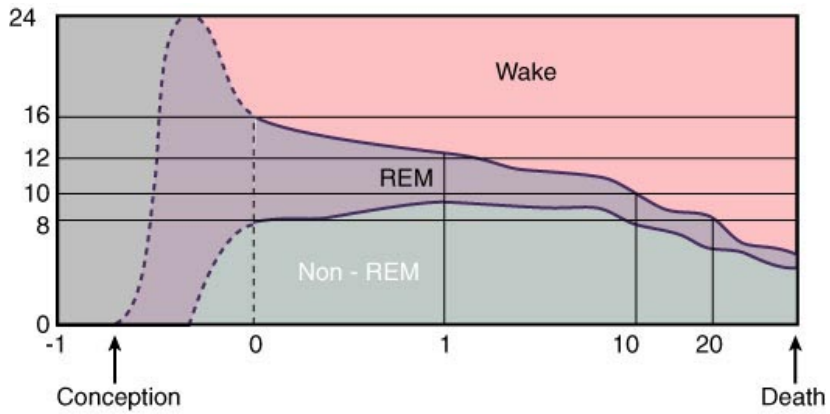

From Purves et al., 2004

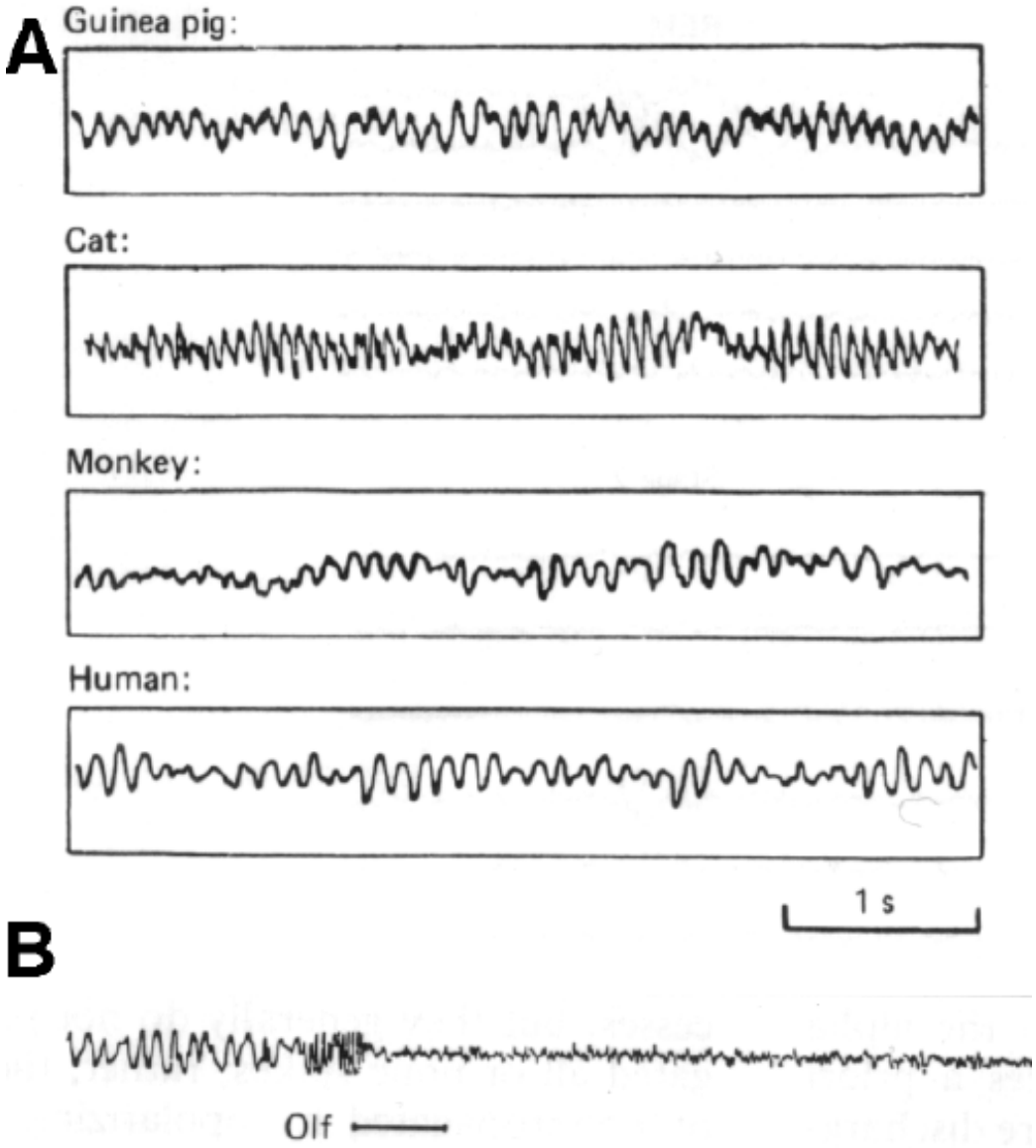

Alpha rhythm

A: EEG records showing alpha rhythm from four species (Brazier, 1960).

B: Desynchronization of the EEG of a rabbit by an olfactory stimulus (Green and Arduini, 1954).

EEG with brainstem transections

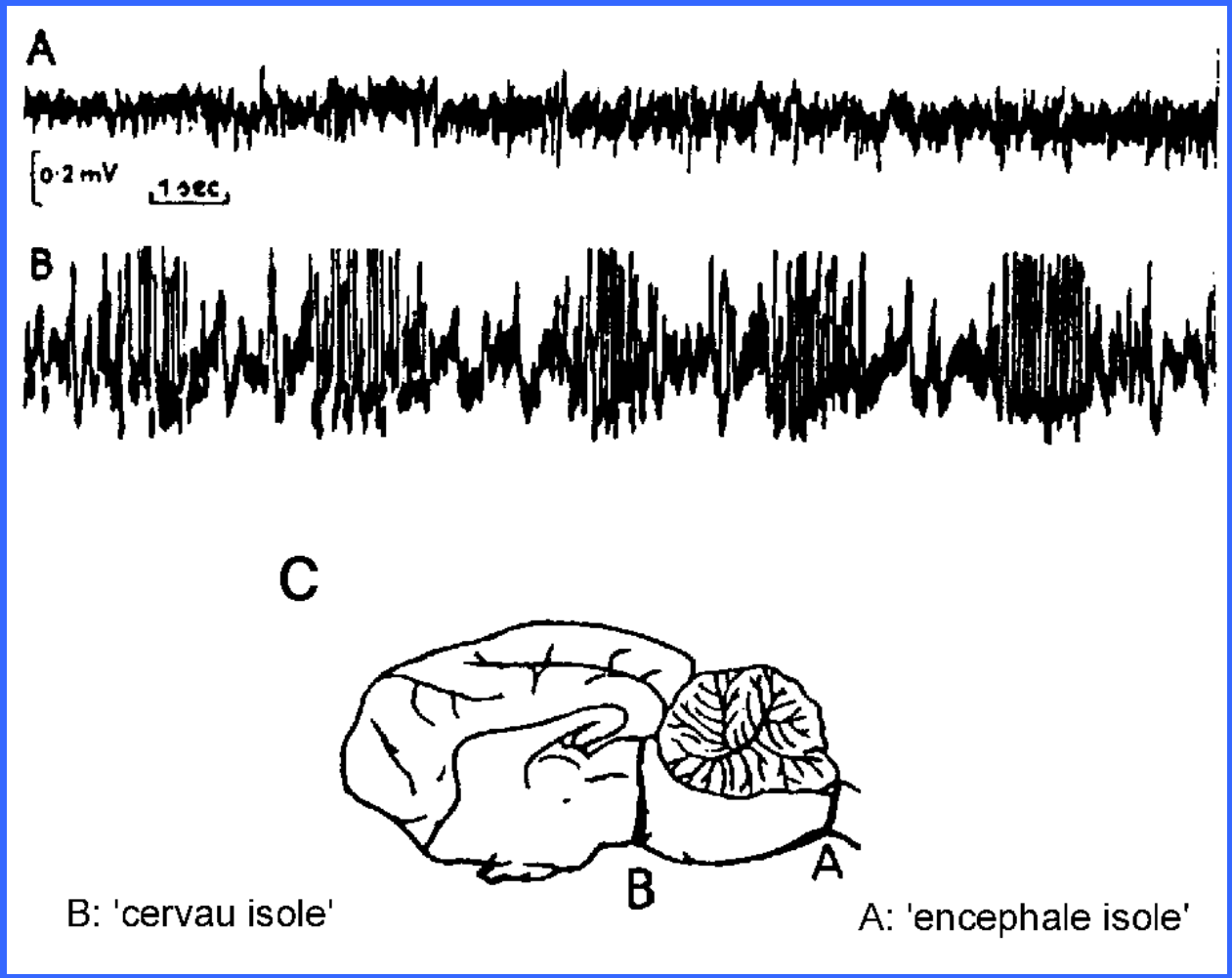

A: Cortical LVFA typical of the alert state in cat (transection at ‘A’).
B: Spindling with cut at ‘B’ (Bremer, 1937).

EEG with brainstem lesions (Lindsley et al., ’49)

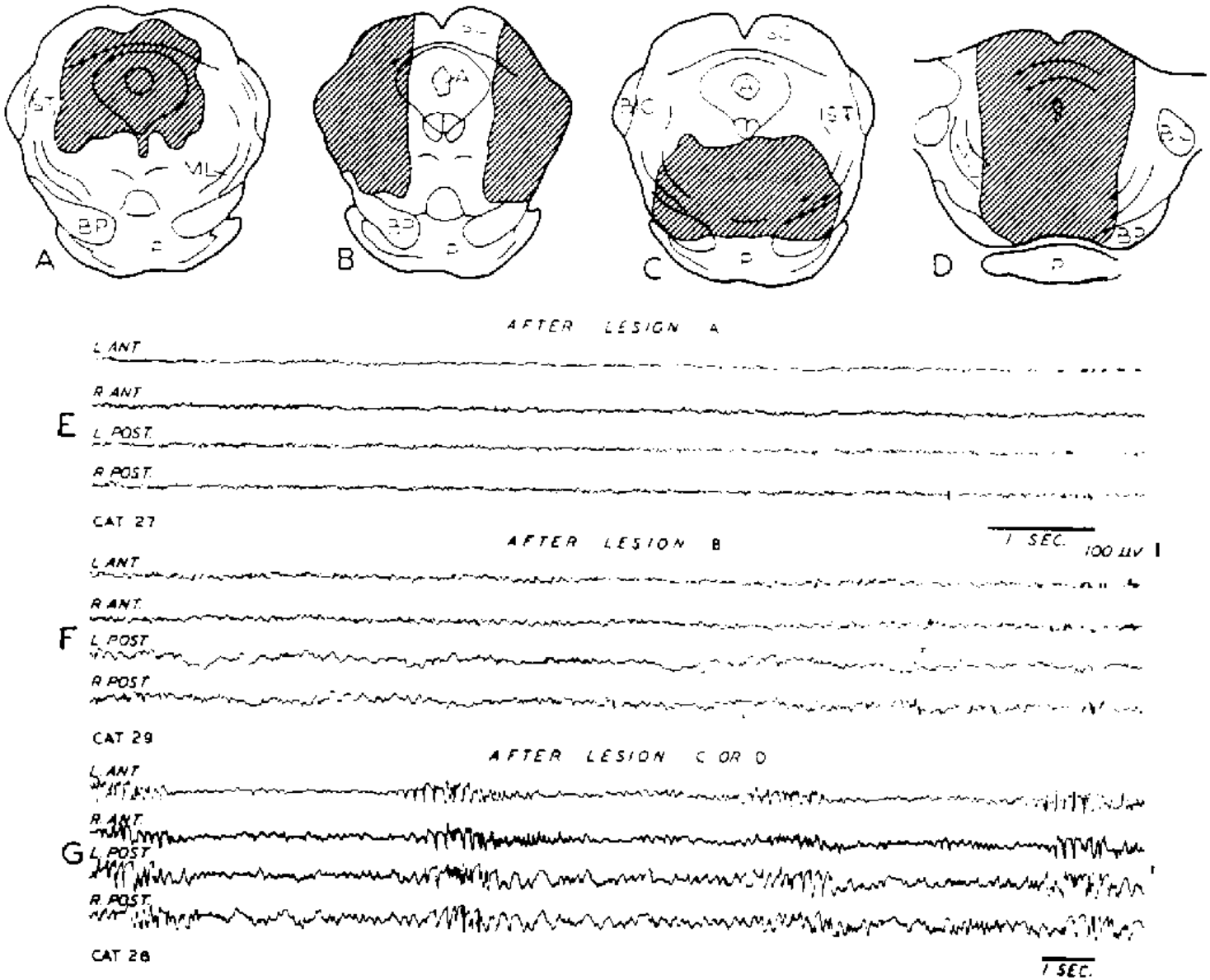

Ascending modulatory systems: The past

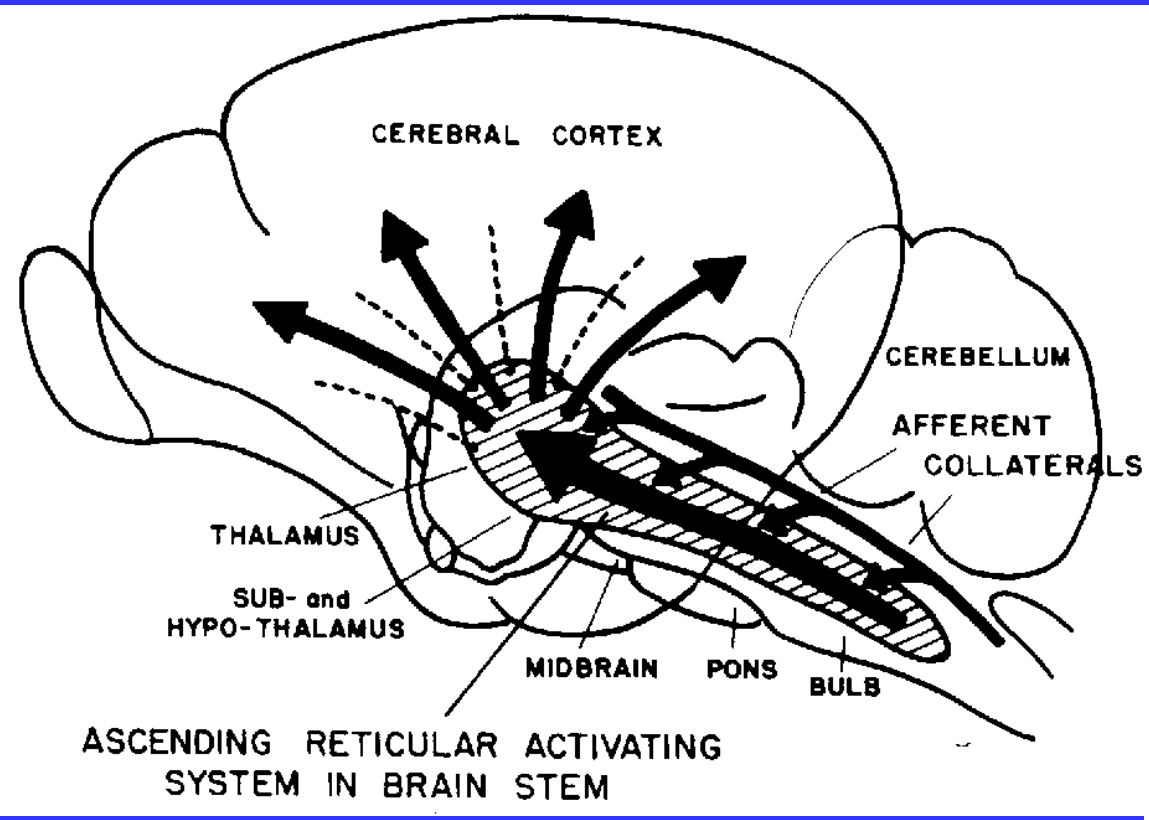

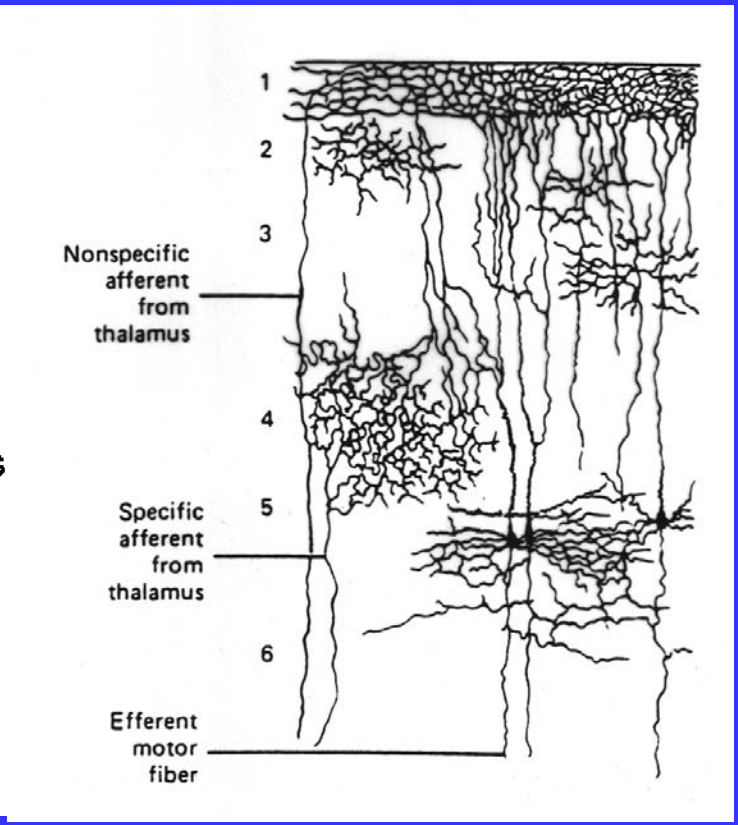

Magoun, Moruzzi et al, 1951

Lorente de No, 1938

Hypothalamic sleep-wake ‘centers’

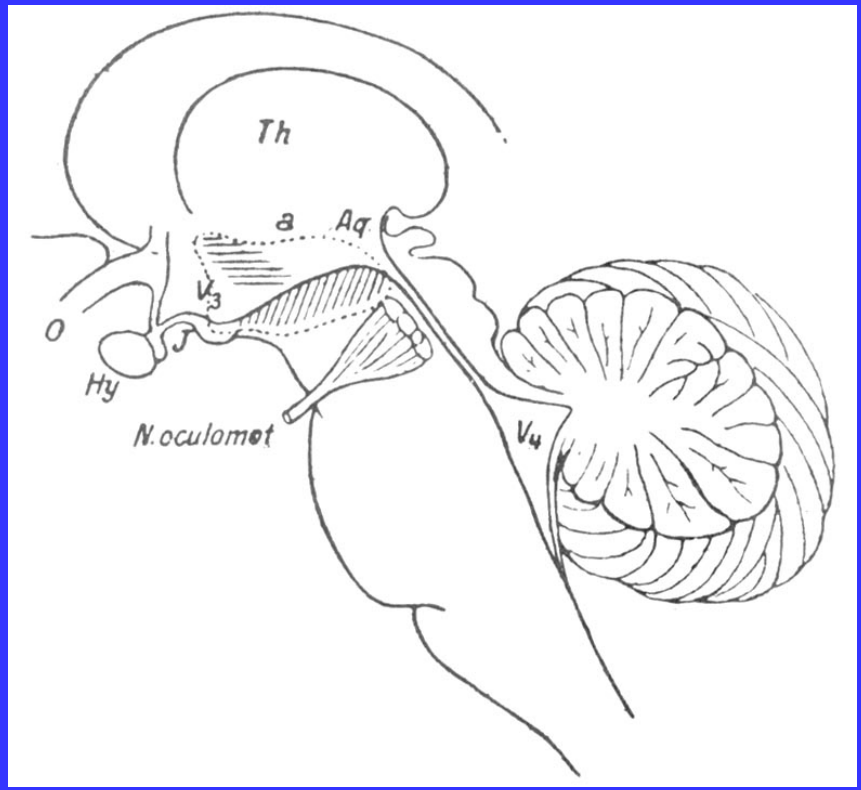

Lesion of the anterior hypothalamus resulted in insomnia, lesion of the posterior hypothalamus was associated with comatose state. (Von Economo, 1931)

Subcortical modulatory systems

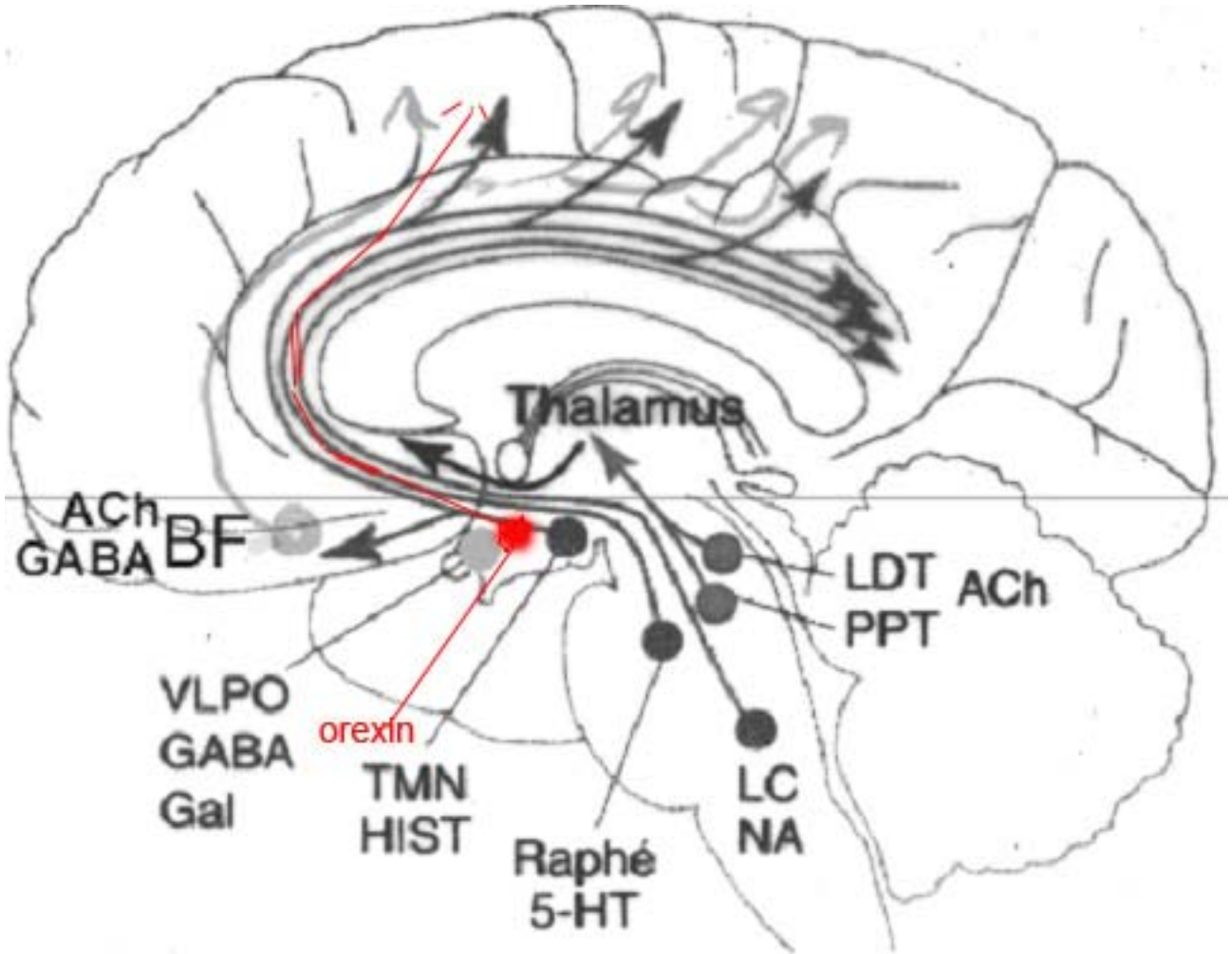

Fuxe, Mesulam, Saper,Kiduff

Dorsal view of the brainstem

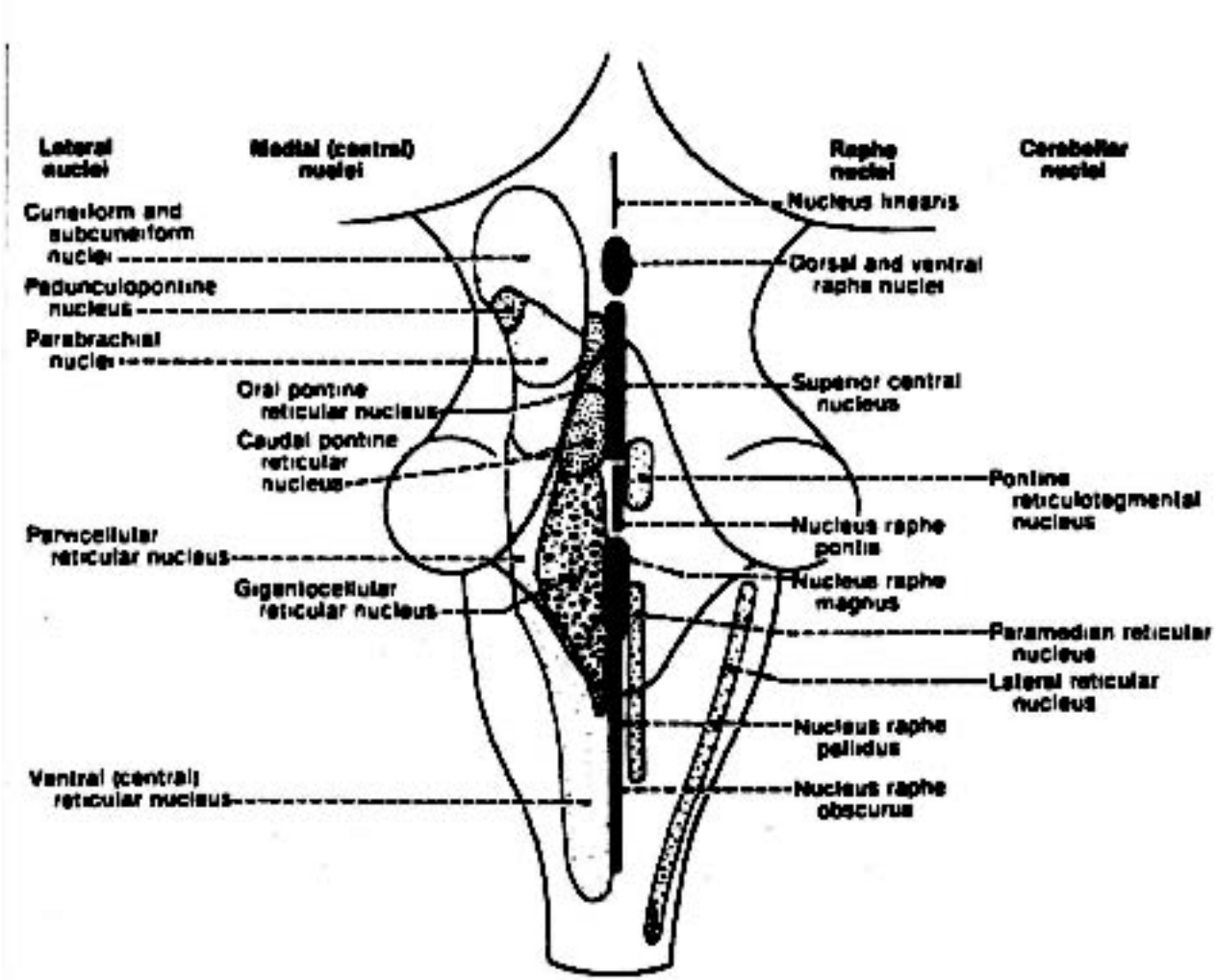

Various cell groups of the reticular formation and the raphe nuclei are indicated.

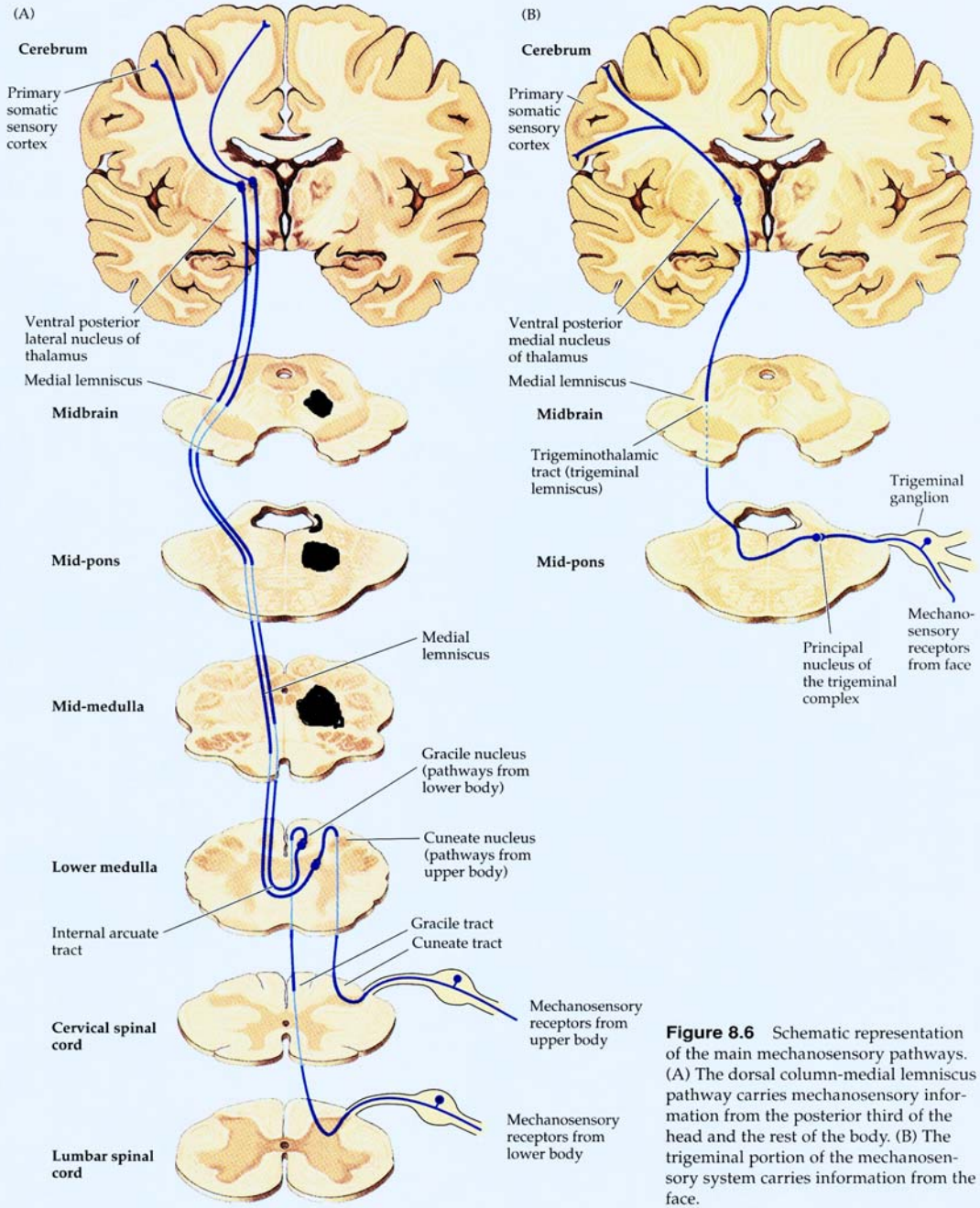

Figure 8.6 Schematic representation of the main mechanosensory pathways. (A) The dorsal column-medial lemniscus pathway carries mechanosensory information from the posterior third of the head and the rest of the body. (B) The trigeminal portion of the mechanosensory system carries information from the face.

The dorsal column-medial lemniscus pathway

Dark shaded are corresponds to the reticular formation

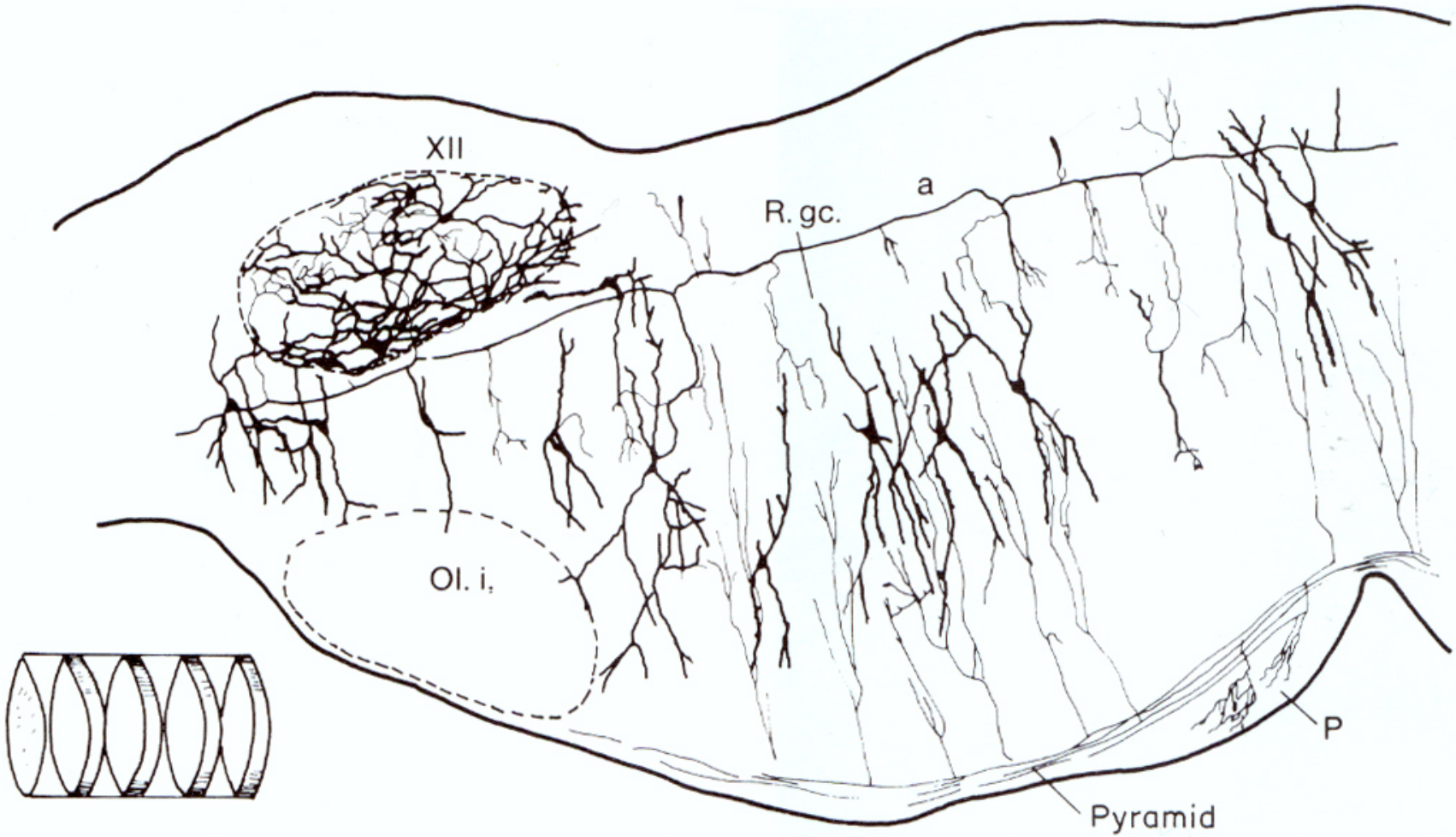

Fig. 12.4. *Orientaion of dendrites in the reticular formation.* Sagittal section through the medulla (rat). Note the long, straight dendrites, which are typical of the neurons of the reticular formation, in contrast to the neurons of a cranial nerve nucleus (XII) and other specific brain stem nuclei. A long axon (a) with numerous collaterals extending ventrally in the transverse plane is also shown. Collaterals of the pyramidal tract fibers (Pyr.) also enter the reticular formation. P = pontine nuclei; R.gc. = the gigantocellular nucleus of the reticular formation; Ol.i. = the inferior olivary nucleus. From Scheibel and Scheibel (1958).

Classification of neurons according their dendritic arborization

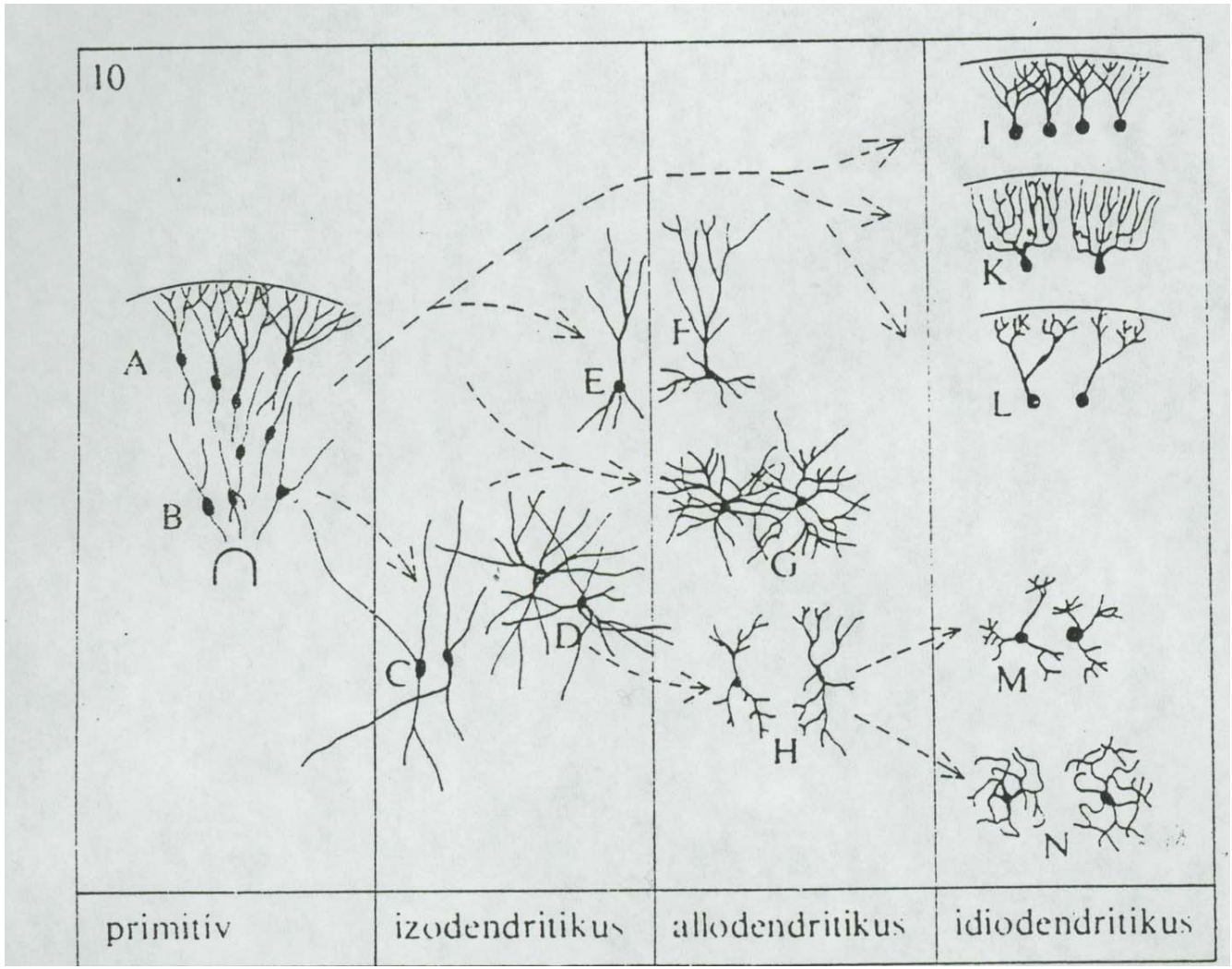

A,B: invertebrates; C-E: brainstem reticular core; F: pyramidal; I: dentate granule; K:Purkinje; L: mitral cell; M: tufted; N: wavy pattern (inferior olive). Monoaminergic cells of the brainstem, cholinergic neurons of the braisntem and basal forebrain show isodendritic arborization

Monoaminergic cell groups in the brainstem

Dahlstrom and Fuxe, 1964

ACTA PHYSIOLOGICA SCANDINAVICA
VOL. 62. SUPPLEMENTUM 232

FROM THE DEPARTMENT OF ANATOMY, KAROLINSKA INSTITUTET, STOCKHOLM, SWEDEN

15013

EVIDENCE FOR THE EXISTENCE OF MONOAMINE-CONTAINING NEURONS IN THE CENTRAL NERVOUS SYSTEM

I. Demonstration of Monoamines in the Cell Bodies of Brain Stem Neurons

BY

ANNICA DAHLSTRÖM and KJELL FUXE

UPPSALA 1964

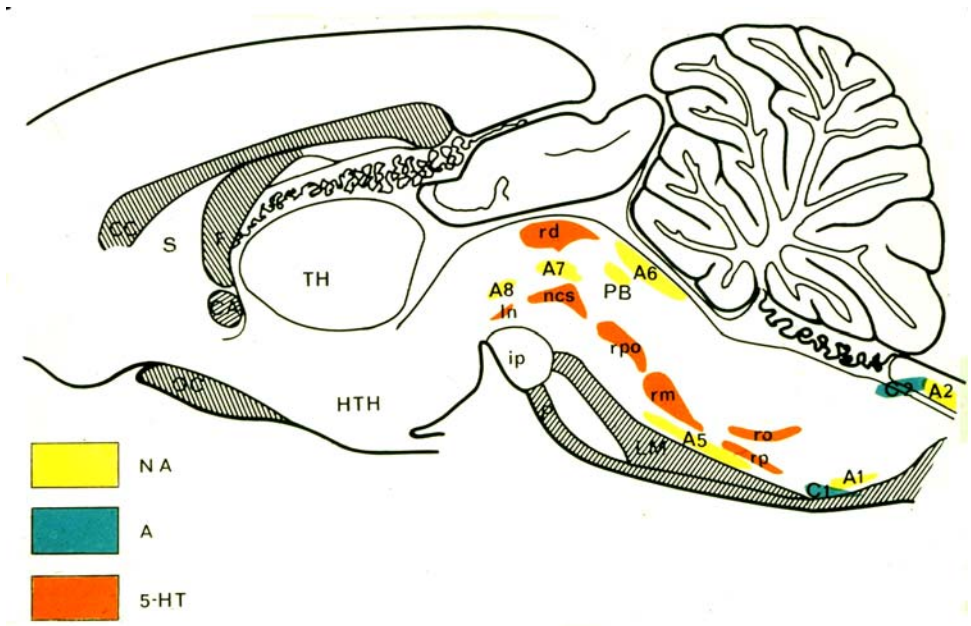

Monoamine synthesis

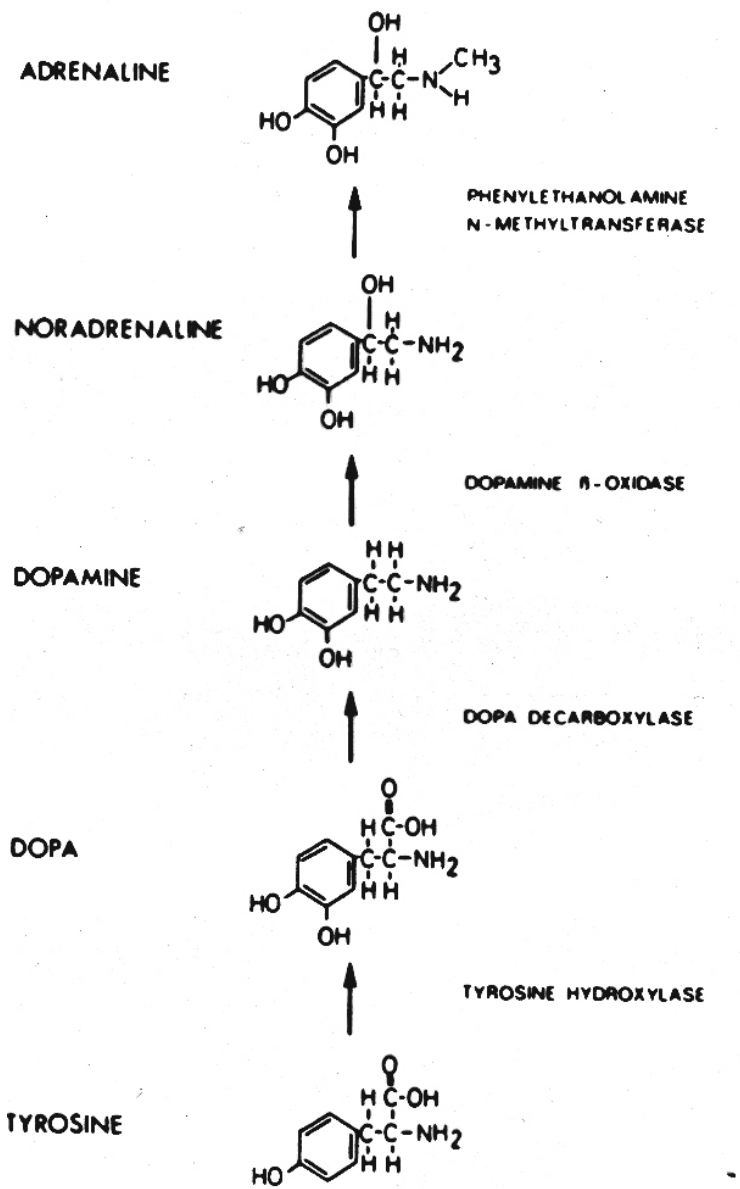

SEROTONIN

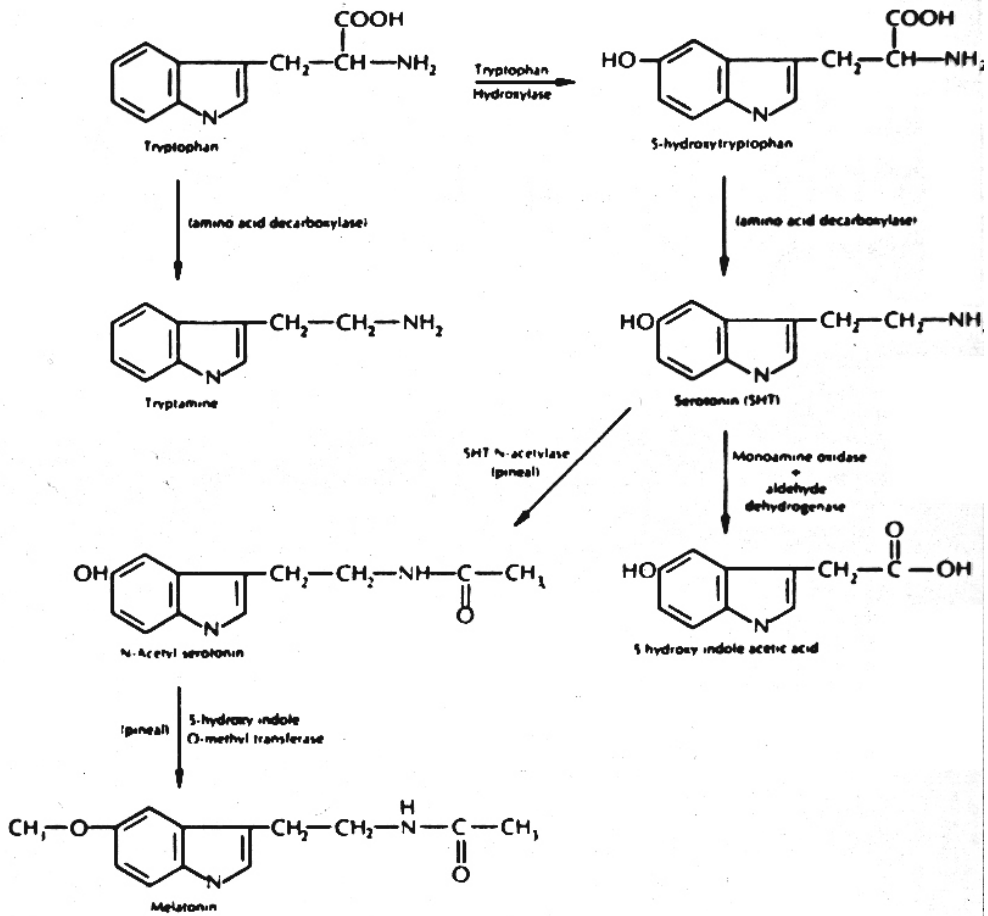

Cortical EEG and ACh output I

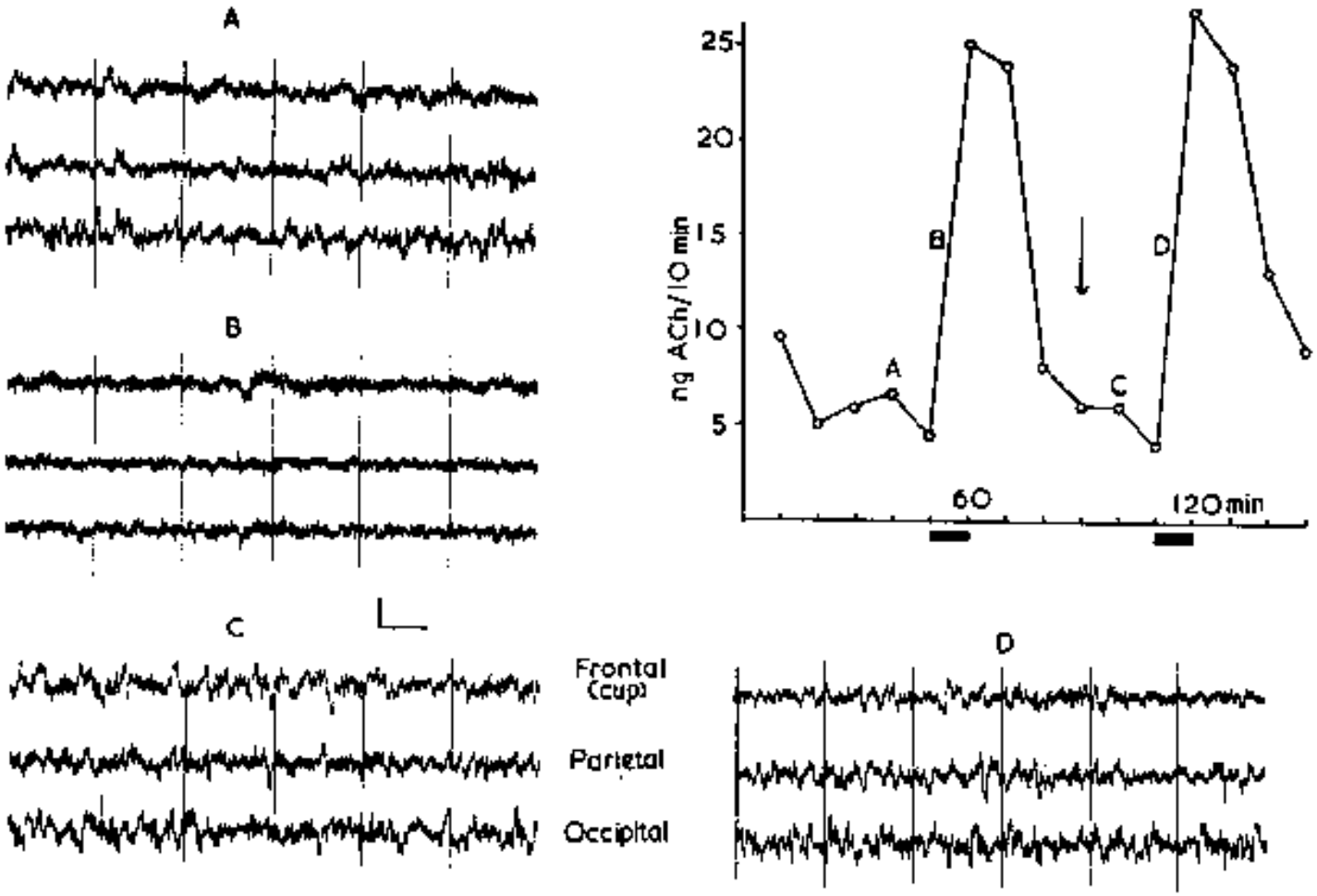

During period marked by thick line, stimulation of the RF. At arrow, 1mg/kg atropine injected iv. EEG calibration: 0.1 mV, 1 sec (Szerb et al., 1965).

EEG, BEHAVIOR, ATROPINE, RESERPINE

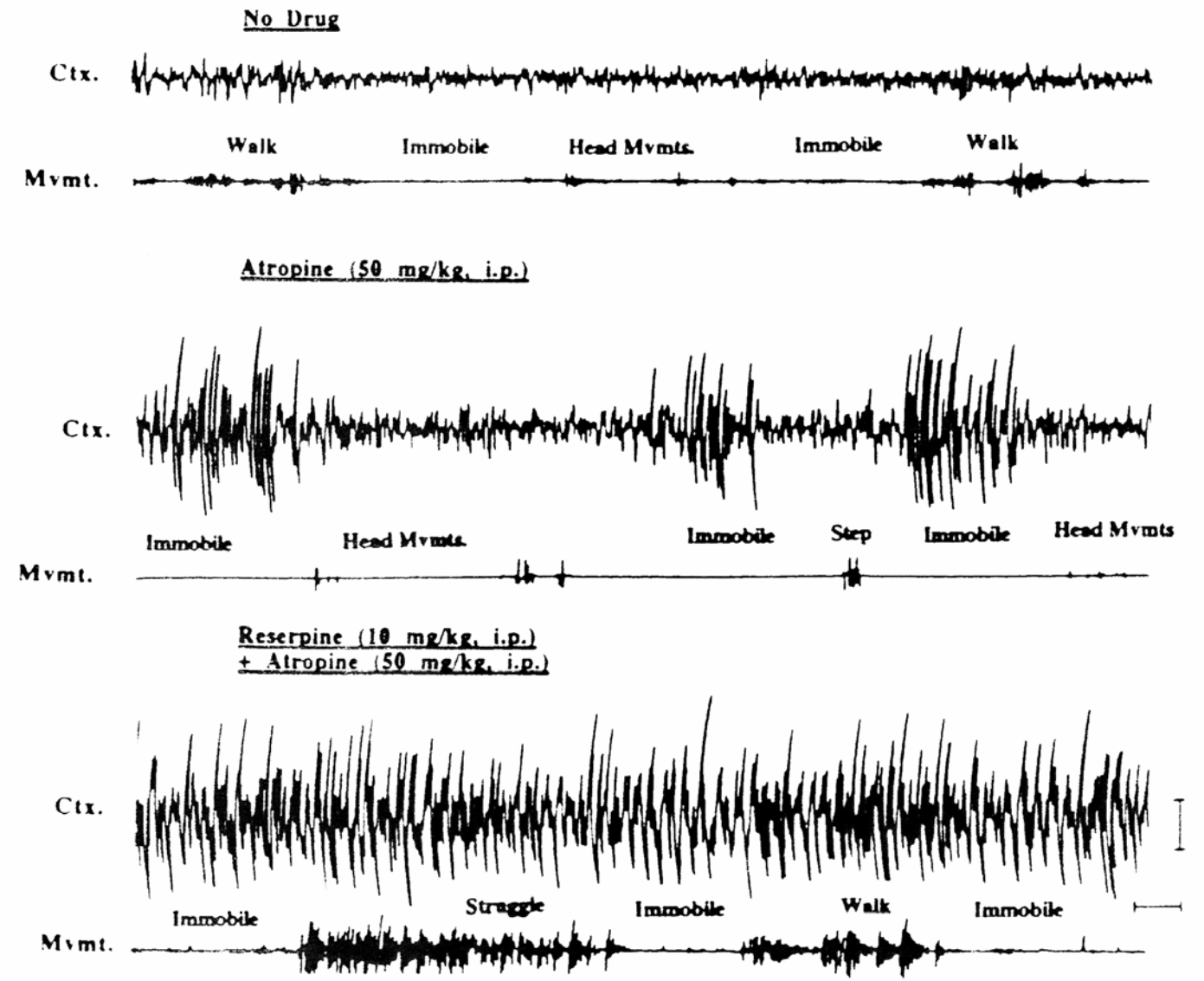

The A1-A7 NE cell groups

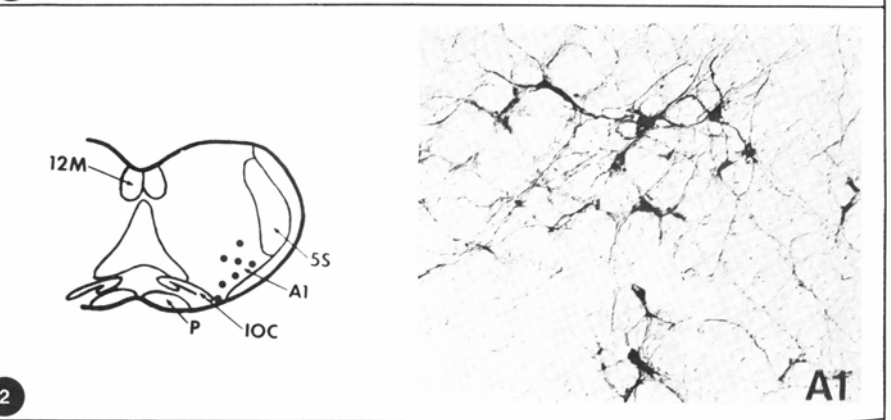

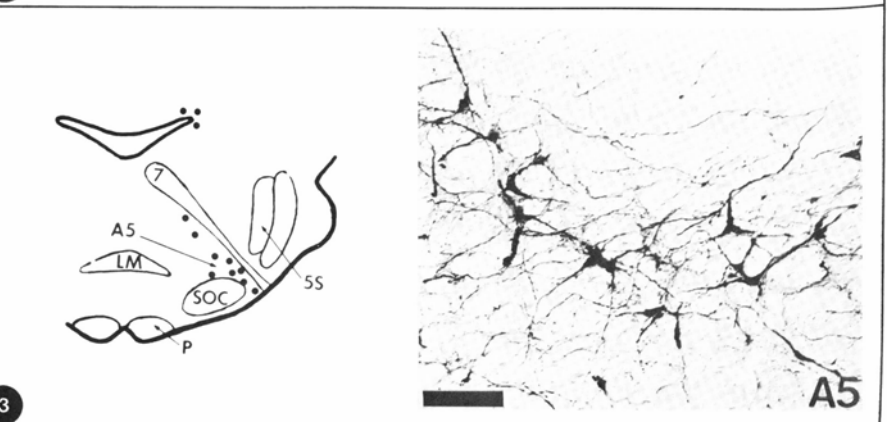

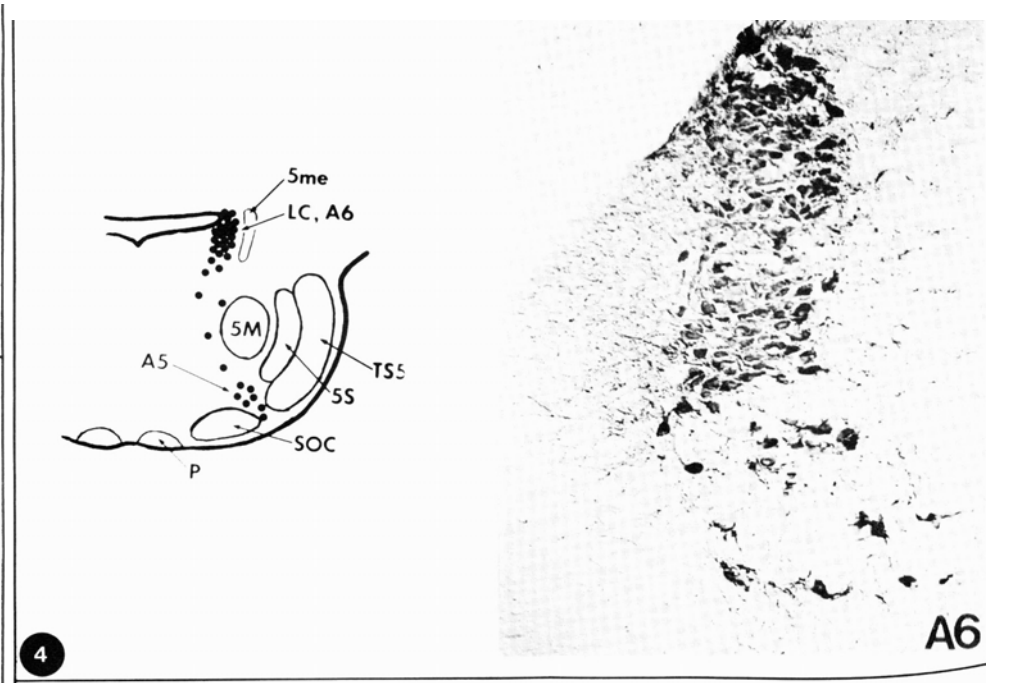

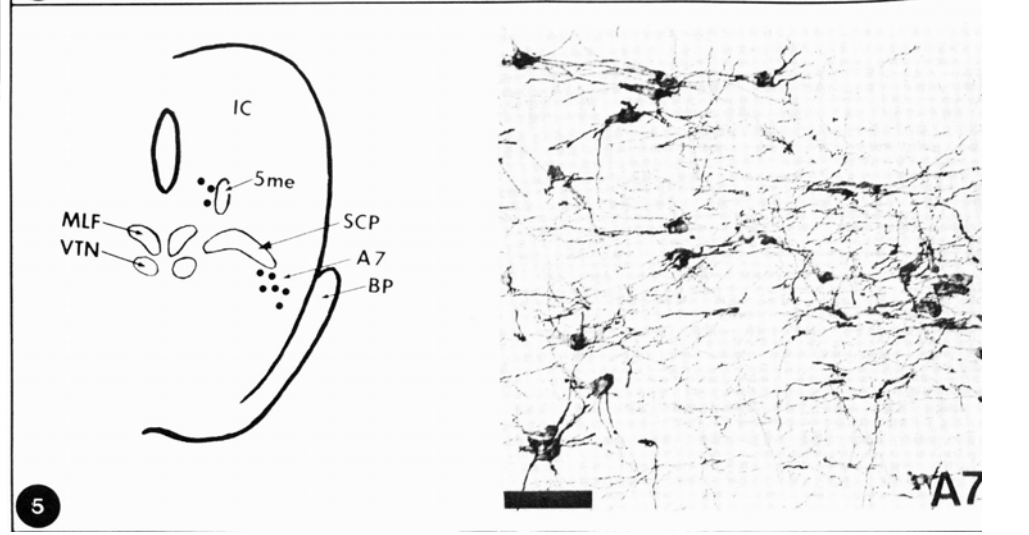

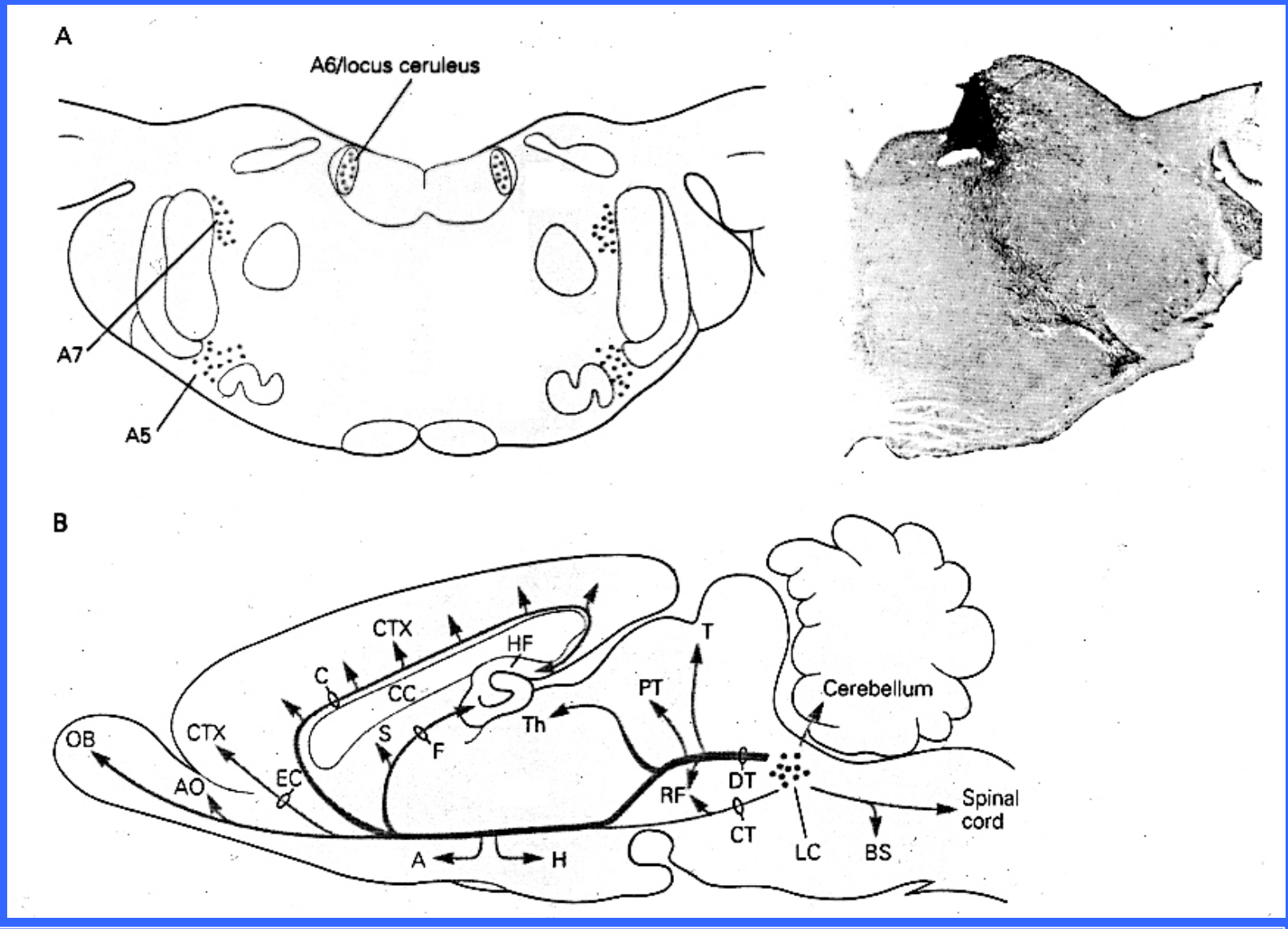

LC provides a major ascending output to the thalamus and cerebral cortex as well as descending projections to the brainstem, cerebellum and spinal cord.

Noradrenergic pathways in humans

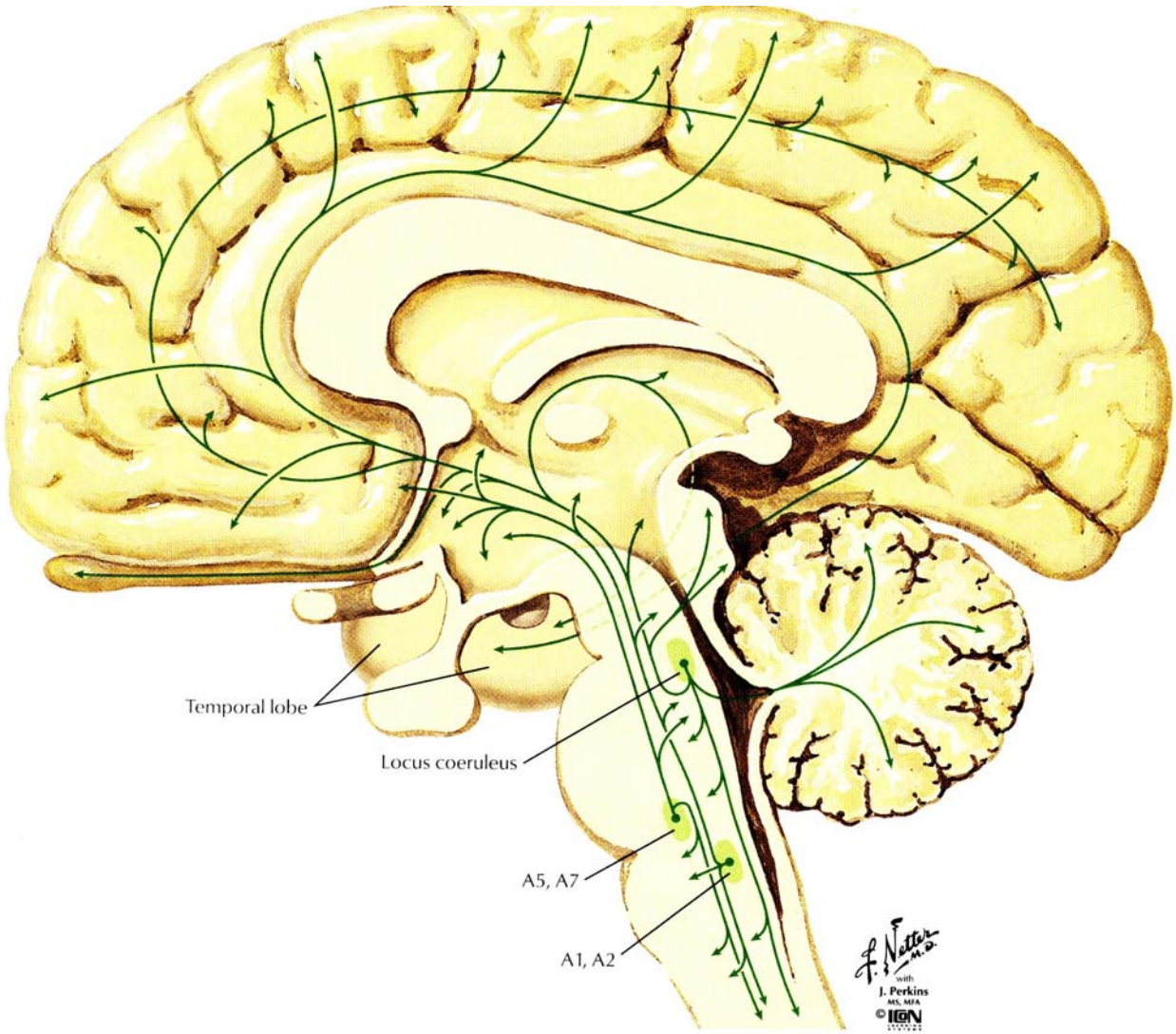

FIGURE II.96: NORADRENERGIC PATHWAYS

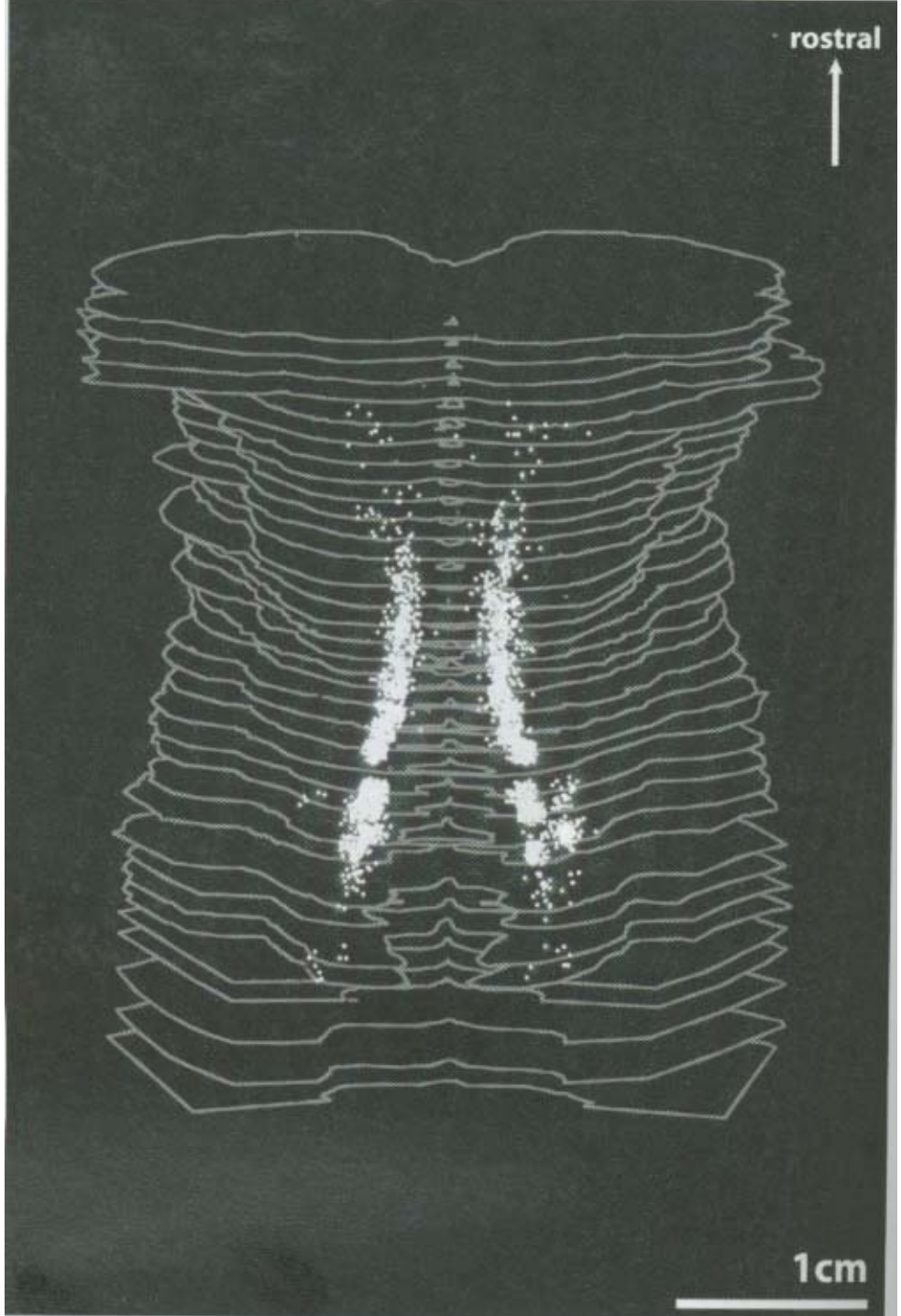

3D reconstruction of transverse cell plots of pigmented LC neurons. One in 15 cells is shown in transverse sections spaced 750 um apart. The locus coeruleus and subcorueleus form a continuous cell column in the upper pons and caudal midbrain (From Holliday, 2005)

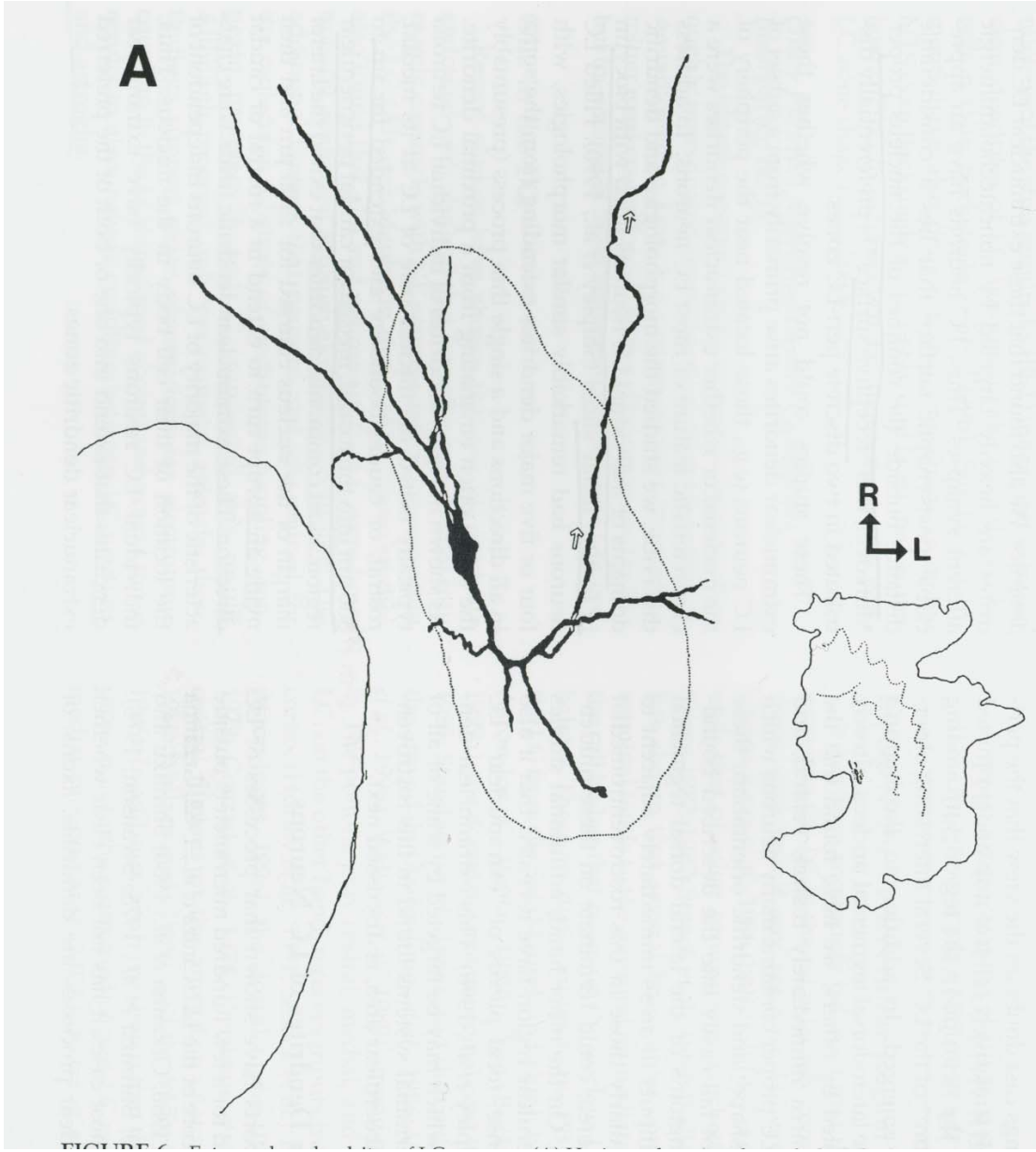

Neuron from the LC (Aston-Jones, 2004)

Effect of LC stimulation (100Hz, 20uA) on neocortical and hippocampal activity in urethane-anaesthetized rat.

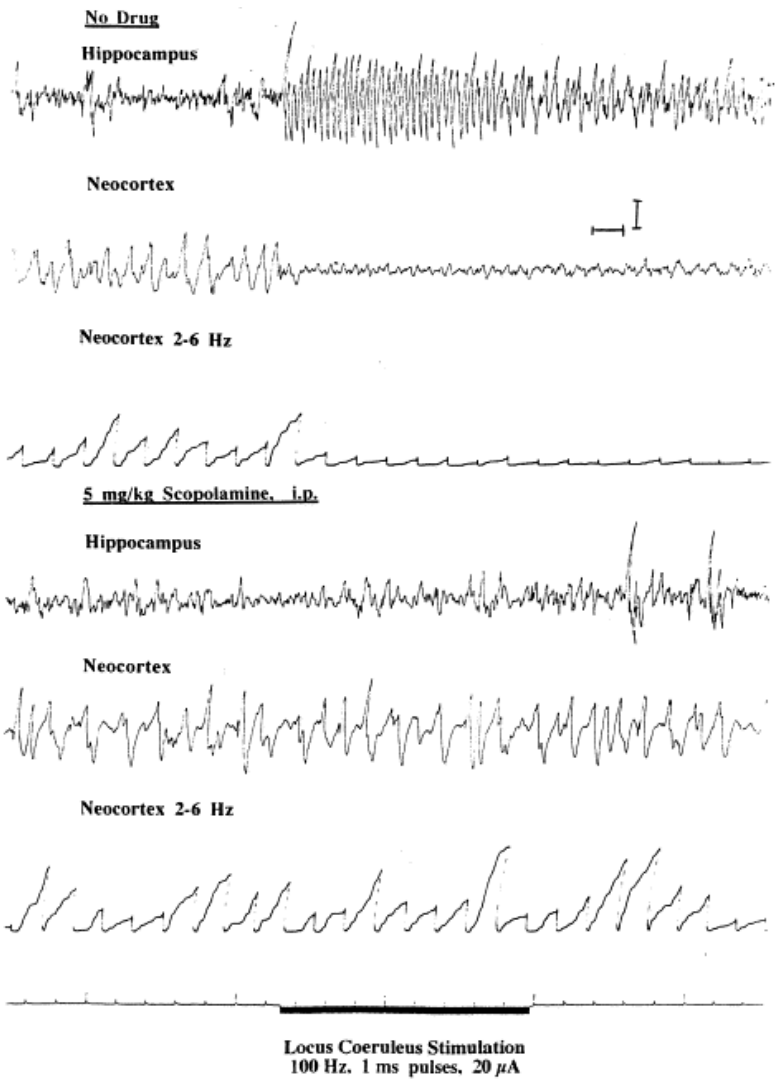

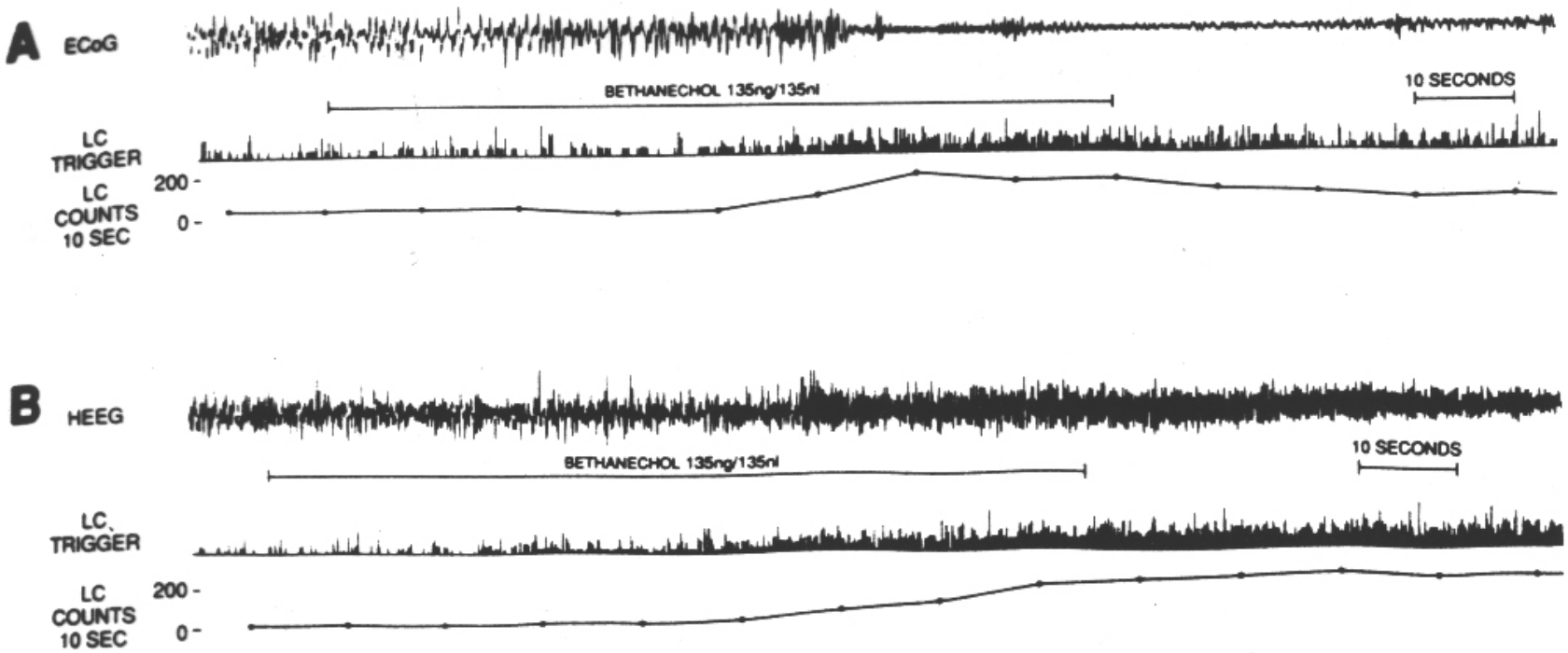

Relationship of LC activity to cortical ECoG (**A**)and hippocampal EEG (HEEG, **B**) before, during and after peri-LC bethanechol infusion. The raw trigger output from LC activity is shown in the middle trace, and the integrated trigger output(10 sec intervals)is in the bottom trace.As LC activity is seen to increase during the latter part of the infusion, reduced amplitude and increased frequency become evident in the ECoG trace. As LC activity begins to decrease, ECoG amplitude begins to increase and its frequency decreases.Similar changes can be observed in the HEEG (Aston-Jones)

LC activity and attention

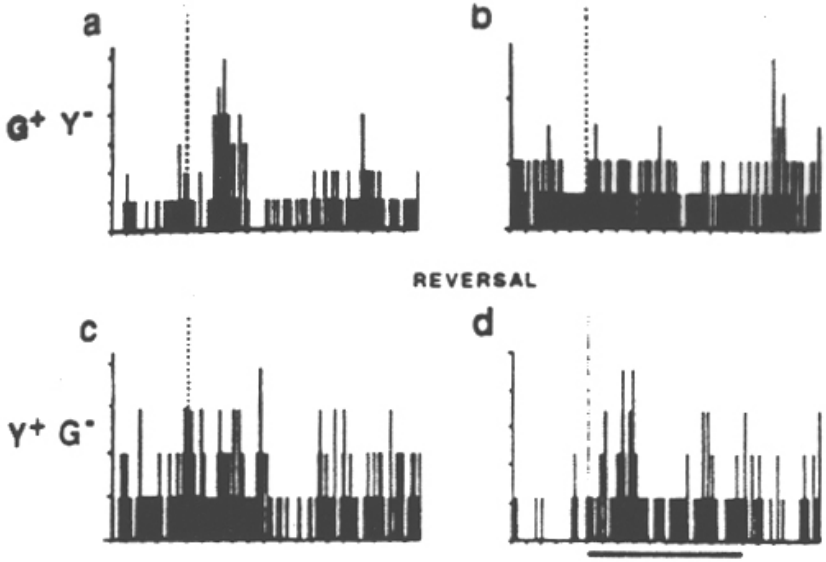

A reversal procedure in a visual discrimination task in monkeys reveals responses for LC neurons specific to meaningful stimuli. Target stimuli occur on 10% of trials, and non-target stimuli occur on 90%; stimuli are presented at *vertical dashed lines* in each histogram. The animal receives a drop of juice when it responds after a target stimulus. **a** and **b:** Post-stimulus-time histograms (PSTHs) for response of an LC neuron to green (target), but not to yellow (non-target) stimuli. **c** and **d:** Similar PSTHs for the same LC neuron after reversal training such that target stimuli are now yellow and non-target stimuli green. Note that green stimuli (**c**) no longer elicit responses, whereas yellow stimuli (**d**) now elicit a small response. Thus, the response is selectively elicited by meaningful stimuli. Calibration bar represents 1 sec. (Aston-Jones)

NE effect on cortical network function

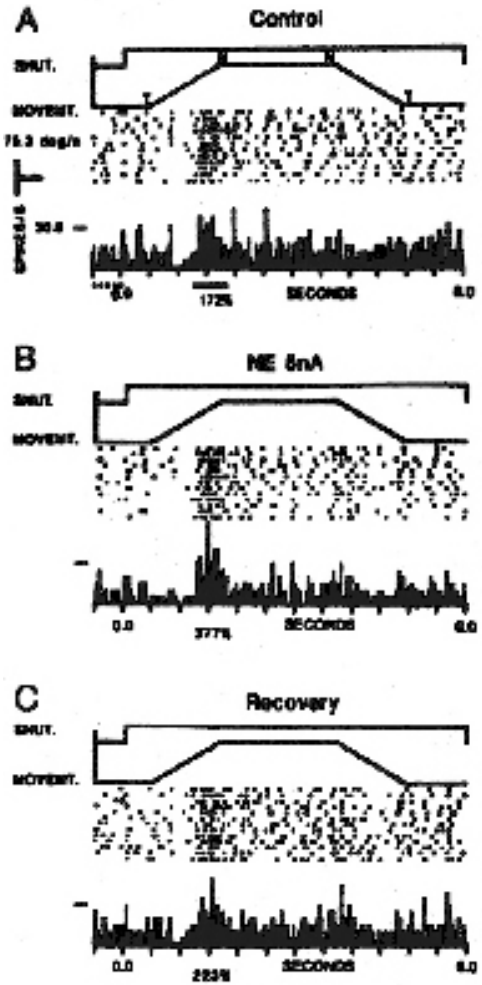

Serotoninergic neurons along the midline of the brainstem

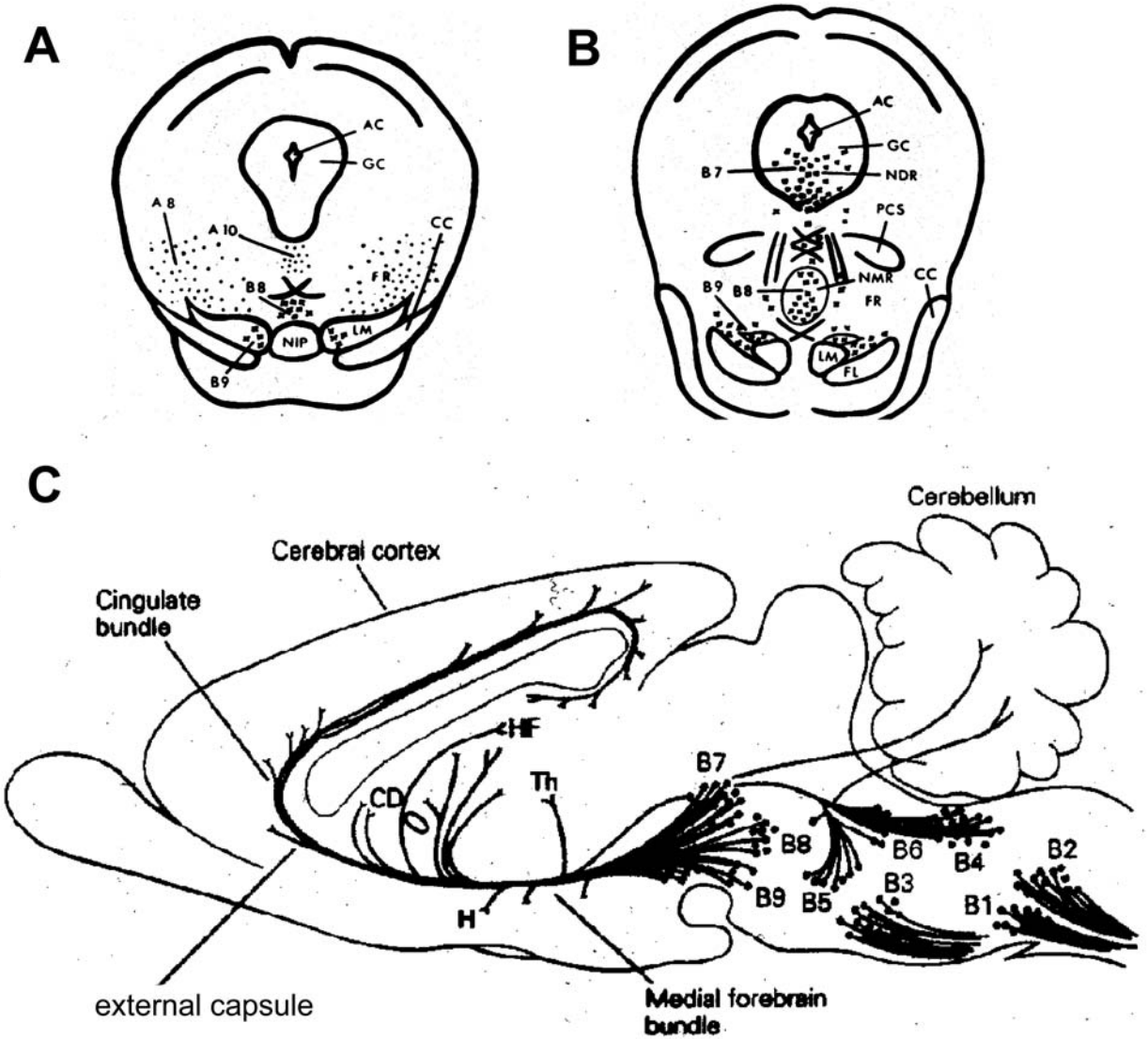

A, B coronal, **C** sagittal sections. Neurons in the B1-B3 groups project to the lower brains stem and spinal cord. Neurons in the raphe pontis (B6), median raphe (B7) and dorsal raphe (B8) project to the upper brainstem, hypothalamus, thalamus and cerebral corte.,

5HT neurons in the human

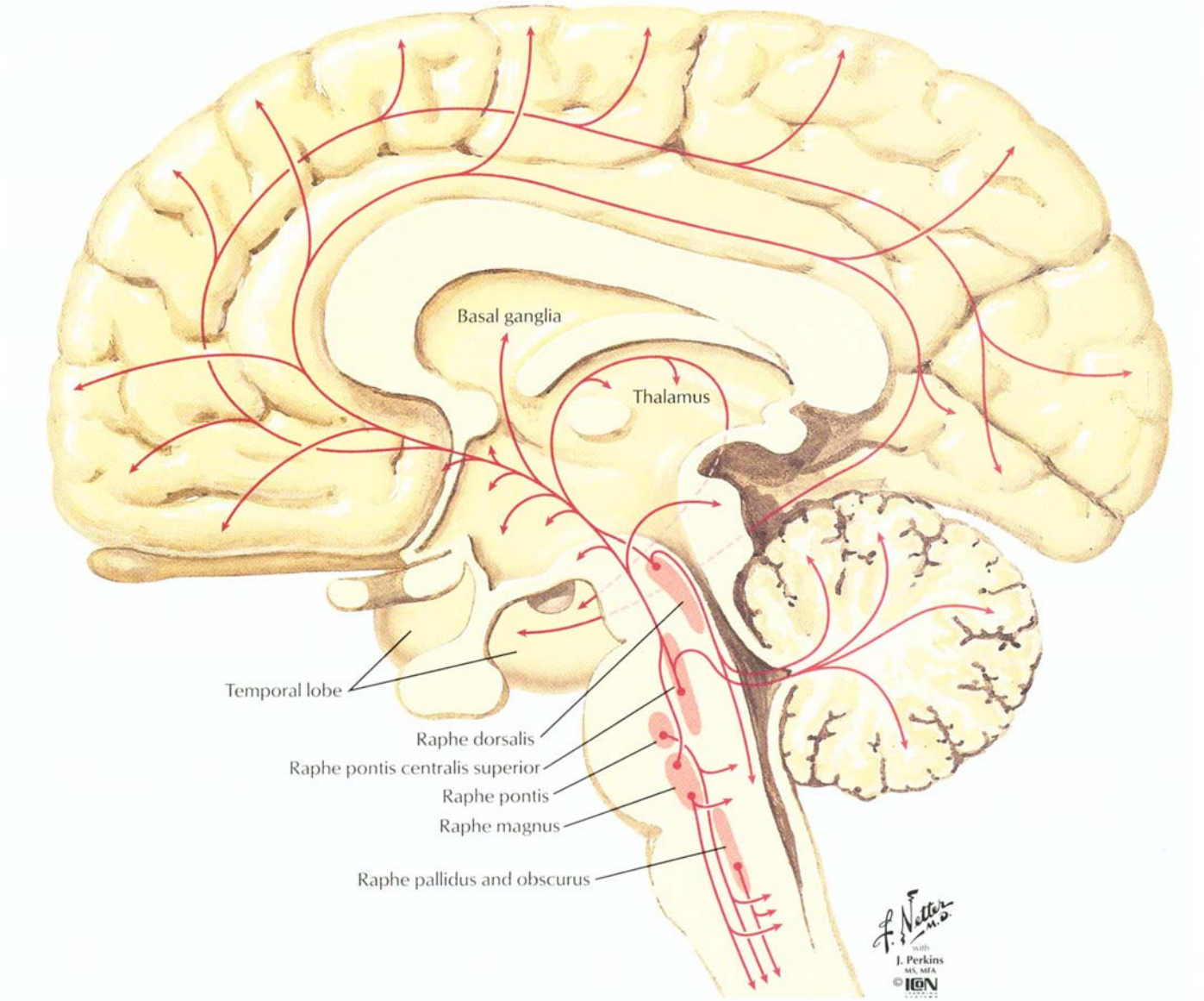

FIGURE II.97: SEROTONERGIC PATHWAYS

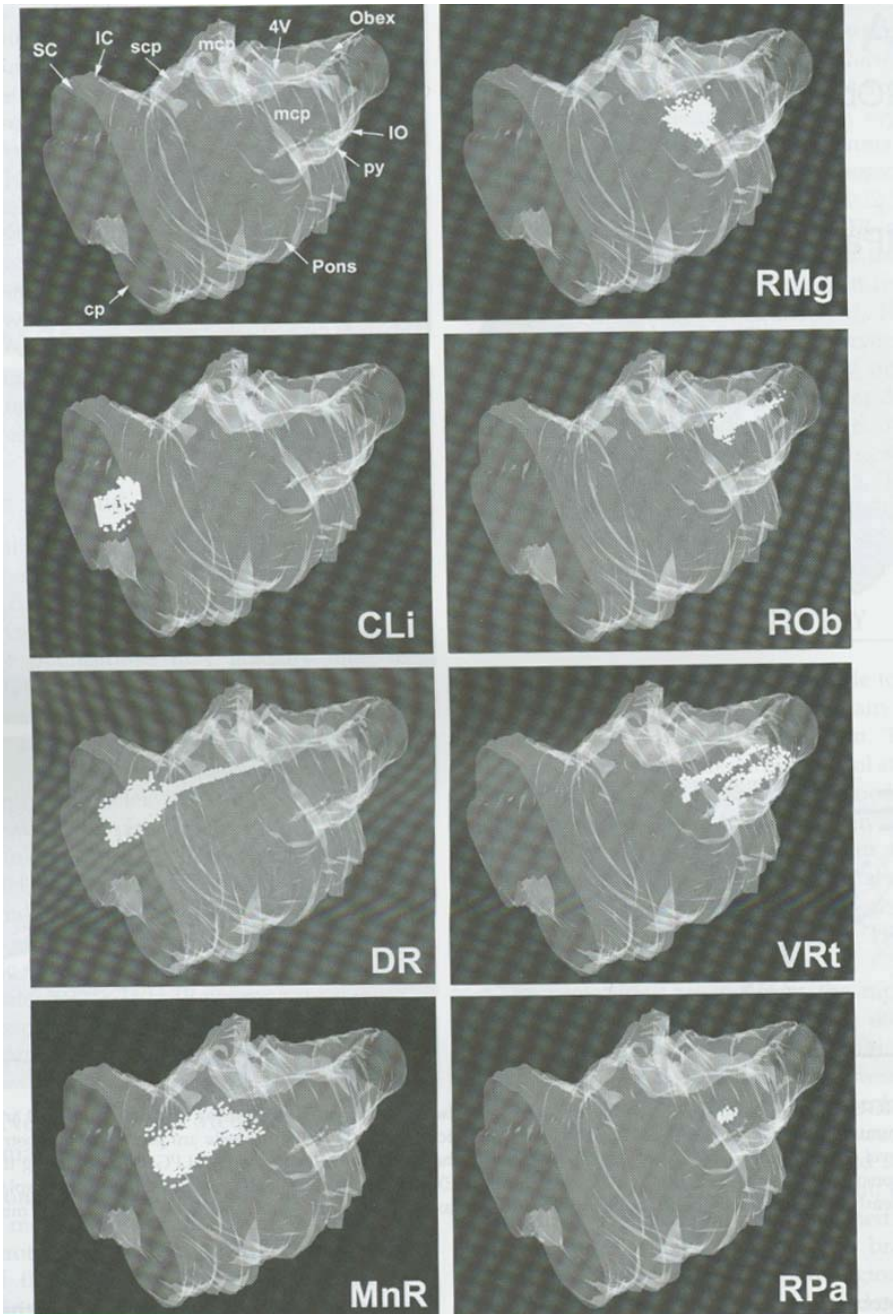

3D representation of the TPH (tryphtophan-hydroxylase) neurons in every 8 sections has been plotted in reference to the outline of the brainstem. The rostro-caudal length of the reconstructed brainstem is 62 mm. From Hornung, 2004)

DR neuron activity and EEG

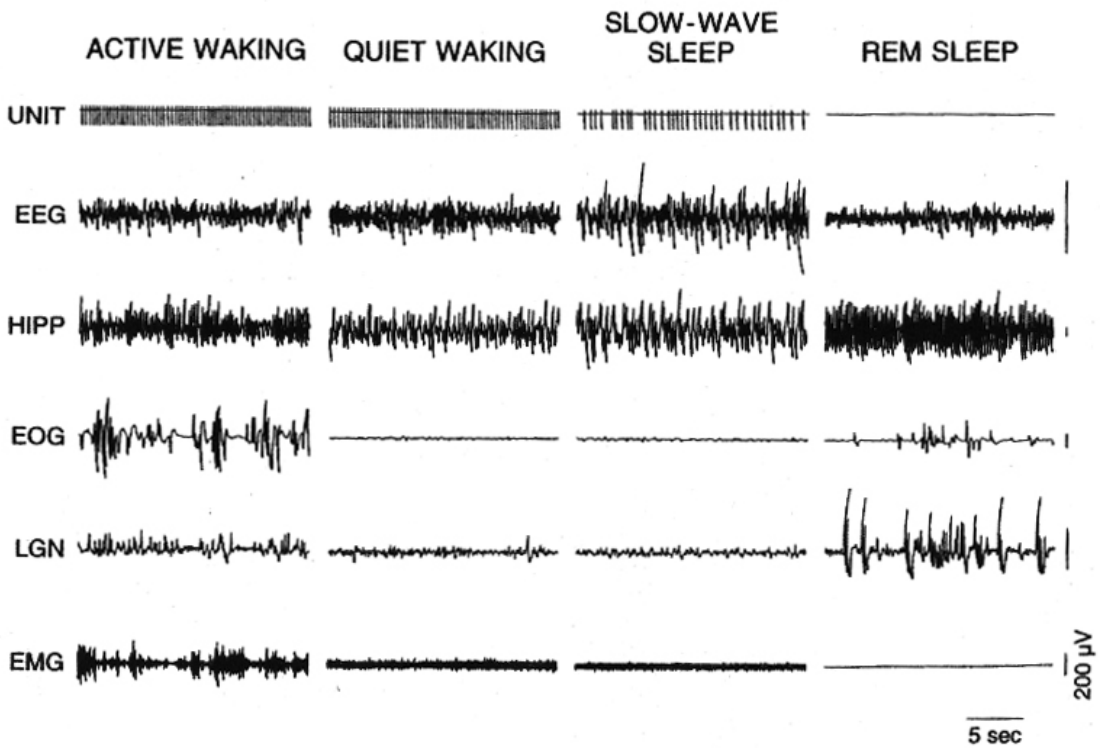

Polygraph records showing the activity of a typical dorsal raphe (DR) neuron and gross potentials across the sleep/wake cycle.Note the positive relationship between the firing rate and the level of behavioral arousal, as well as the cessation of unit activity during REM sleep. During REM sleep, ponto-geniculo-occipital (PGO) waves can be seen in the LGN trace and prominent rhythmic slow activity (theta) in the hippocampus (HIPP) trace (Jacobs and Fornal, 1999).

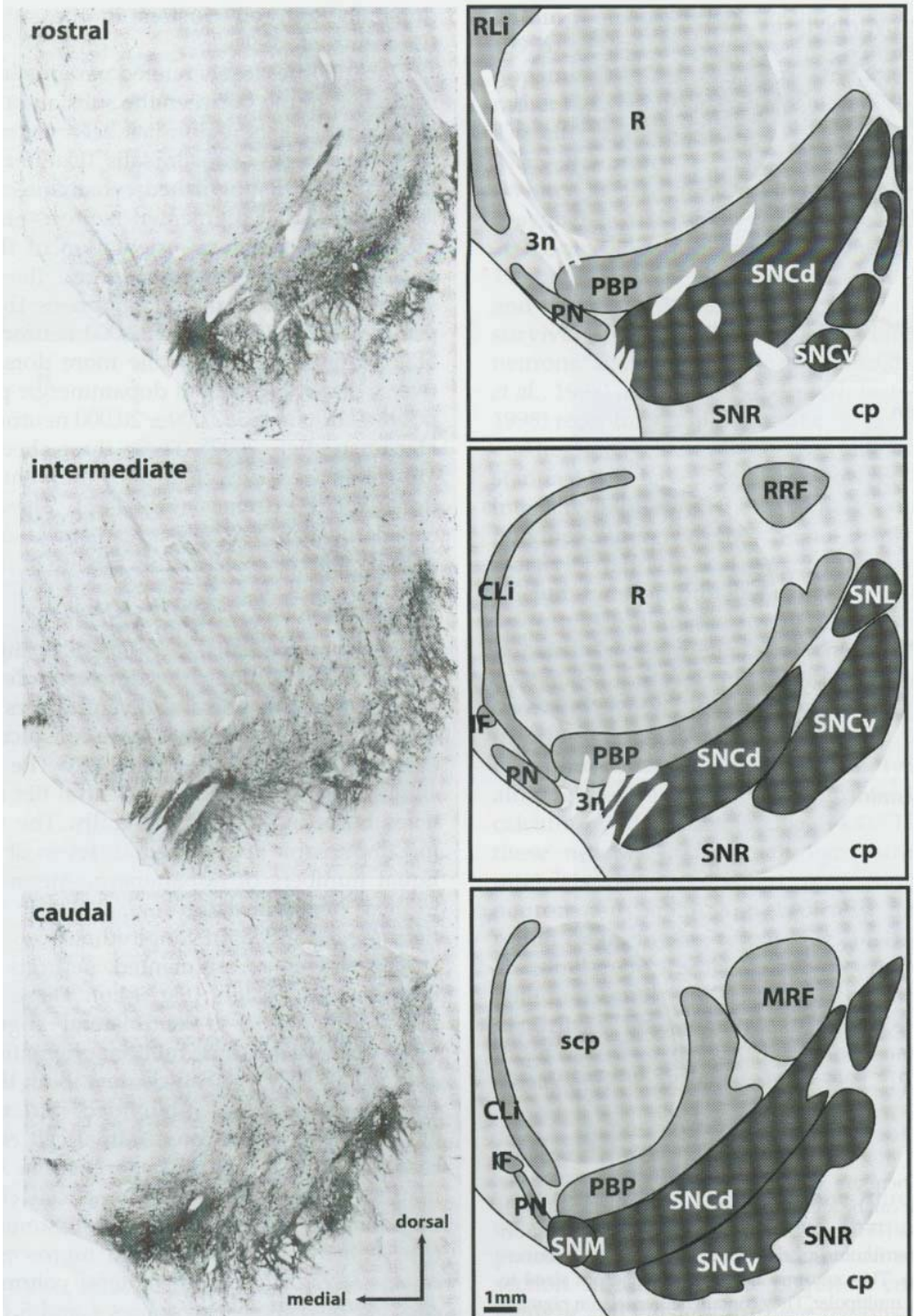

Rostro-caudal transverse levels of the midbrain stained for TH (tyrosine hydroxylase).

Dopaminergic neurons in the brain

Dopaminergic neurons in the brain stem and hypothalamus.

A. Dopaminergic neurons in the substantia nigra (**A9** group) and the adjacent retrorubral field (**A8** group) and ventral tegmental area (**A10** group) provide a major ascending pathway that terminates in the striatum, the frontotemporal cortex, and the limbic system, including the central nucleus of the amygdala and the lateral septum.

B. Hypothalamic dopaminergic neurons in the **A11** and **A13** cell groups, in the zona incerta, provide long descending pathways to the autonomic areas of the lower brain stem and the spinal cord. Neurons in the **A12** and **A14** groups, located along the wall of the third ventricle, are involved with endocrine control. Some of them release dopamine as a prolactin release inhibiting factor in the hypophysial portal circulation.

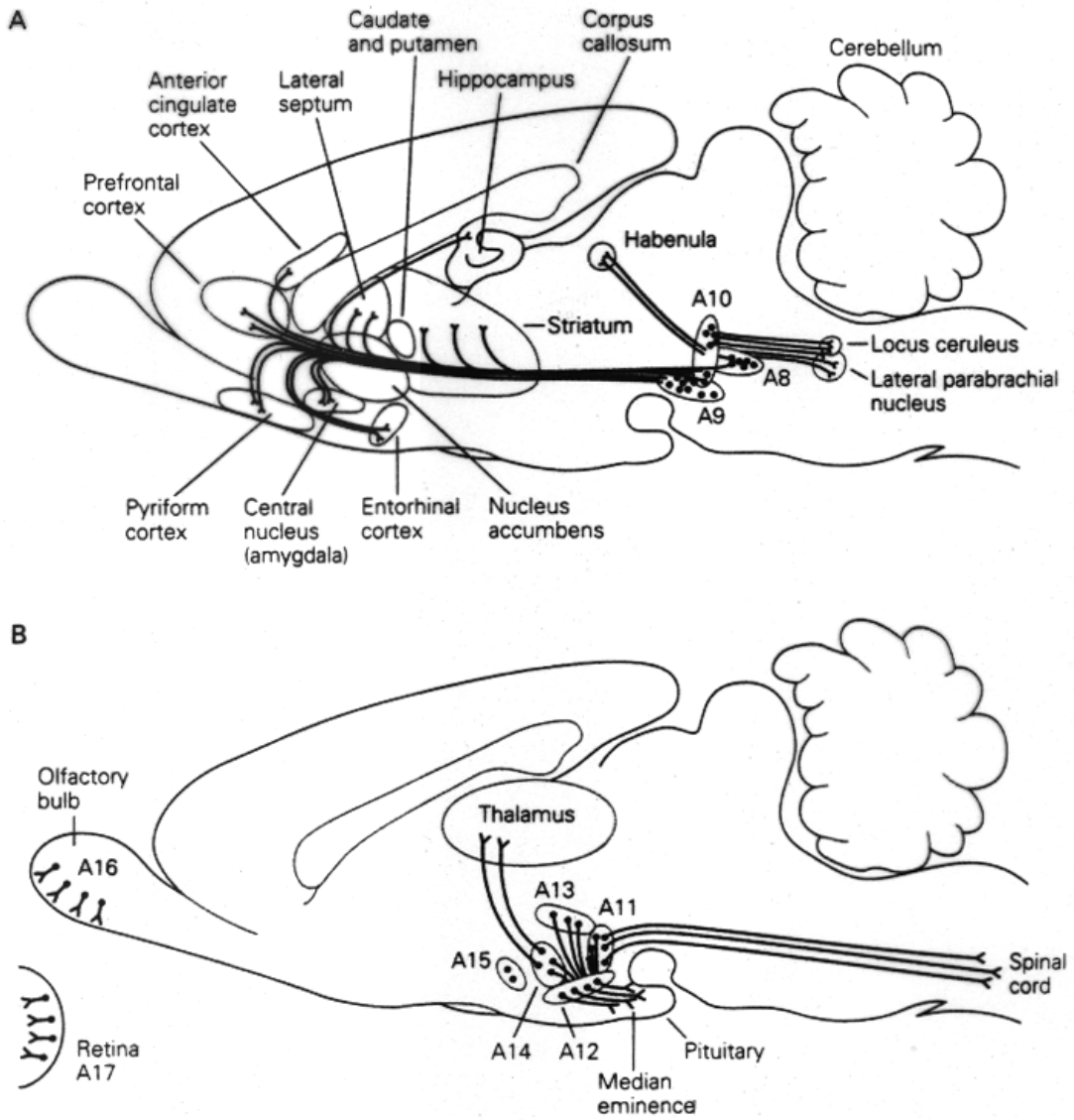

Activity of DA neurons relate to prediction of reward

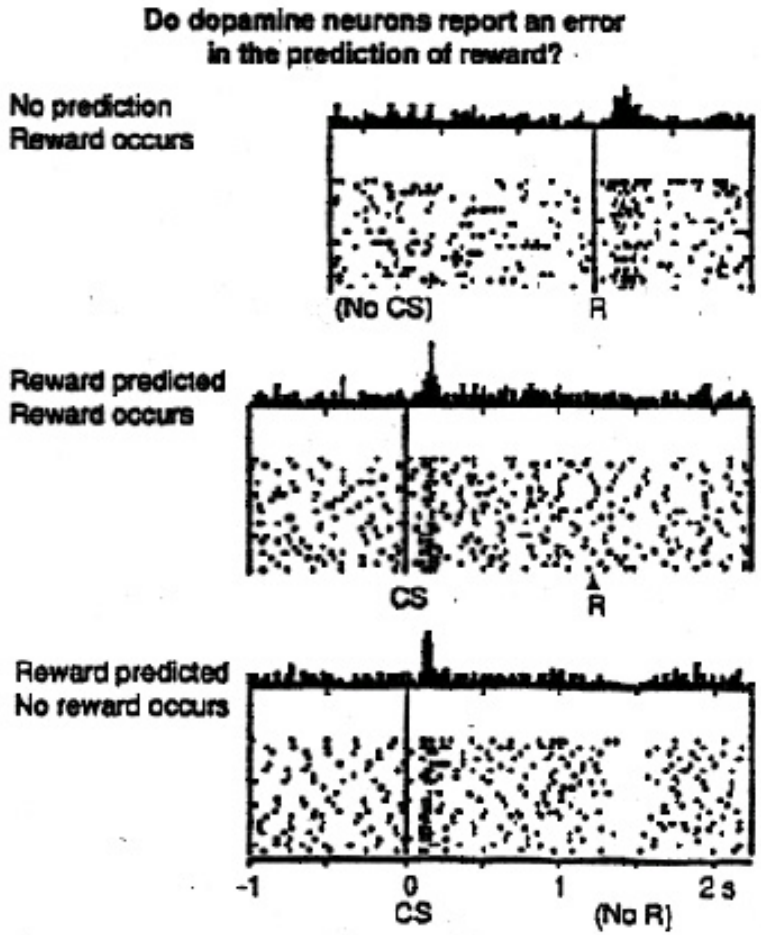

Fig. 1. Changes in dopamine neurons' output code for an error in the prediction of appetitive events. (**Top**) Before learning, a drop of appetitive fruit juice occurs in the absence of prediction—hence a positive error in the prediction of reward. The dopamine neuron is activated by this unpredicted occurrence of juice. (**Middle**) After learning, the conditioned stimulus predicts reward, and the reward occurs according to the prediction—hence no error in the prediction of reward. The dopamine neuron is activated by the reward-predicting stimulus but fails to be activated by the predicted reward (right). (**Bottom**) After learning, the conditioned stimulus predicts a reward, but the reward fails to occur because of a mistake in the behavioral response of the monkey. The activity of the dopamine neuron is depressed exactly at the time when the reward would have occurred. The depression occurs more than 1 s after the conditioned stimulus without any intervening stimuli, revealing an internal representation of the time of the predicted reward. Neuronal activity is aligned on the electronic pulse that drives the solenoid valve delivering the reward liquid (top) or the onset of the conditioned visual stimulus (middle and bottom). Each panel shows the peri-event time histogram and raster of impulses from the same neuron. Horizontal distances of dots correspond to real-time intervals. Each line of dots shows one trial. Original sequence of trials is plotted from top to bottom. CS, conditioned, reward-predicting stimulus; R, primary reward.

The mesopontine cholinergic nuclei

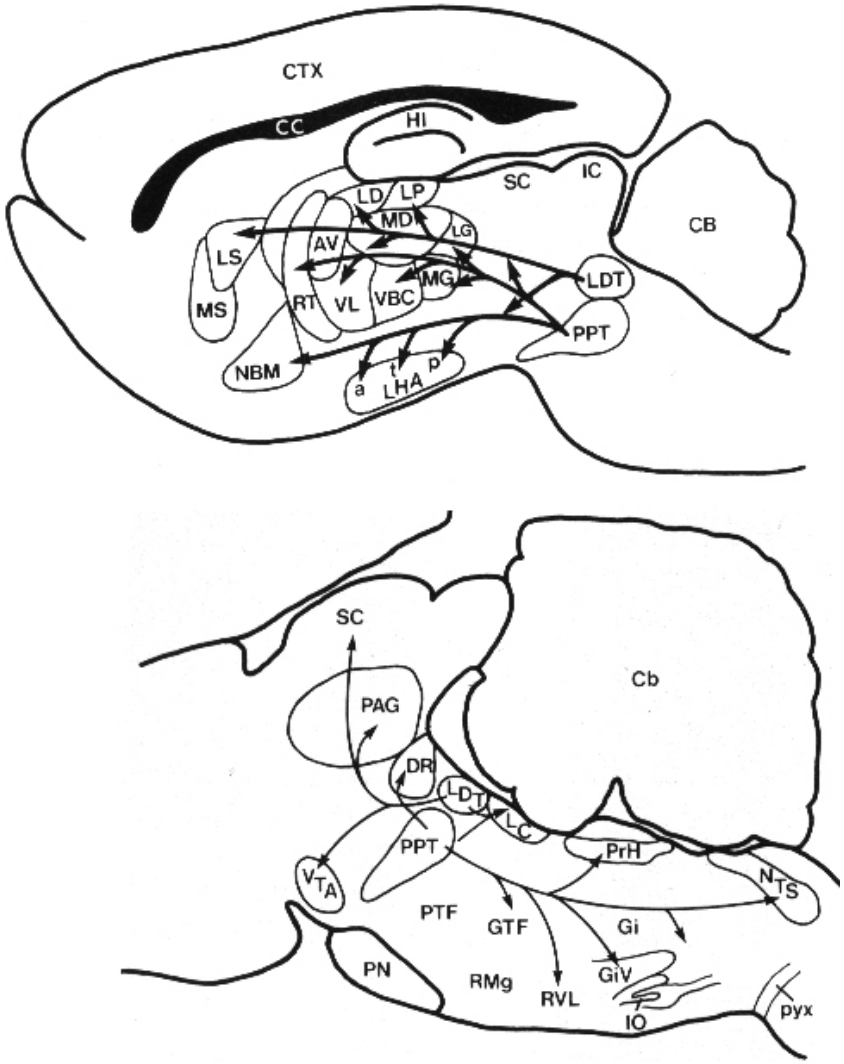

Summary of ascending and descending projections of the latero-dorsal (LTD) and pedunculo-pontine (PPT) tegmental nuclei. The most substantial ascending projections are to the thalamus, including relay and limbic nuclei. This pattern of thalamic innervation is in marked contrast to the surrounding tegmentum which innervates midline and intralaminar nuclei. The PPT also innervates the reticular (RT) nucleus, however, this nucleus also receive a substantial cholinergic innervation from the basal forebrain. A major target of the descending projection is the medial pontine reticular formation (Wainer et al., 1993).

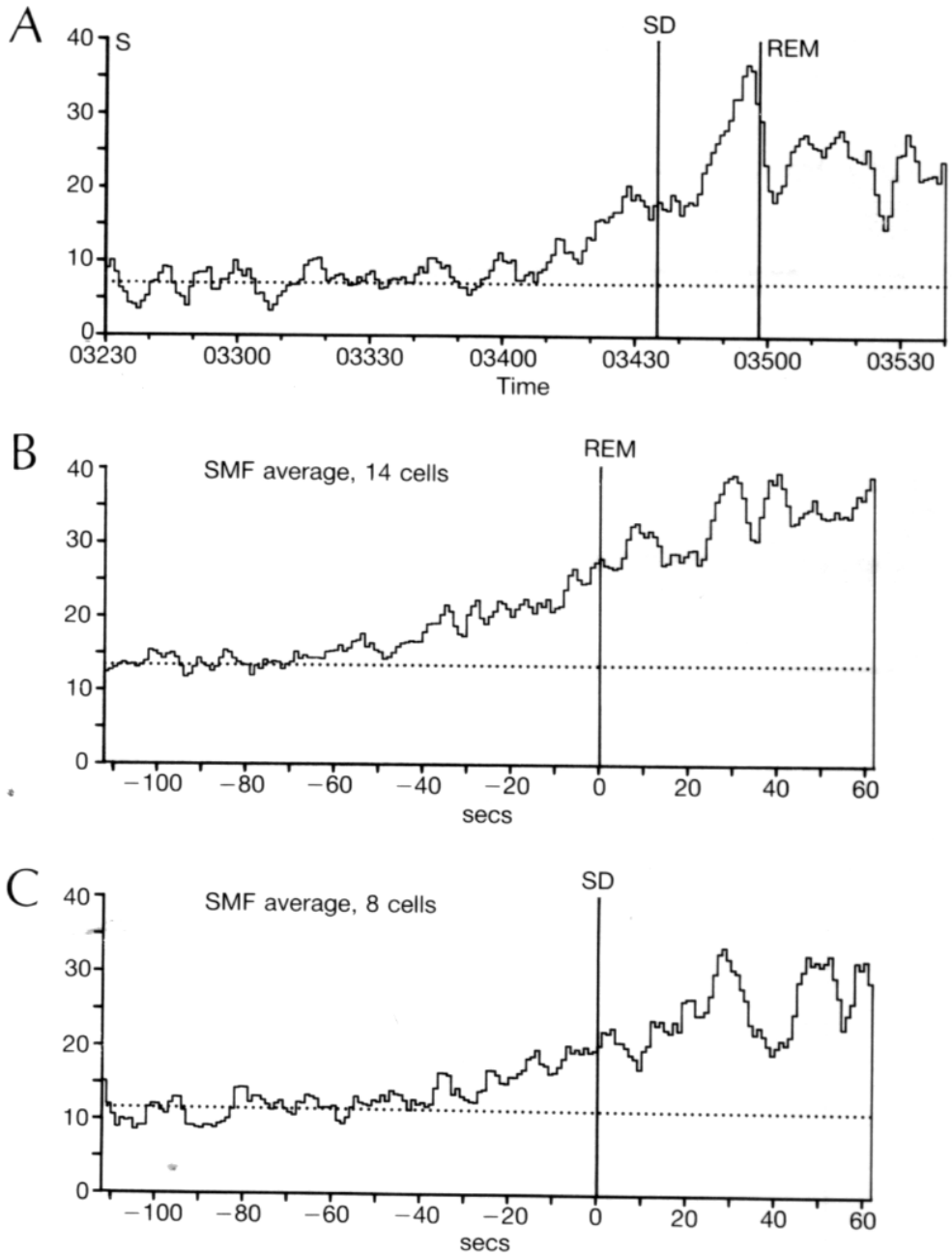

PPT neuron firing and EEG

Brainstem PPT neurons of cat increase firing rates in advance of EEG desynchronization during REM sleep.Sequential mean frequency (SMF) of one (A), 14 (B) and eight PPT (C) neurons.

S= synchronized sleep, SD= transitional epoch. Time 0 of SD epoch is the appearance of the first PGO wave. The spontaneous firing baseline in S is indicated by dotted line. (Steriade, Data, Oakson, Pare).

HYPOTHALAMO-CORTICOPETAL SYSTEMS

Histaminergic neurons in the postero-lateral hypothalamus

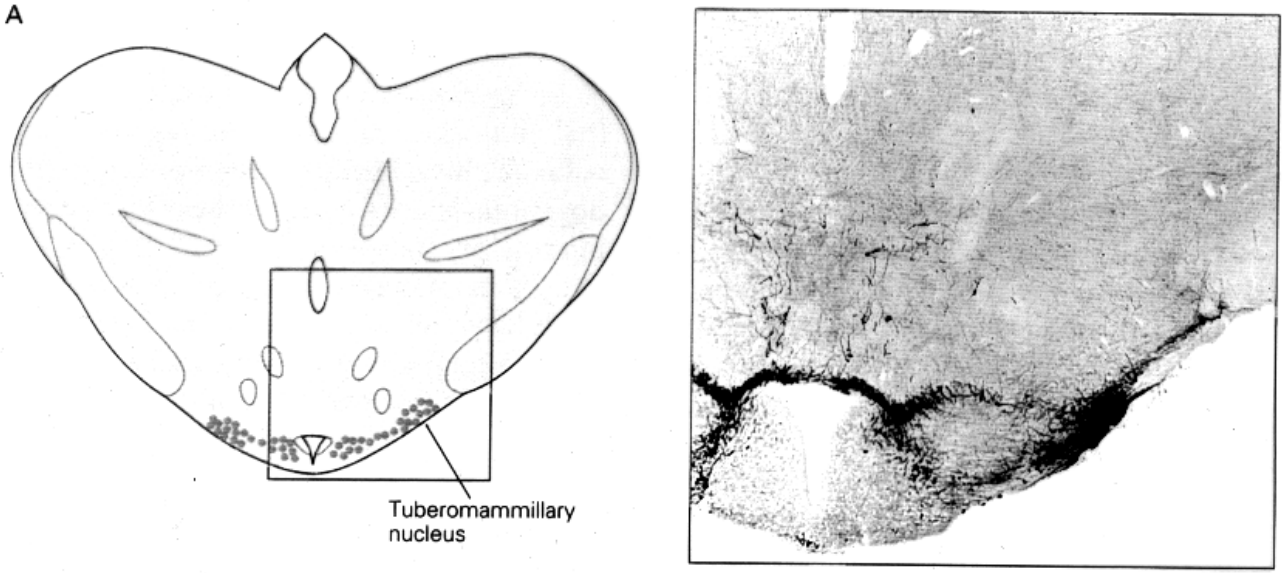

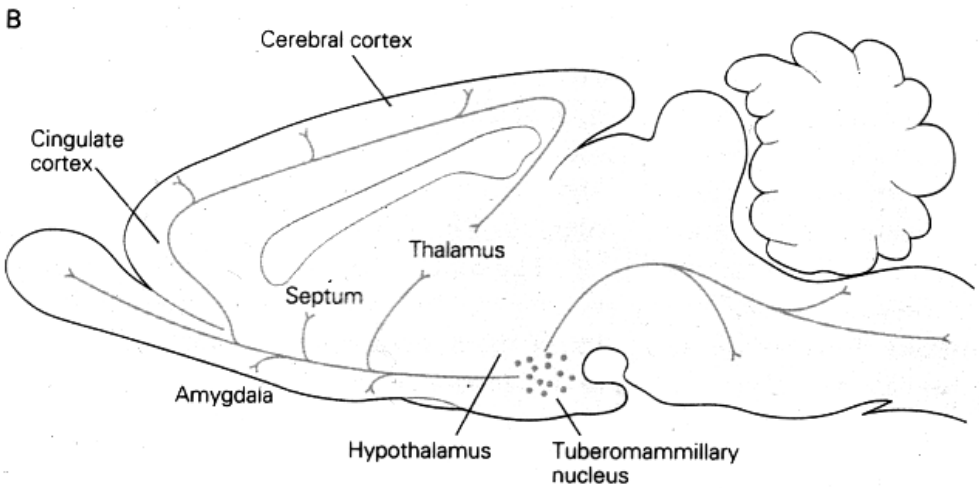

Histaminergic cells are clustered in the tuberomammilary nucleus in the posterior-lateral hypothalamus. The histaminergic neurons innervate the entire neuraxis, from the cerebral cortex to the spinal cord (From Saper, 2000)

Waking-related neuron in the post-lat. hypothalamus

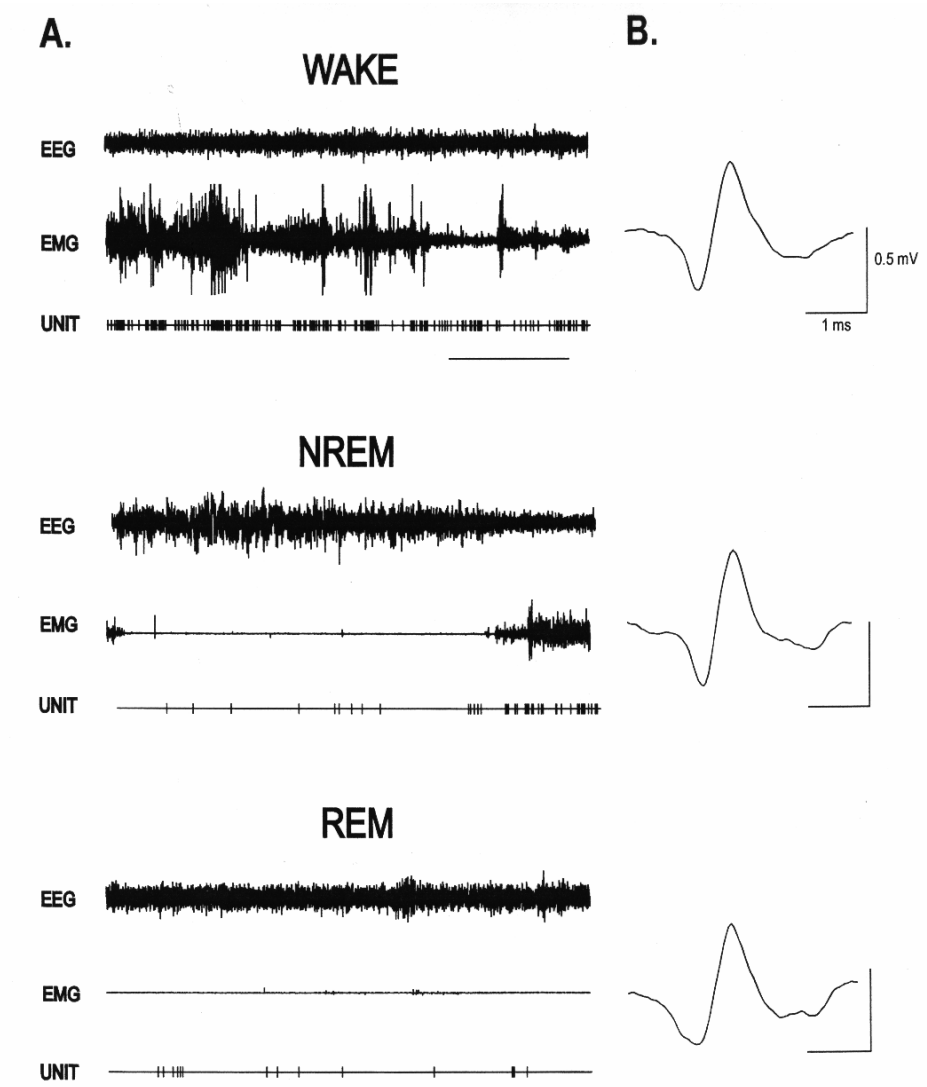

Waking-related neuron in the post-lat hypothalamus, in the area that is rich in histaminergic neurons. Unit firing in waking: 2.03 Hz, NREM: 0.15 Hz and REM sleep: 0.14 Hz. Note the resumption of firing coincident with the appearance of waking in the second trace. (From Steininger et al., 1999).

The orexin/hypocretin system of the lateral hypothalamus

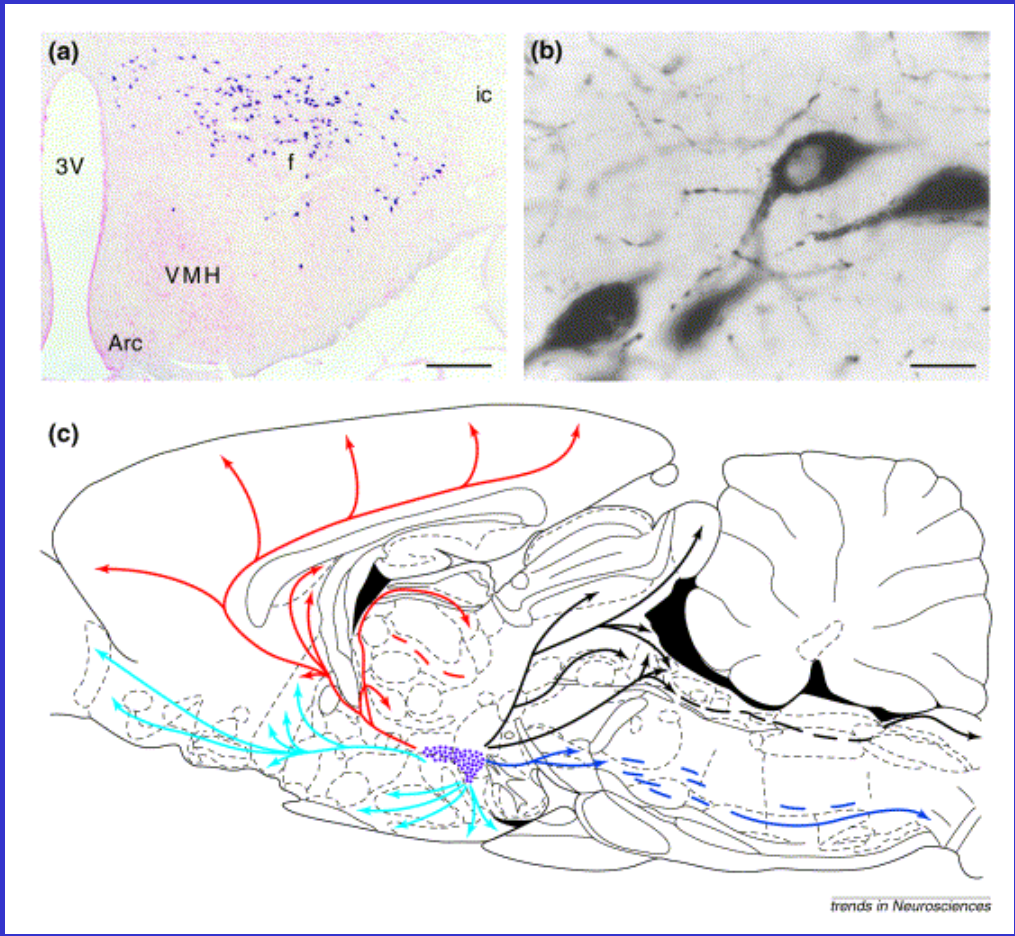

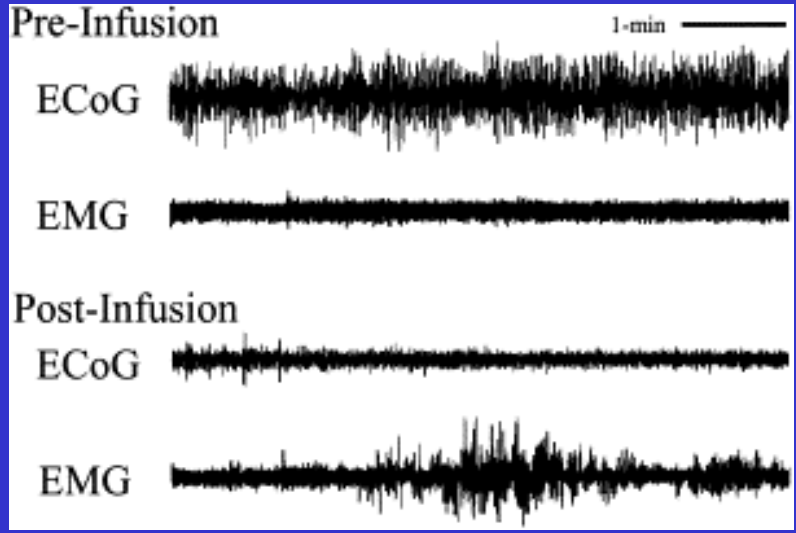

Effect of 0.7 nmol HCRT-1 infused into the lateral ventricle on ECoG and EMG activity. Immediately, prior to the infusion (pre-infusion), the animal spent the majority of time in slow-wave sleep. Following infusion, behavioral, ECoG and EMG indices of waking were observed. Note the decrease in large-amplitude, sSWS activity in ECoG and th eincrease in EMG activity post-infusion.

DISCHARGE OF OREXIN NEURONS ACROSS SLEEP-WAKE STATES

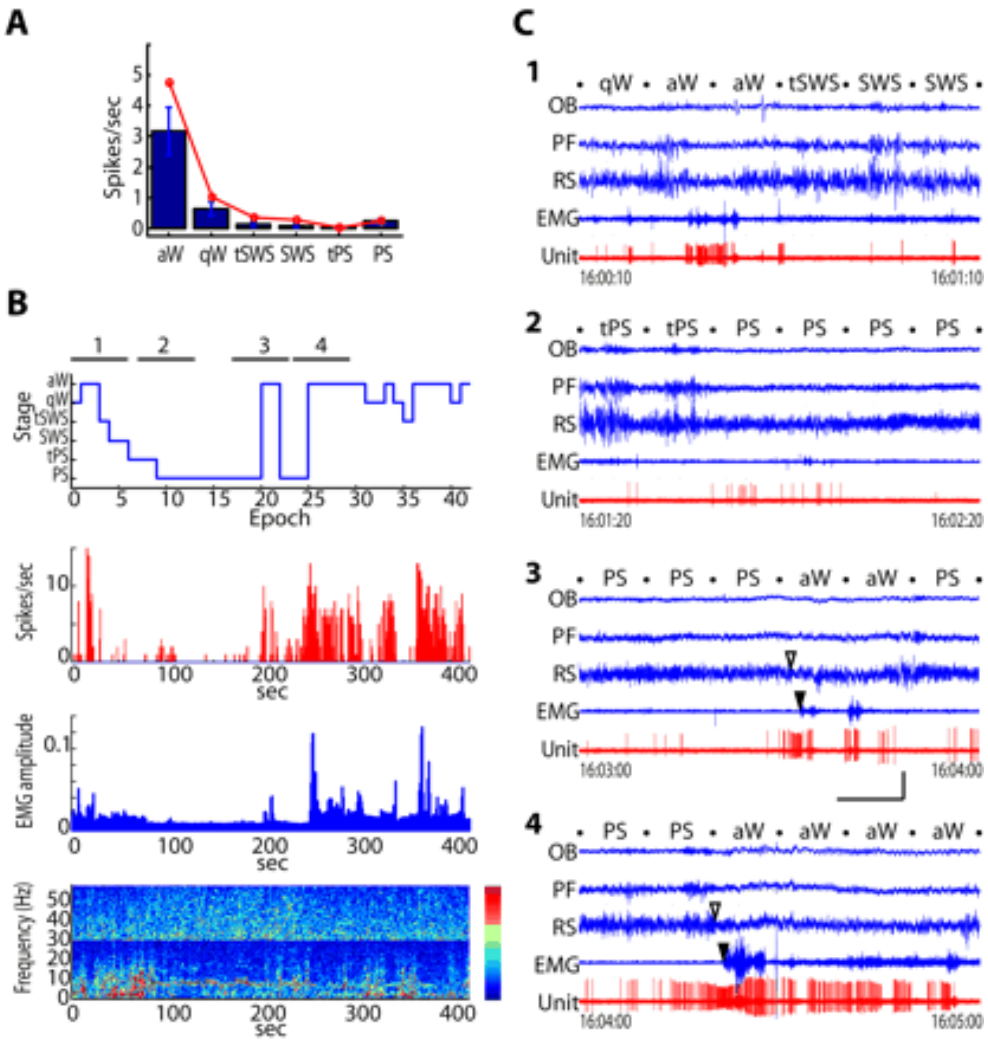

A, Bar graph showing mean spike rate that varied significantly as a function of sleep-wake stage across cells.The rate during aW was significantly higher than that during qW and all sleep stages, including PS. The line graph (in red) shows the discharge rate of the Nb+/Orx+ neuron (#c32u10) shown in ***B*** and ***C***.

B, Hypnogram, spike rate histogram, and EMG amplitude and EEG frequency spectra over the recording session (of 400 s corresponding to 40 10 s epochs).

C, Four 1 min segments (as indicated by time below) of unit, EEG, and EMG activity during state transitions: from qW through aW, tSWS to SWS (***1***), from tPS to PS (***2***), from PS through aW back to PS; (***3***), and from PS to aW (***4***)., Olfactory bulb; PF, prefrontal cortex; RS, retrosplenial cortex. From Lee et al., 2005

Hypocretin modulates LC firing

A

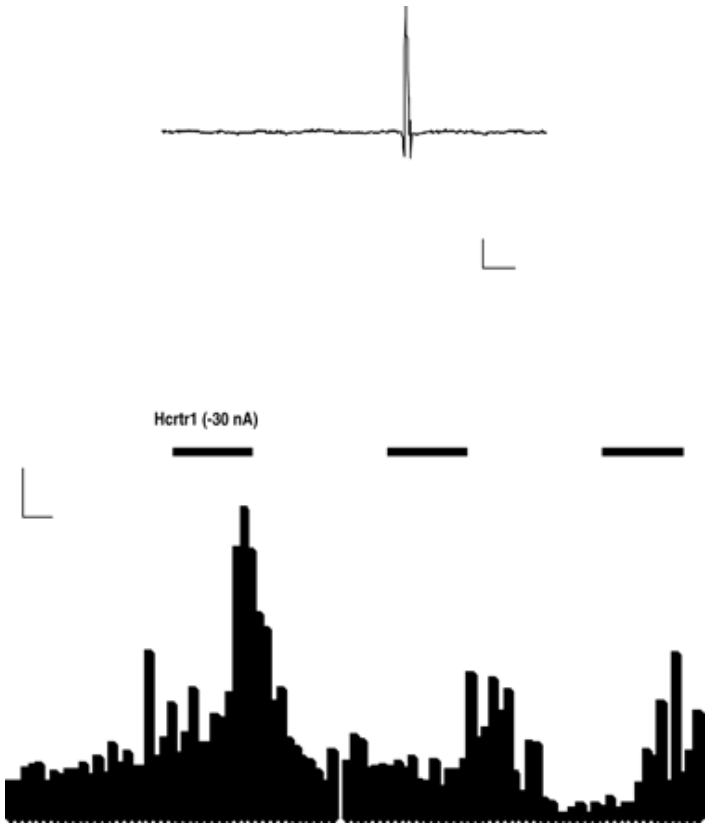

B

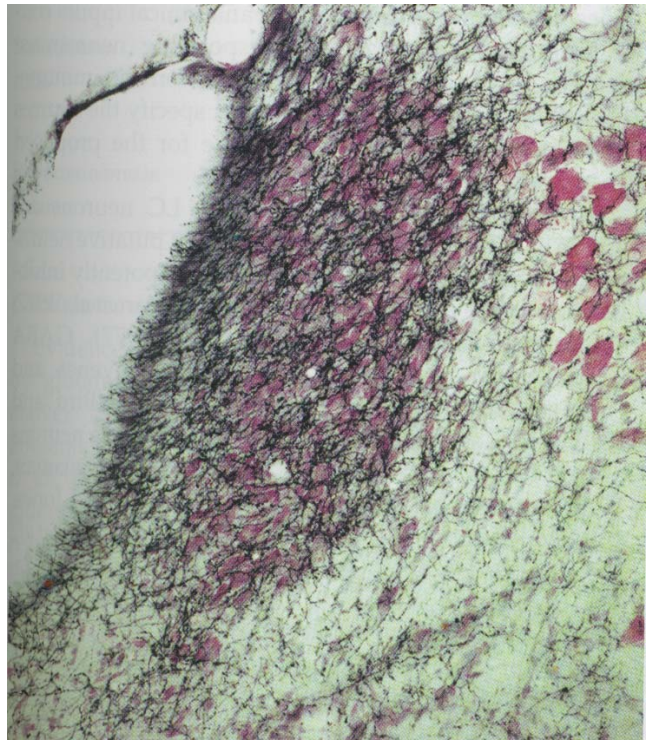

B: Hypocretin innervation of the LC (Aston-Jones, 2004)

A: Activation of hypocretin 1 receptors increases the firing rate of locus coeruleus neurons. *Bottom*, Rate meter record demonstrating that *in situ* microelectrophoretic application of hypocretin 1 (1 mg/ml) produced a marked activation of a spontaneously active LC neuron. Calibration: 5 Hz, 5 sec. (Bourgin et al., 2000).

Ascending modulatory systems so far

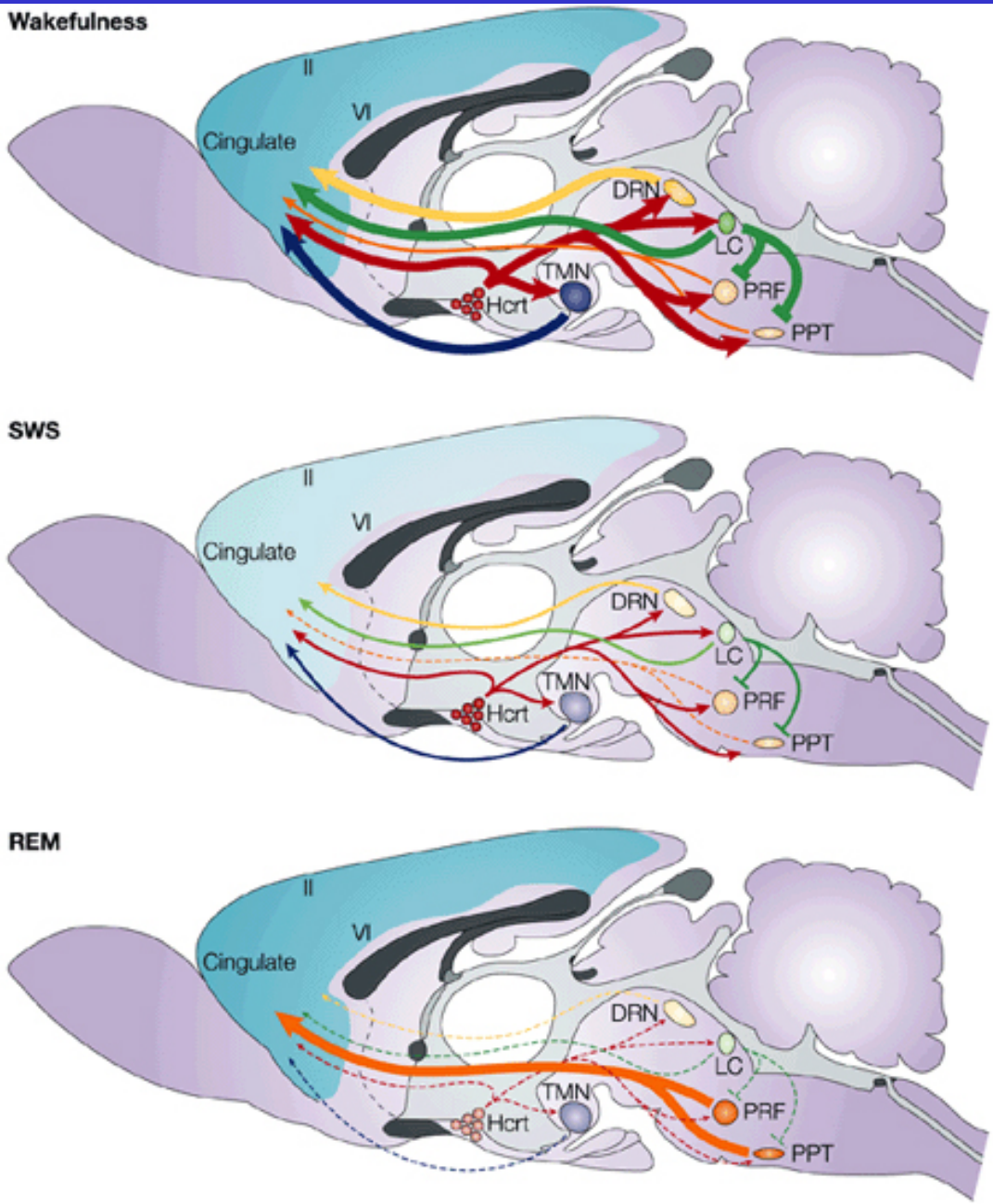

DRN-5HT (yellow)

LC-NE (green)

PPT-Ach (orange)

TMN-His

Hcrt/Orexin (red)

Sutcliffe and De Lecea, 2002;

THE BASAL FOREBRAIN CORTICOPETAL SYSTEM

DISTRIBUTION OF CHOLINERGIC CORTICOPETAL NEURONS IN RAT

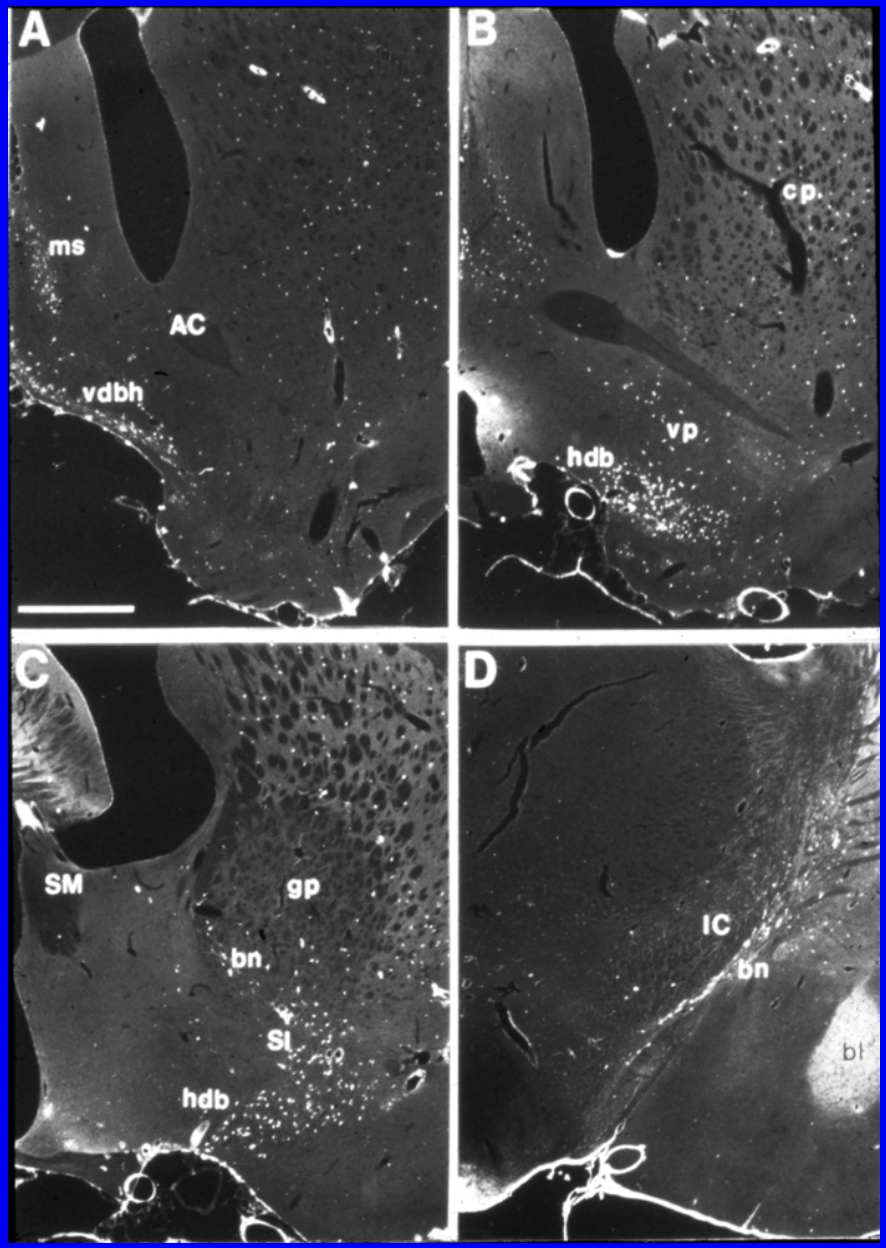

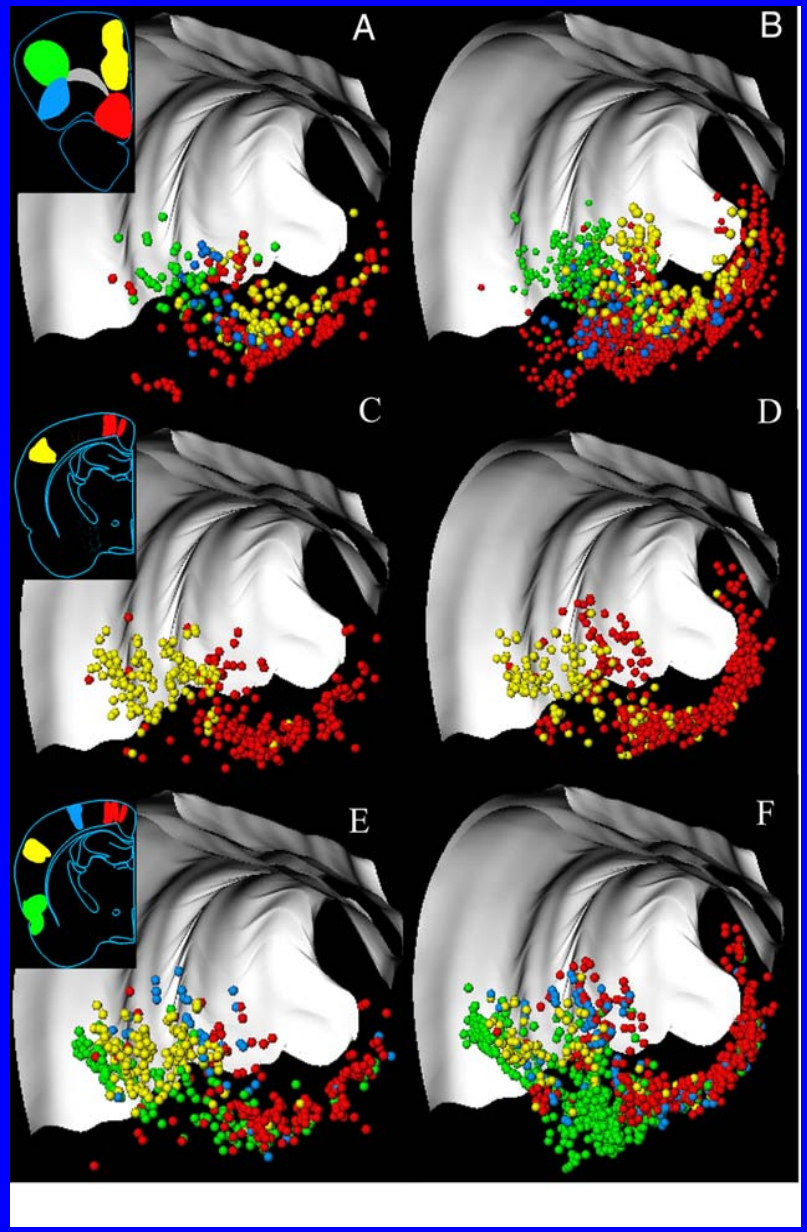

Basal forebrain cholinergic neurons in human

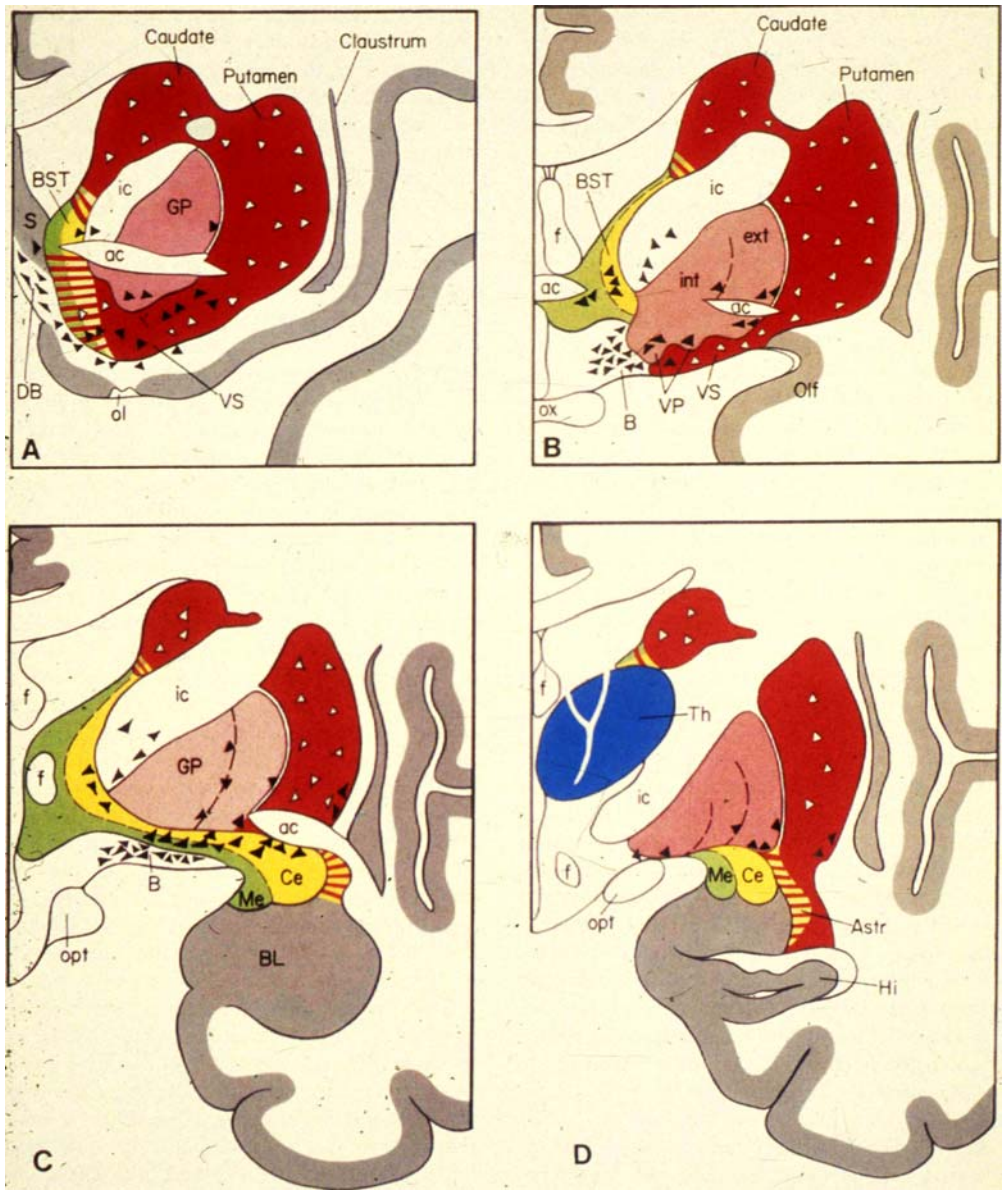

ACHE cell staining (Saper)

ChAT terminals (Mesulam)

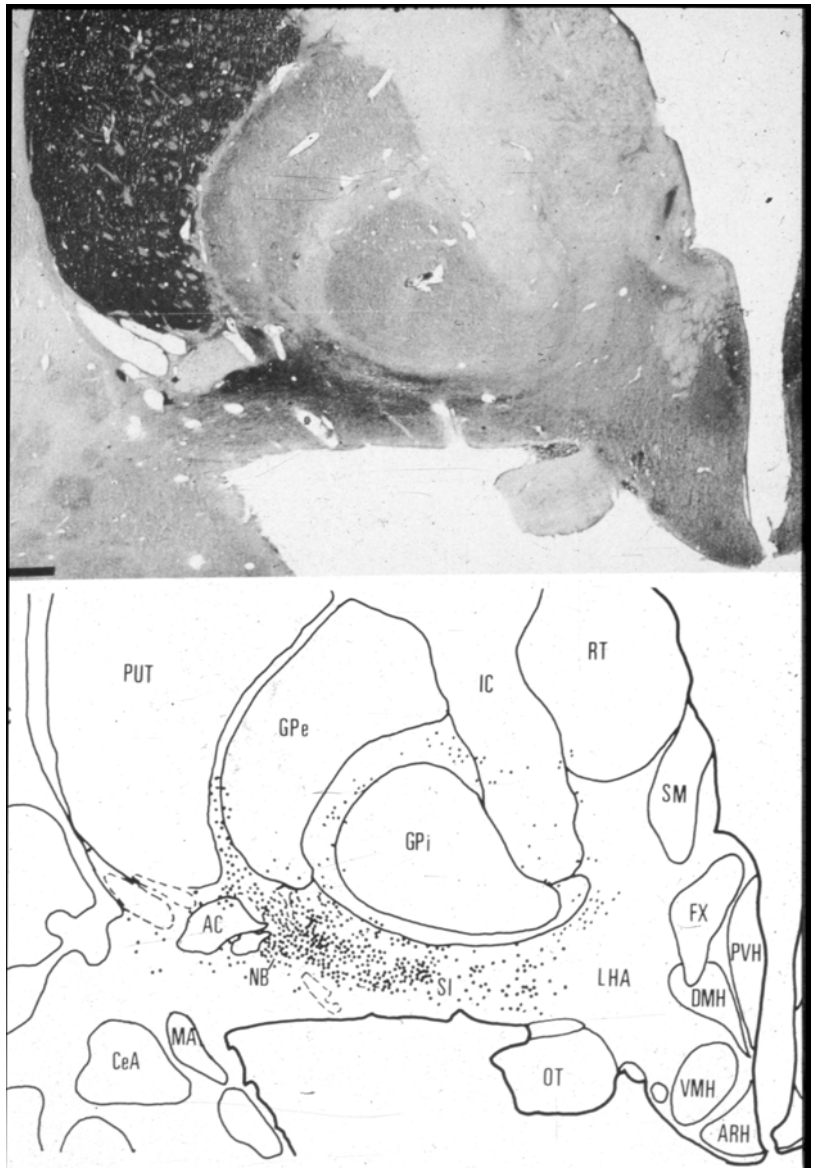

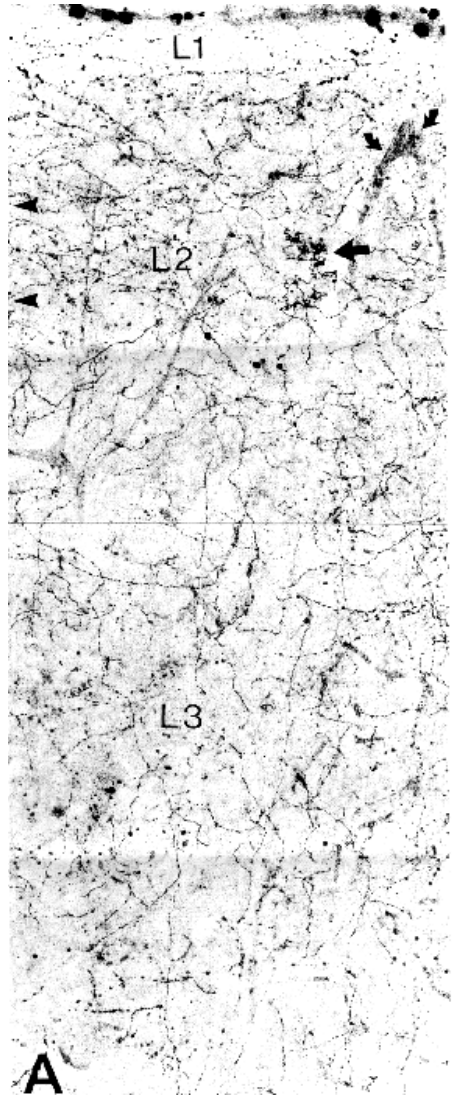

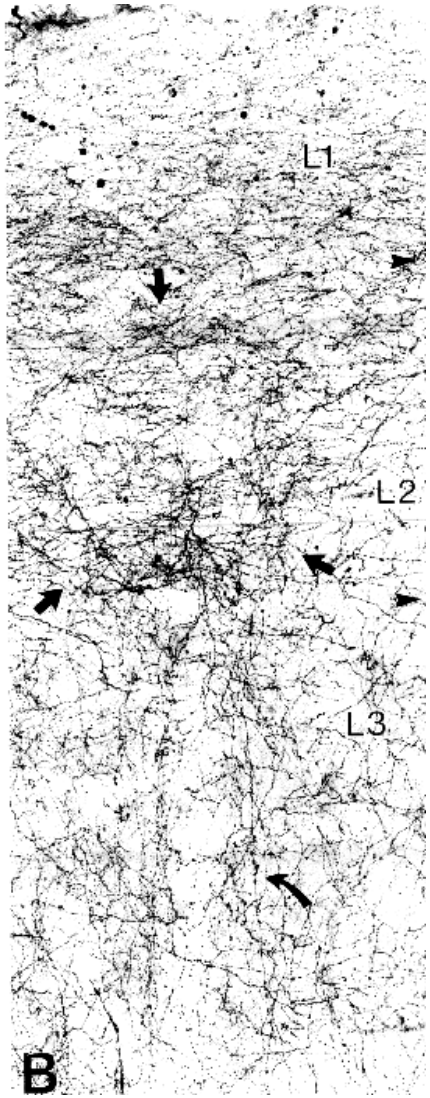

Basal forebrain cholinergic system in human

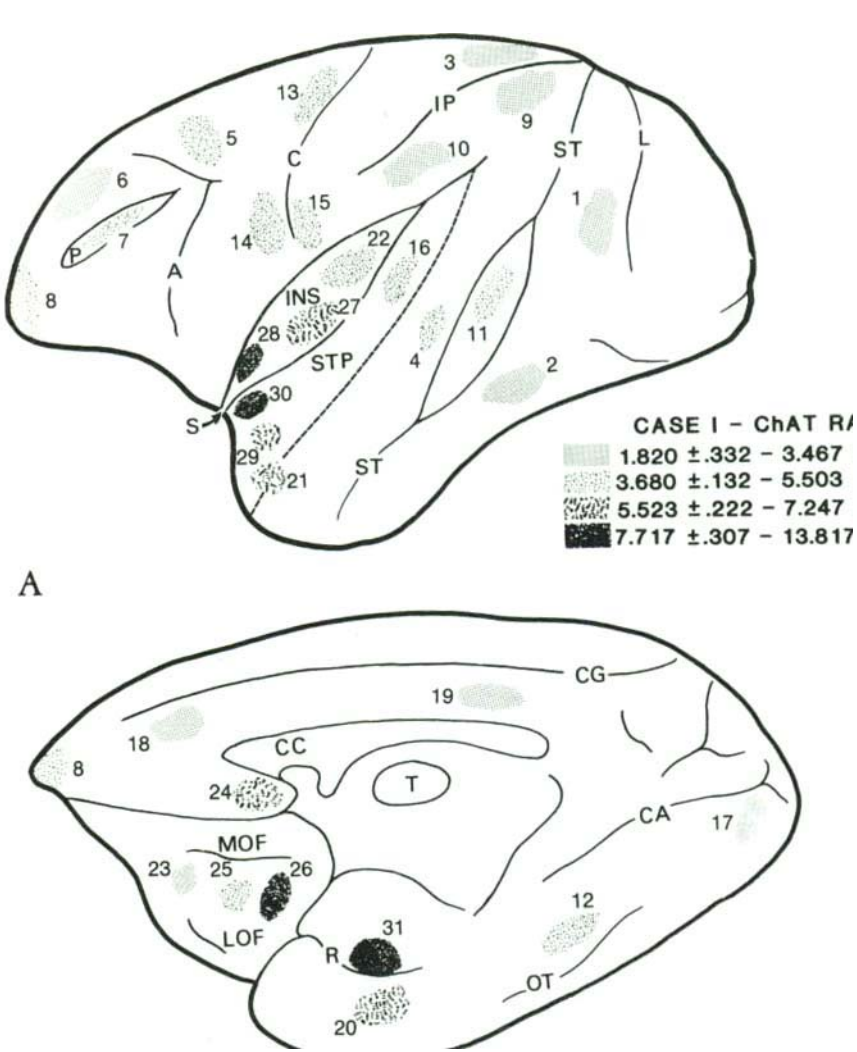

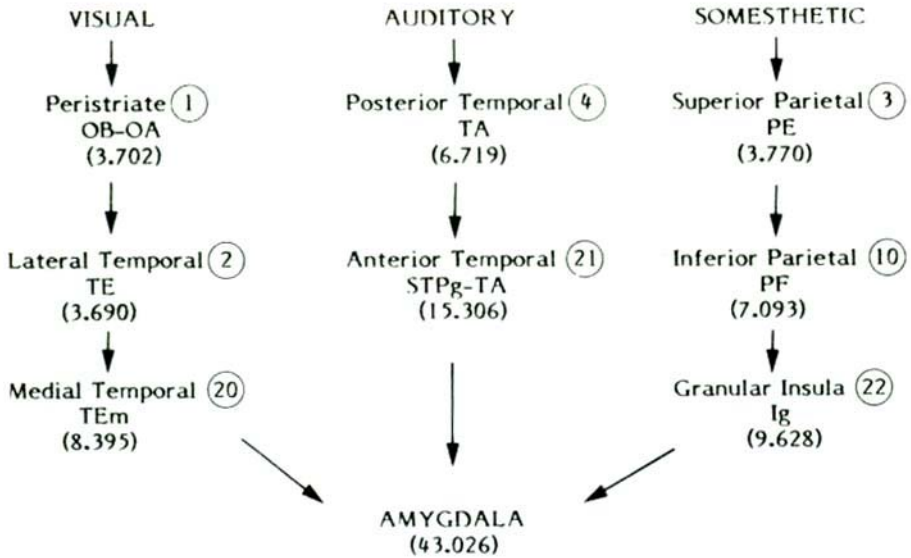

Regional Chat activities in rhesus monkey (Mesulam et al., 1986)

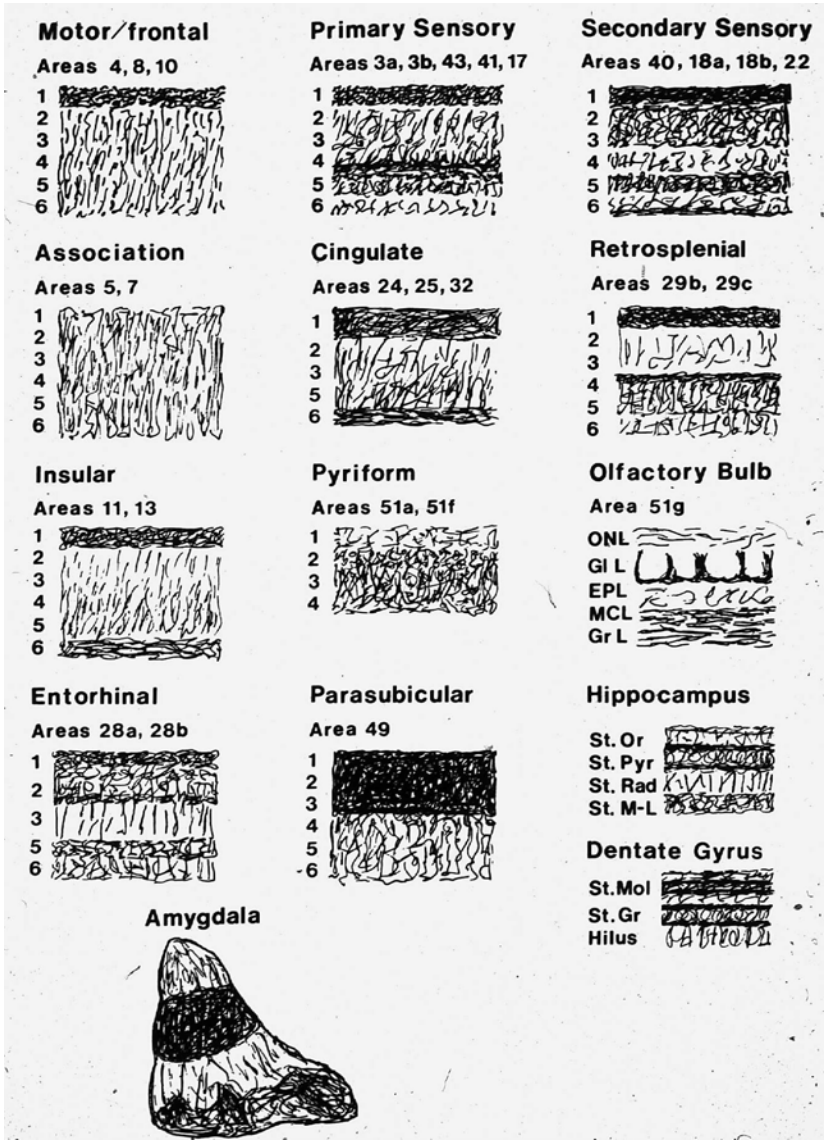

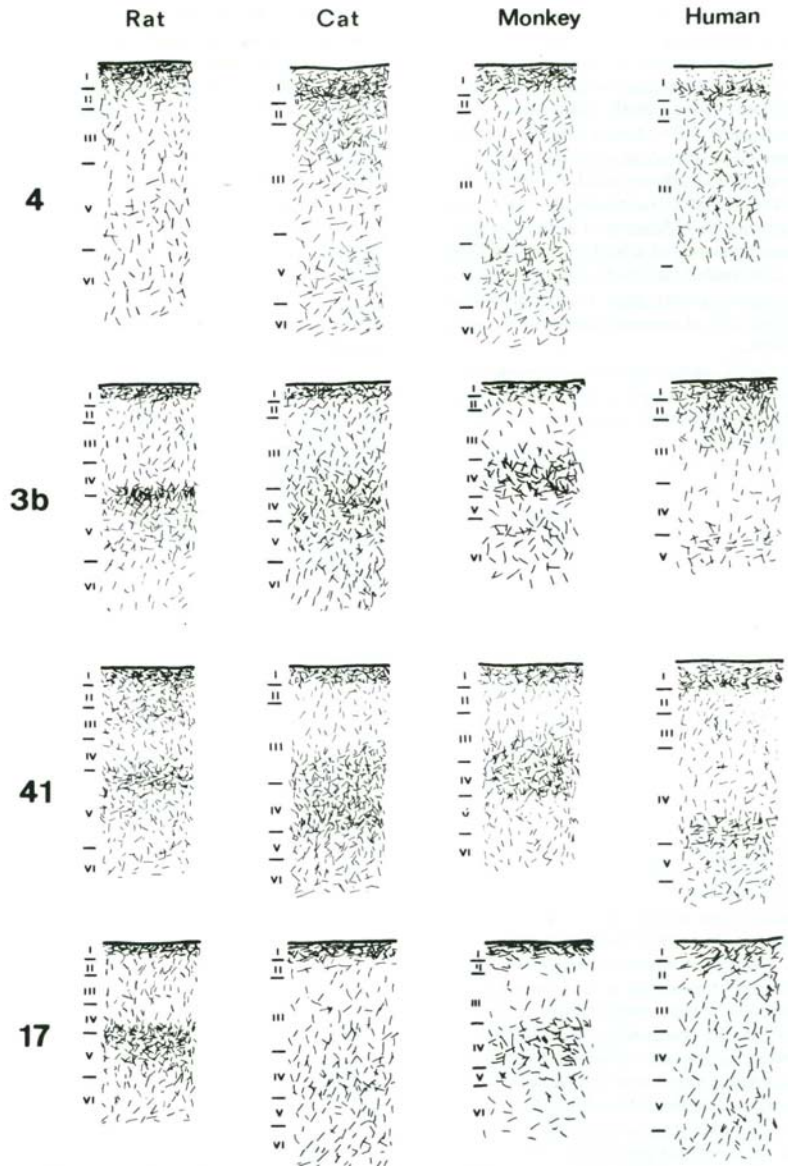

Cholinergic innervation in rat (Lysakowski et al., 1988)

Comparing the ACh innervation of motor (4) and sensory regions of the rat, cat, monkey and human). From Avendano et al.,1996

BF stimulation, EEG I.

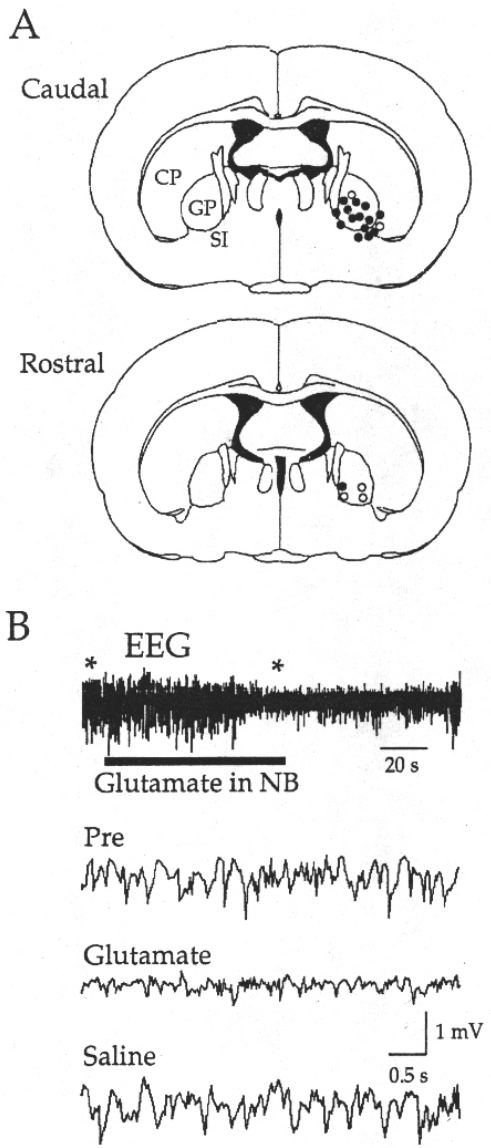

A, Effective (*solid circles*) and ineffective (*open circles*) stimulation sites for eliciting EEG activation in 20 consecutive experiments. Caudal stimulation sites (mean rostrocaudal distance from the anterior commissure, 0.77 mm; range, 0.54–1.04 mm) were more effective (87.5 %; $n = 14$ of 16), whereas rostral stimulation sites (mean distance, 0.28 mm; range, 0.08–0.46 mm) were less effective (25%; $n = 1$ of 4). Effective stimulation sites lay in middle and ventral aspects of the caudal globus pallidus (GP) and substantia innominata (SI), source of the NB cholinergic projection to auditory cortex (Wenk et al., 1980; Saper, 1984). Atlas sections modified from Paxinos and Watson (1986). CP, caudate putamen. *B*, Glutamate (180 nmol in saline), delivered via a 30 gauge cannula attached to the stimulating electrode, desynchronized the EEG for >1 min (recovery can be seen at *end of trace*). Portions of the EEG before and during glutamate-induced desynchronization are marked by *asterisks* and shown below at higher resolution. Subsequent saline infusion of equal volume was without effect.

METHERATE and ASHE, 1992

BF stimulation, EEG II

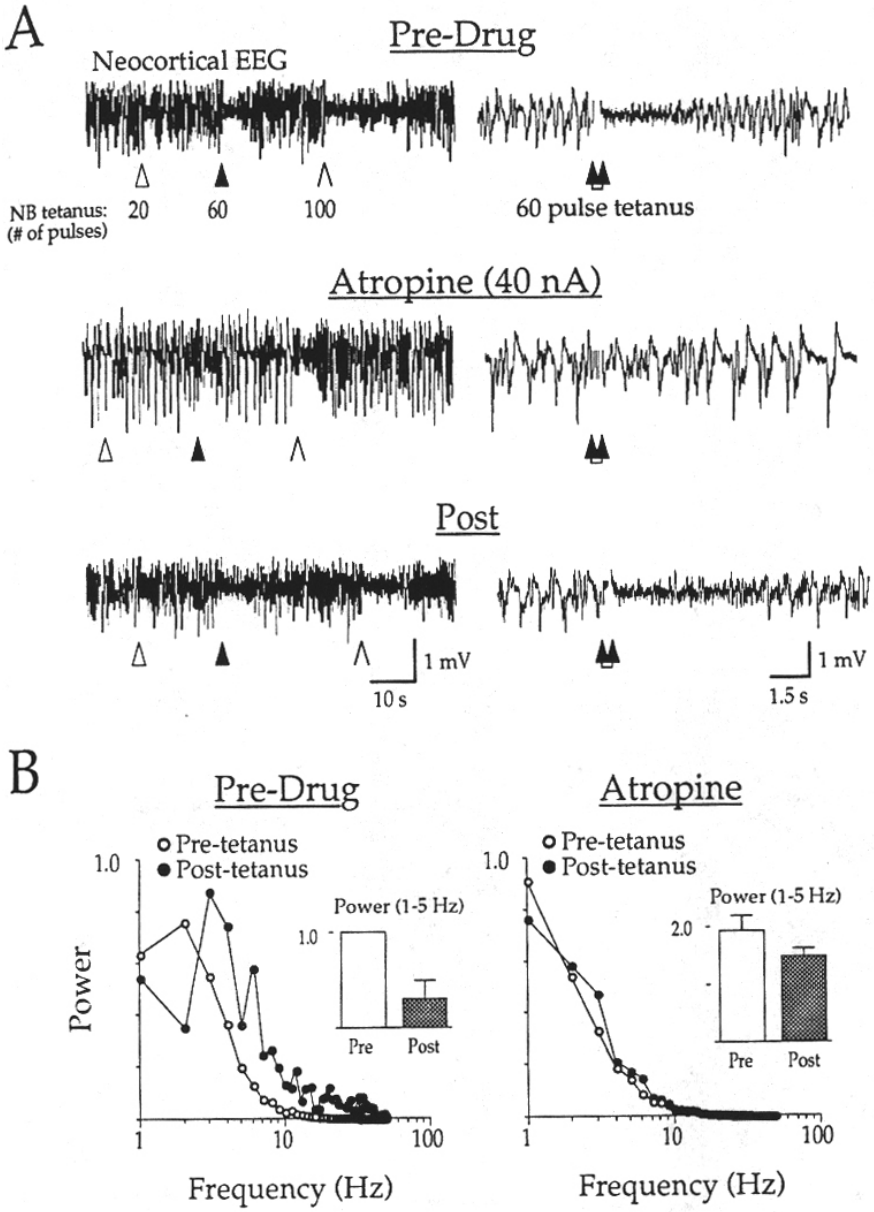

Metherate and Ashe, 1992

NB stimulation *in vivo* elicited EEG activation mediated by cortical muscarinic receptors. *A*, NB tetani (200/sec, 500 μA) of increasing number of pulses (*arrowheads*) elicited correspondingly longer durations of EEG desynchronization. Effect of 60 pulse tetanus is shown at faster speed to the *right* (duration of tetanus indicated by *arrows*; artifacts are blanked). Atropine, administered iontophoretically (40 nA) within auditory cortex, enhanced synchronous oscillations and antagonized the effect of NB stimulation. Increasing stimulus intensity (e.g., 100 pulse stimulus) partly overcame the atropine blockade. Recovery was seen at about 1 hr (*Post*). *B*, Averaged (n = 5) frequency power spectra show that NB stimulation resulted in increased high-frequency components (*Pre-drug* spectra; individual functions contributing to each average were normalized to the peak power under that condition, i.e., pre- or posttetanus). NB stimulation also produced decreased power in the 1–5 Hz range (histogram in *inset*; power normalized to pretetanus value for each experiment). Atropine antagonized the effect of NB stimulation on EEG frequency components and power in the 1–5 Hz range. Note that the increased EEG amplitude and synchrony under atropine (seen in *A*) resulted in increased power in the 1–5 Hz range relative to control (note change in histogram scale). Data are from five experiments in which (1) atropine was administered within the cortex (either iontophoretically or directly to the cortical surface), and (2) NB-mediated EEG desynchronization endured for longer than 2 sec (to allow for adequate digital sampling).

Correlation of EEG and ACh output II

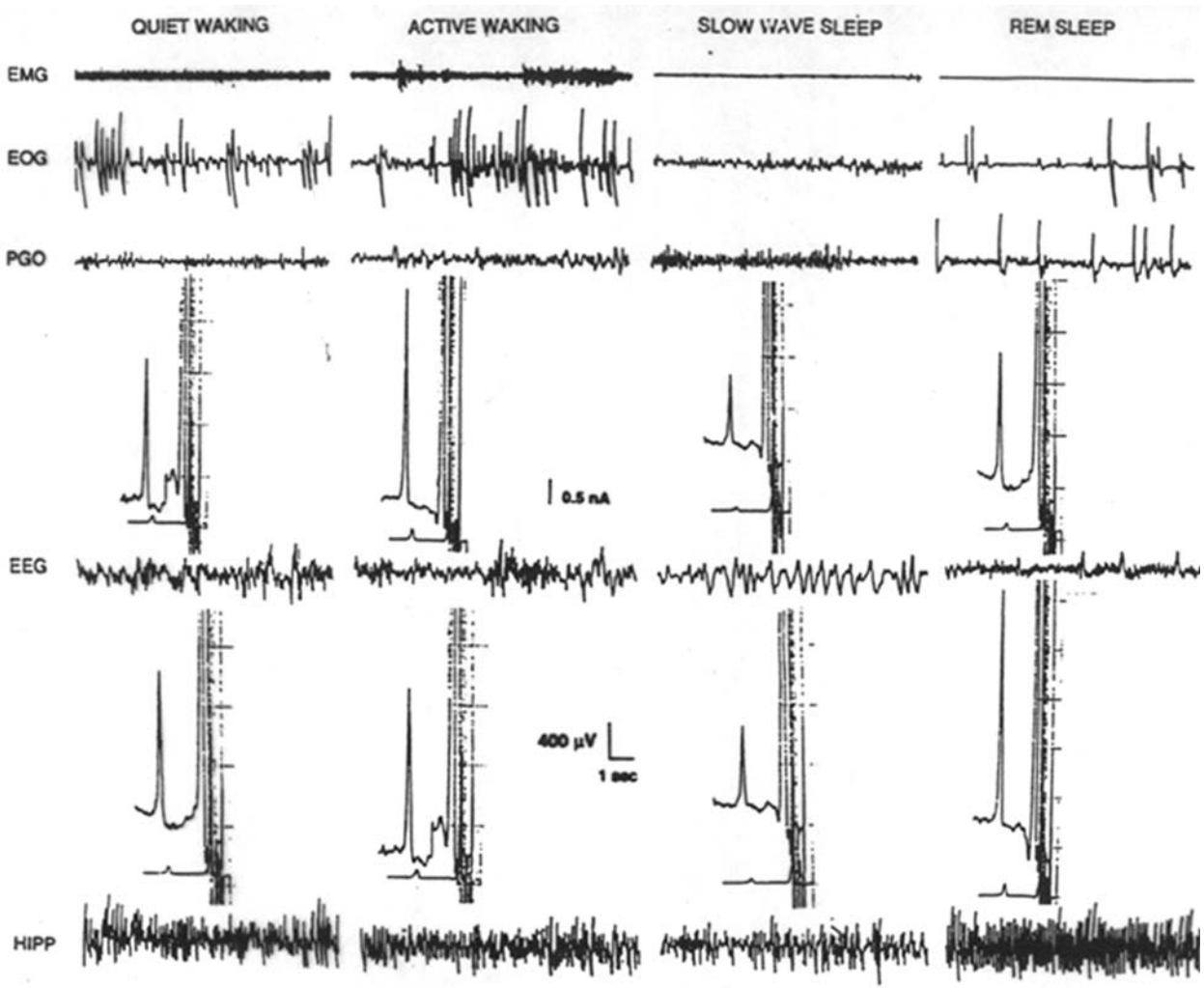

Correlation of EEG and ACh output in cortex and hippocampus in freely-moving cat (Marrosu et al., 1995)

BF stimulation or cortical ACh application enhances sensory evoked responses: Is this part of an arousal reaction or a more selective process (attention)?

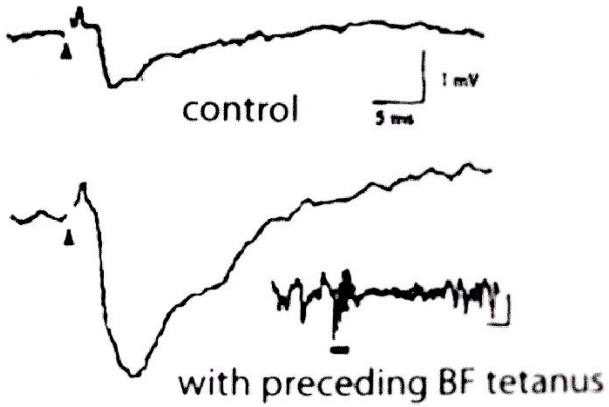

Auditory cortical response to medial geniculate stimulus is modified by preceding (30 msec) basal forebrain stimulation. (Metherate and Ashe, 1991

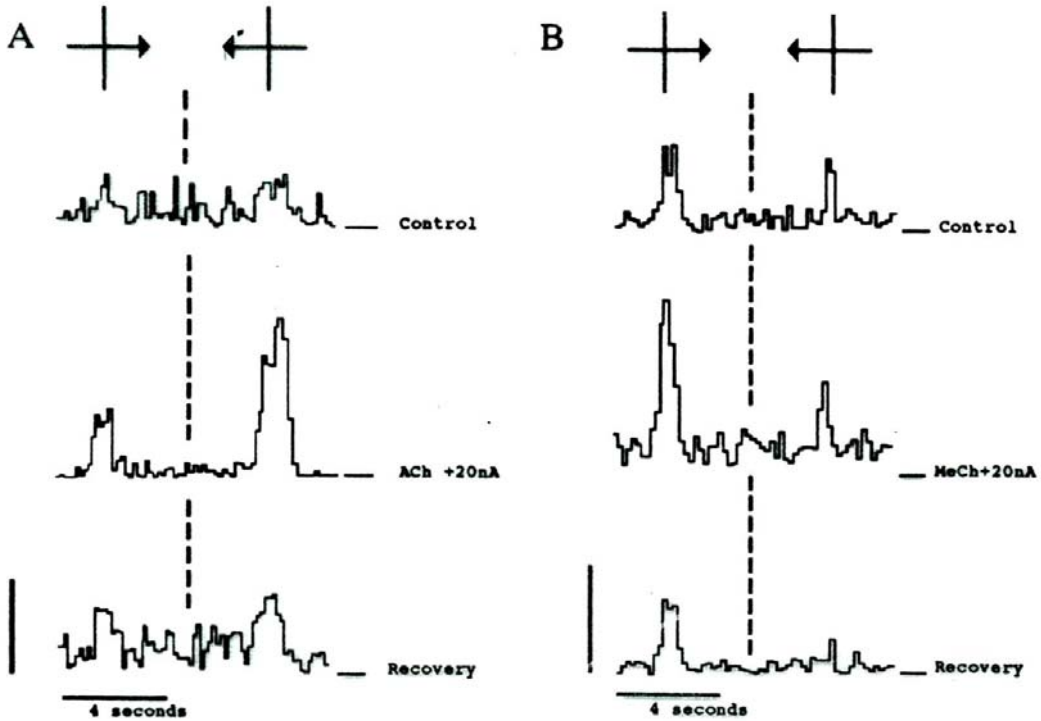

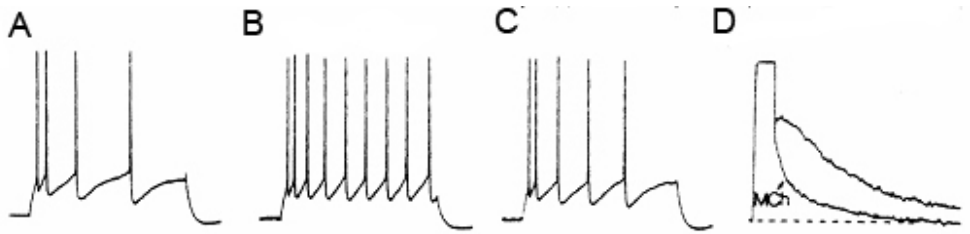

Effect of cholinergic facilitation on the direction selectivity of a LIV simple cell (A) and a LVI complex cell (B). PSTH showing the response of the cells to an optimally oriented bar of light moving forwards and backwards over the receptive field. (Silito, 1993)

BF stimulations elicit heterogeneous cortical MUA responses

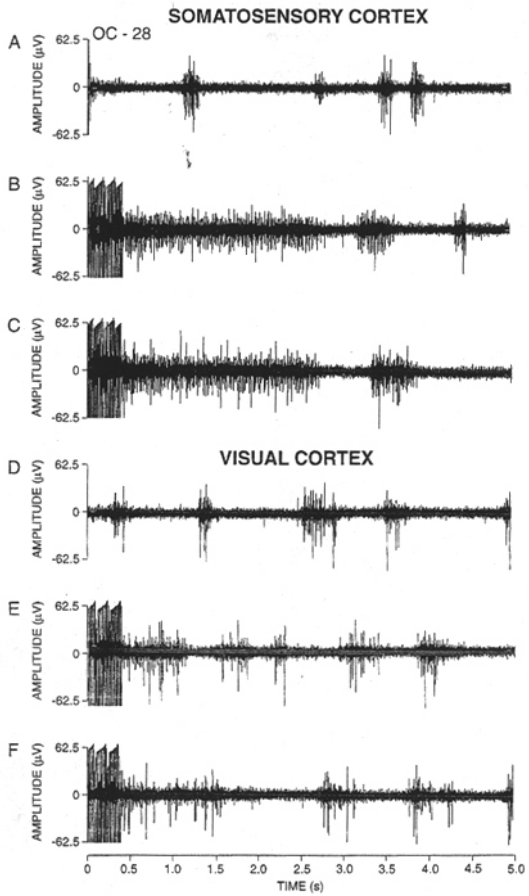

An example of the effects of BF stimulation on the cerebral cortex elicited from a region of the BF that produced increased ACh release from somatosensory cortex. **A:** Spontaneous activity. **B:** Effect of a 400-ms train of pulses at 100 Hz in the BF. **C:** A second example of the response in the somatosensory cortex. **D:** Spontaneous activity in the visual cortex. **E:** The effect of BF stimulation in the visual cortex from the same site that produced the record in (B). **F:** A second example of the response to BF stimulation in the visual cortex. The release of ACh from the visual cortex was much less than from the somatosensory cortex.

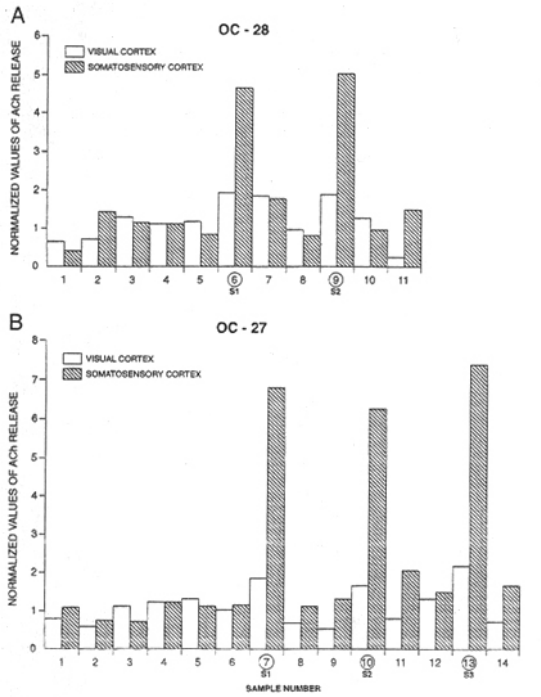

ACh release from sites in the visual and the somatosensory cortex following electrophysiological recordings of the neuronal activity provoked by BF stimulation. **A:** Eleven pairs of 30-minute samples obtained simultaneously from the somatosensory and the visual cortex. The first five pairs provided the baseline levels for both cortical regions. During collection of the sixth pair of samples the BF was stimulated every 4 seconds with a train of 40 pulses at 100 Hz. ACh release increased more in the somatosensory cortex than in the visual cortex. ACh levels returned to normal over the next hour, and the stimulation was repeated during the ninth sampling period. **B:** A second experiment showing the same pattern of differential ACh release following BF stimulation. In this experiment the BF stimulation was performed three times using a train of 50 pulses every 4 seconds for the duration of the 30-minute sampling period (sample pairs 7, 10, and 13). A slight, but significant, increase in ACh occurred in the visual cortex, whereas a 600–700% increase occurred in the somatosensory cortex.

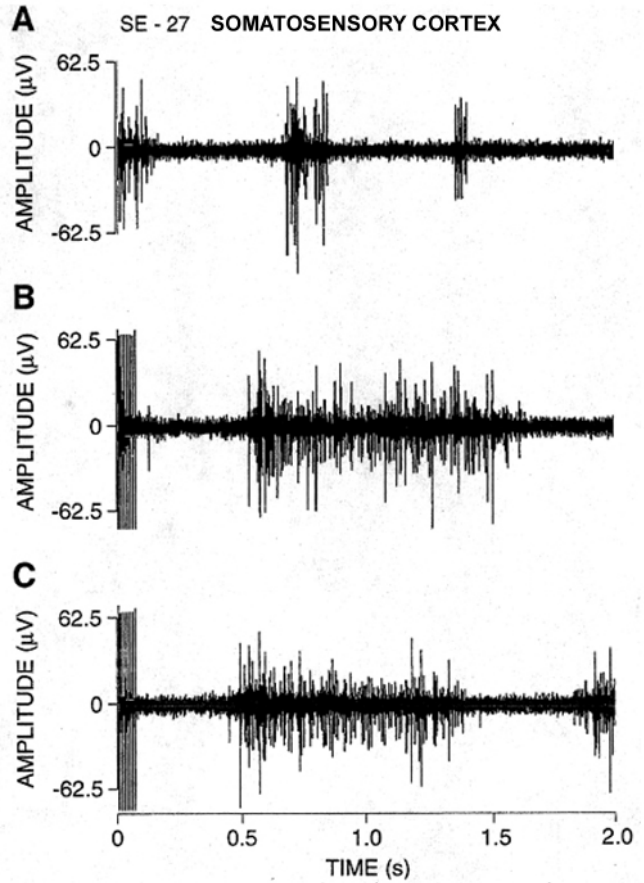

Multiunit recordings from the hindlimb somatosensory cortex showing how BF stimulation could provoke a long suppression of spontaneous activity followed by a large and long increase in neural activity. The several large neurons in this recording were spontaneously active. **A:** A 2-second record of spontaneously active neurons discharging in bursts. **B:** When a 100-ms BF stimulus was administered, all neural activity stopped for about 450 ms after the end of the stimulus; then an intense discharge occurred, lasting for approximately 1.1 second. **C:** A second example of the inhibitory pause produced by BF stimulation.

Dykes et al, 1997

BF neurons are electrophsyiologically heterogeneous

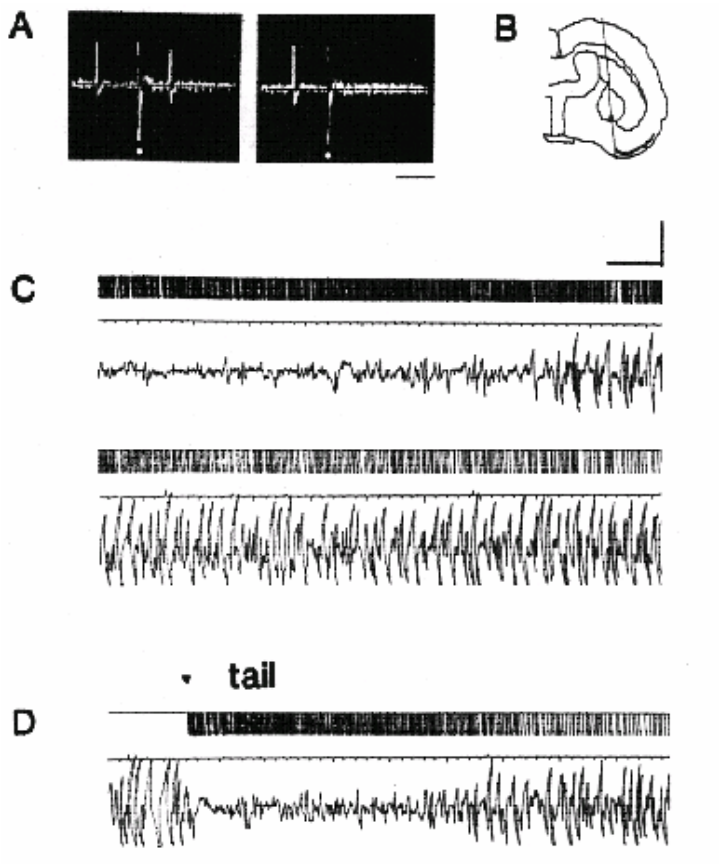

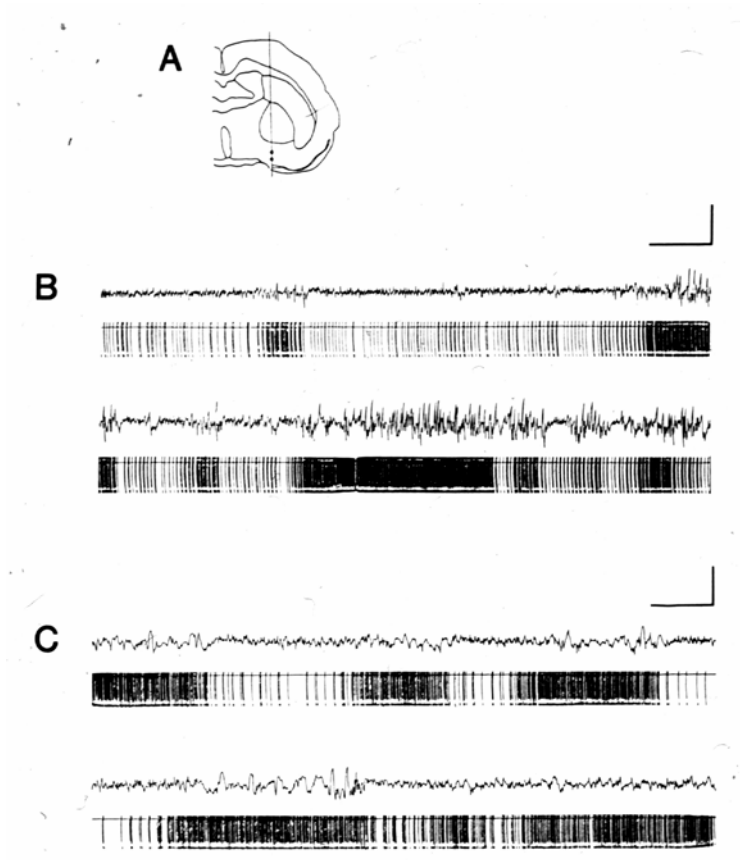

Detari et al., 1987

Basal forebrain corticopetal cholinergic neurons are intermingled with non-cholinergic neurons

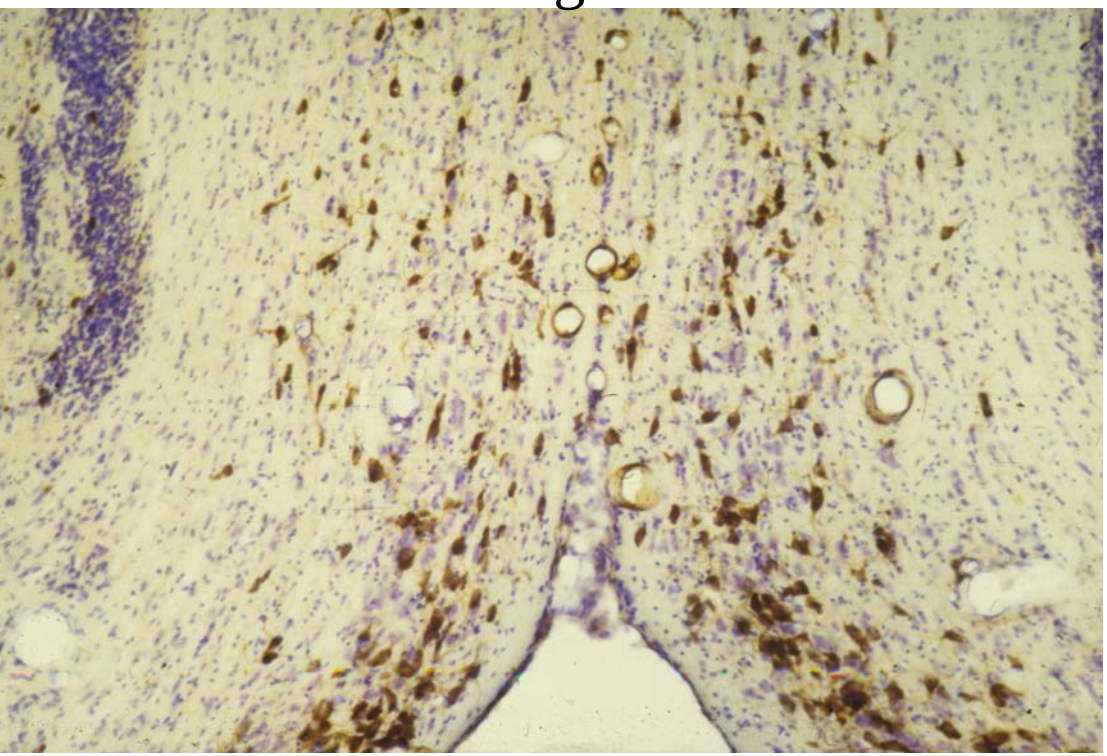

A

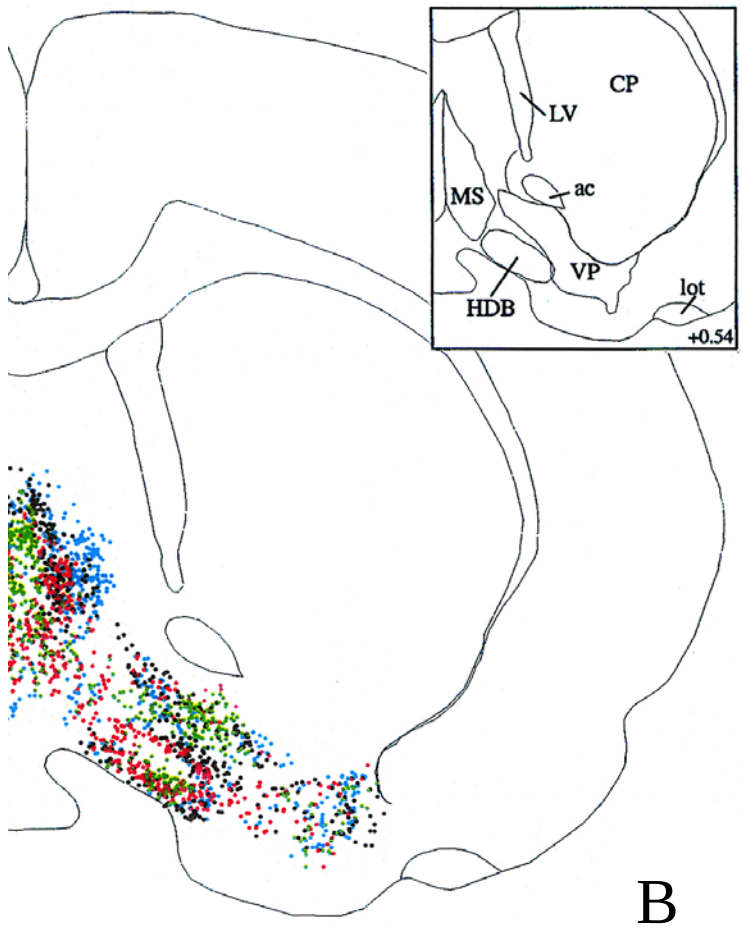

B

A: Choline acetyltransferase (ChAT) and Nissl-staining. B: cholinergic neurons red) are intermingled with Parvalbumin (green), Calretinin (black) and calbindin (blue) neurons

Juxtacellular filling, unit recording, EEG

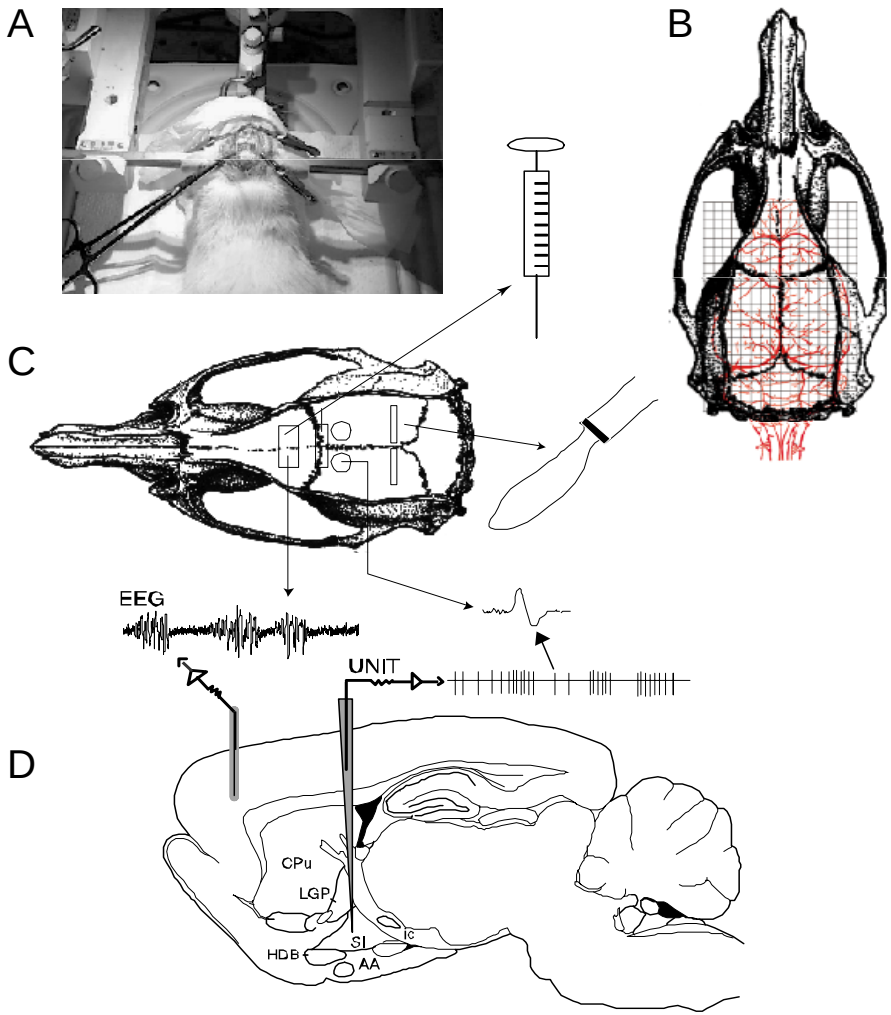

Identified cholinergic neuron

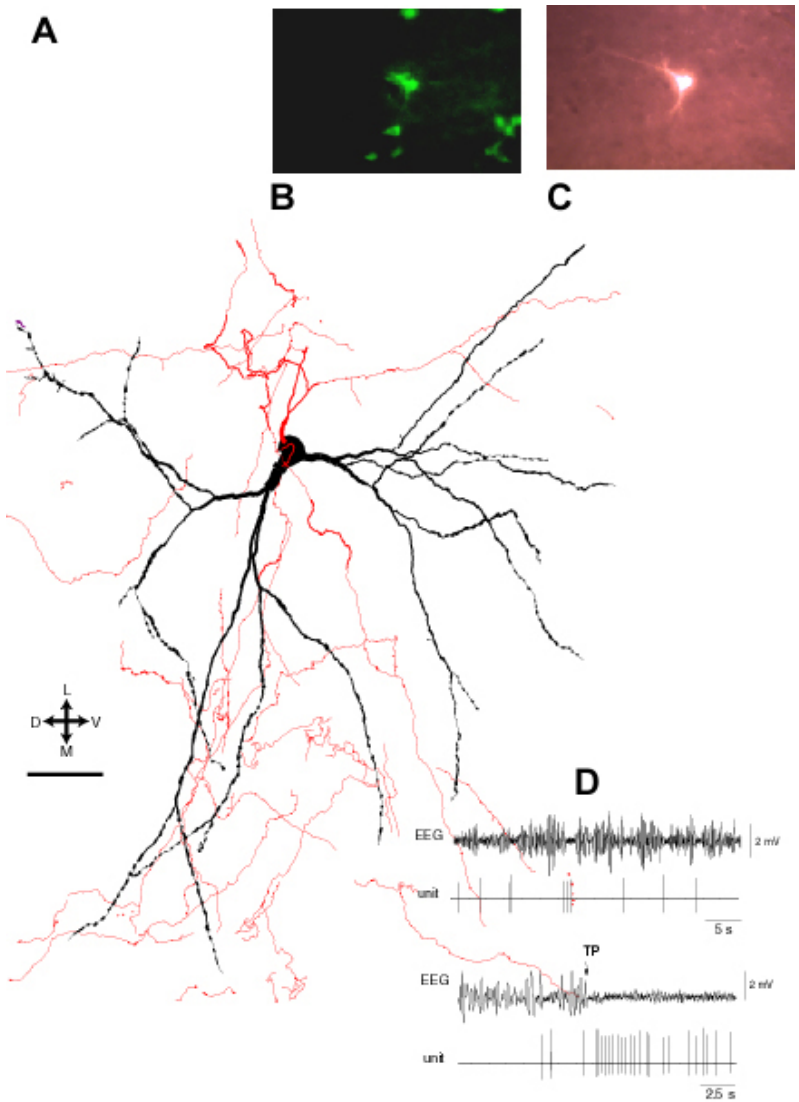

Identified GABAergic neuron (Parvalbumin)

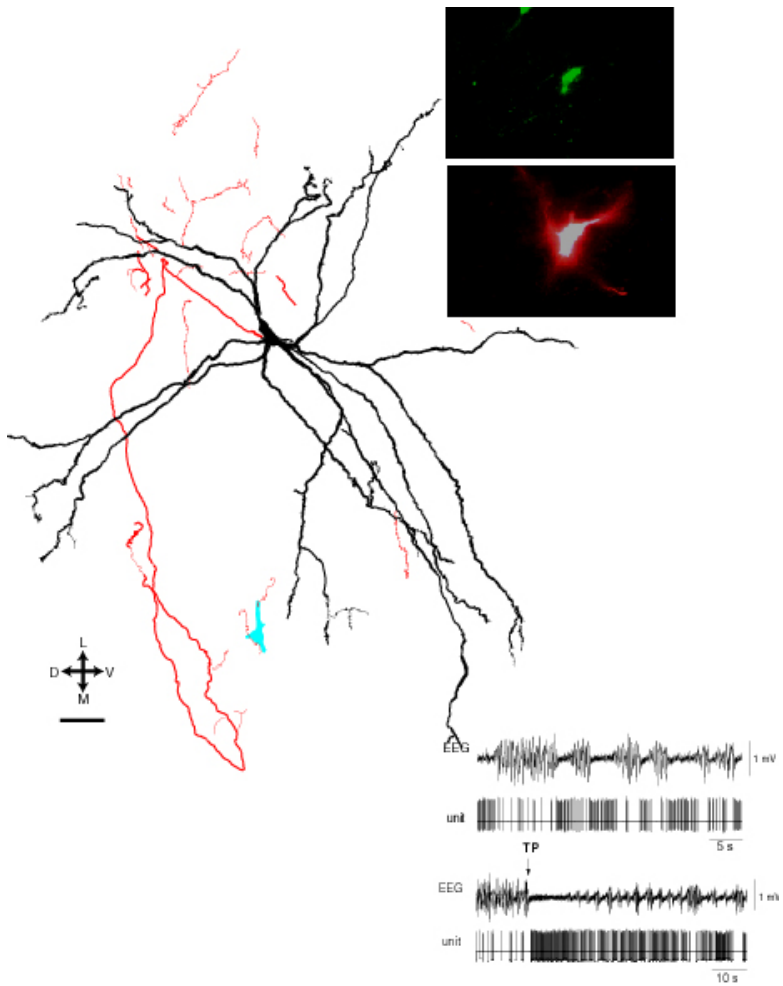

Identified interneuron (GABA-NPY)

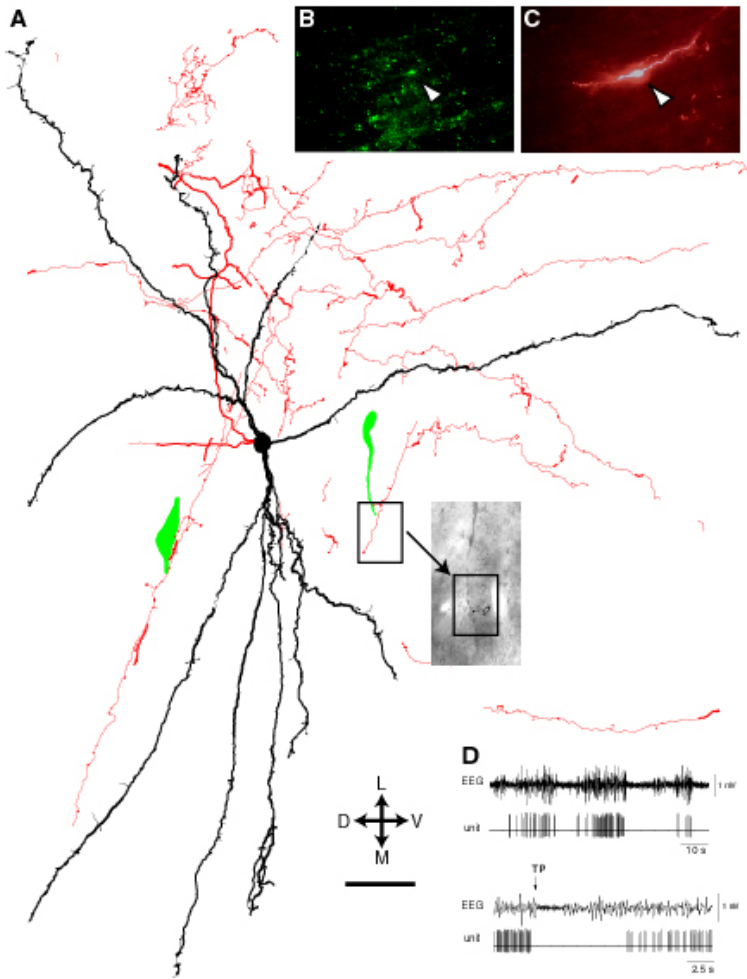

Fig. 38. Putative functional circuitry in the BF

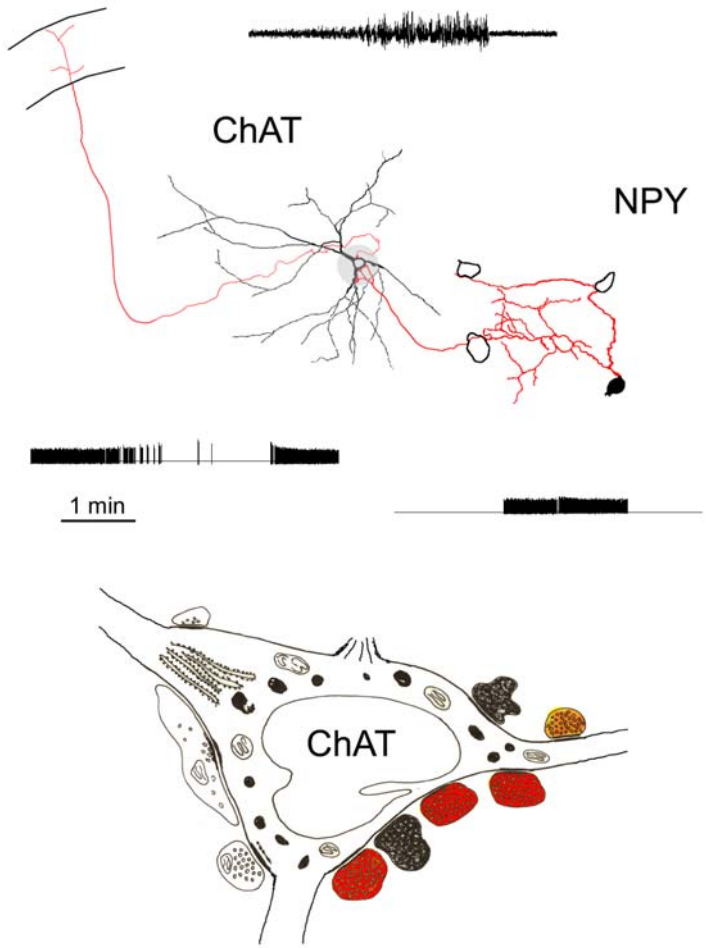

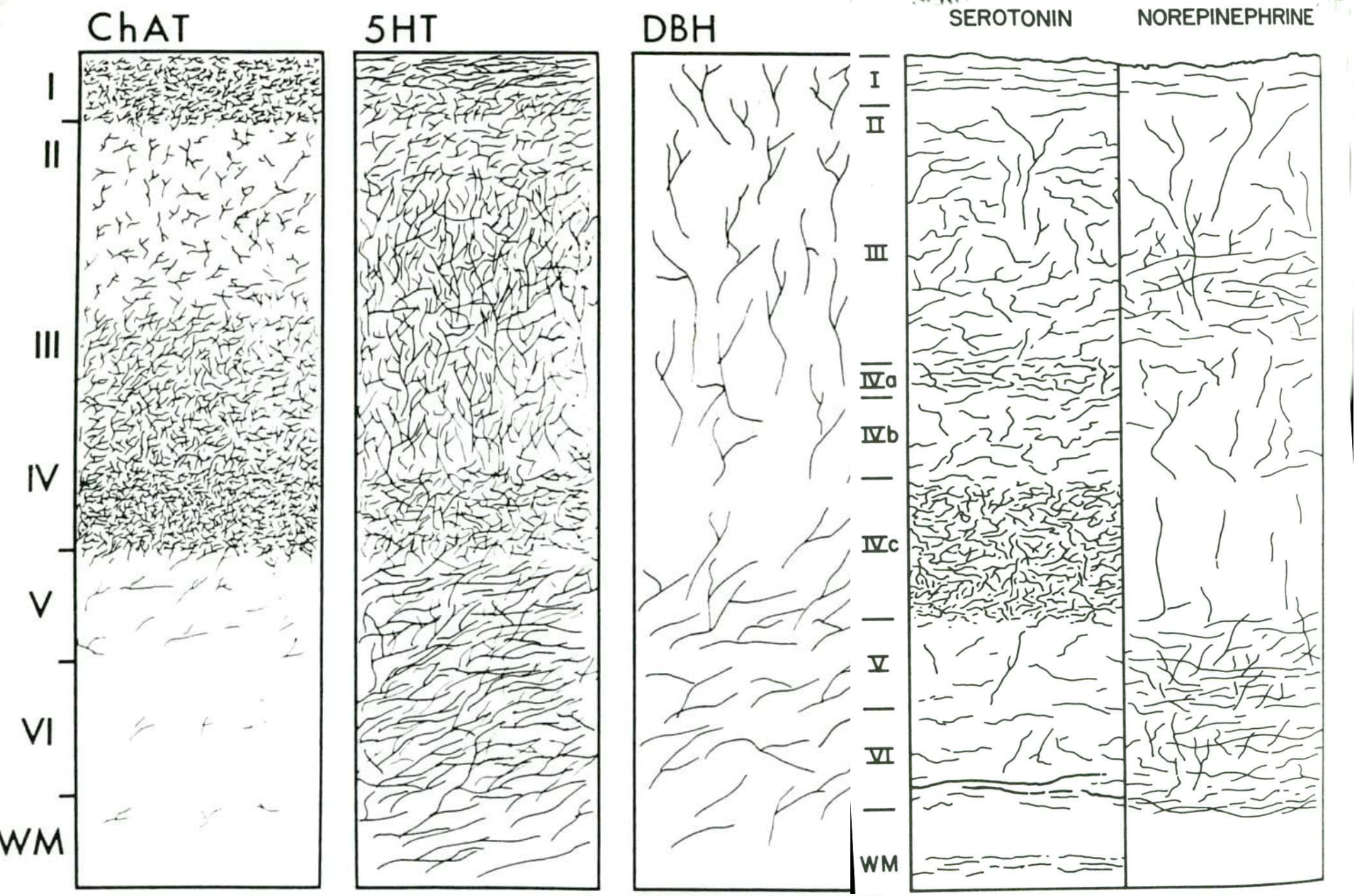

Comparative distribution of ChAT, 5HT, DBH fibers in monkey auditory (first three columns: Campbell et al., 1987) and primary visual cortex (last two columns Morrison et al., 1982)

Effect of monoamines on pyramidal cell firing on vitro and in vivo

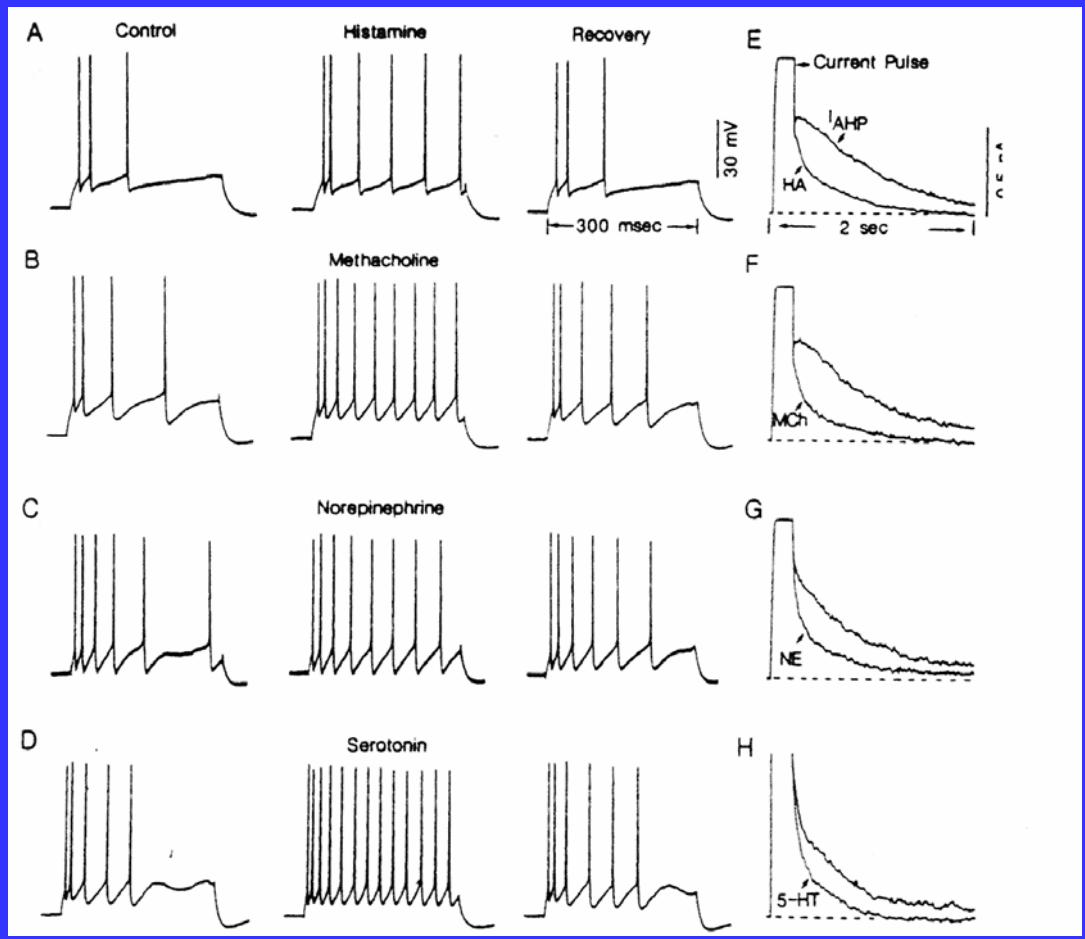

A-D: current clamp; E-H voltage clamp mode; McCormick and Williamson, 1989

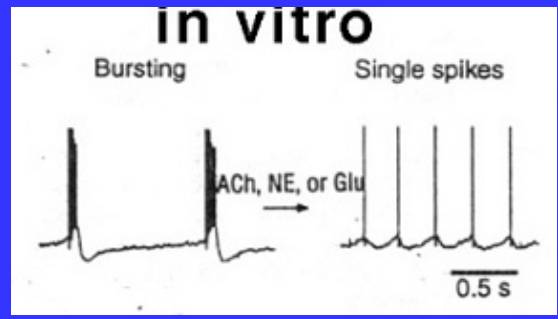

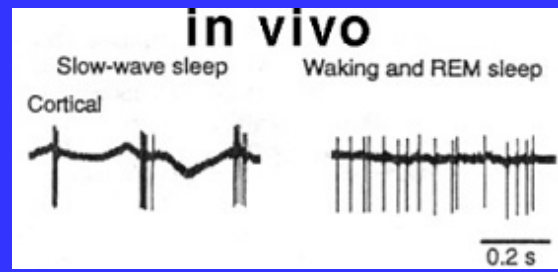

From Steriade et al., 1993

The ascending modulatory systems are interconnected

Diffuse input to BF: LC axons

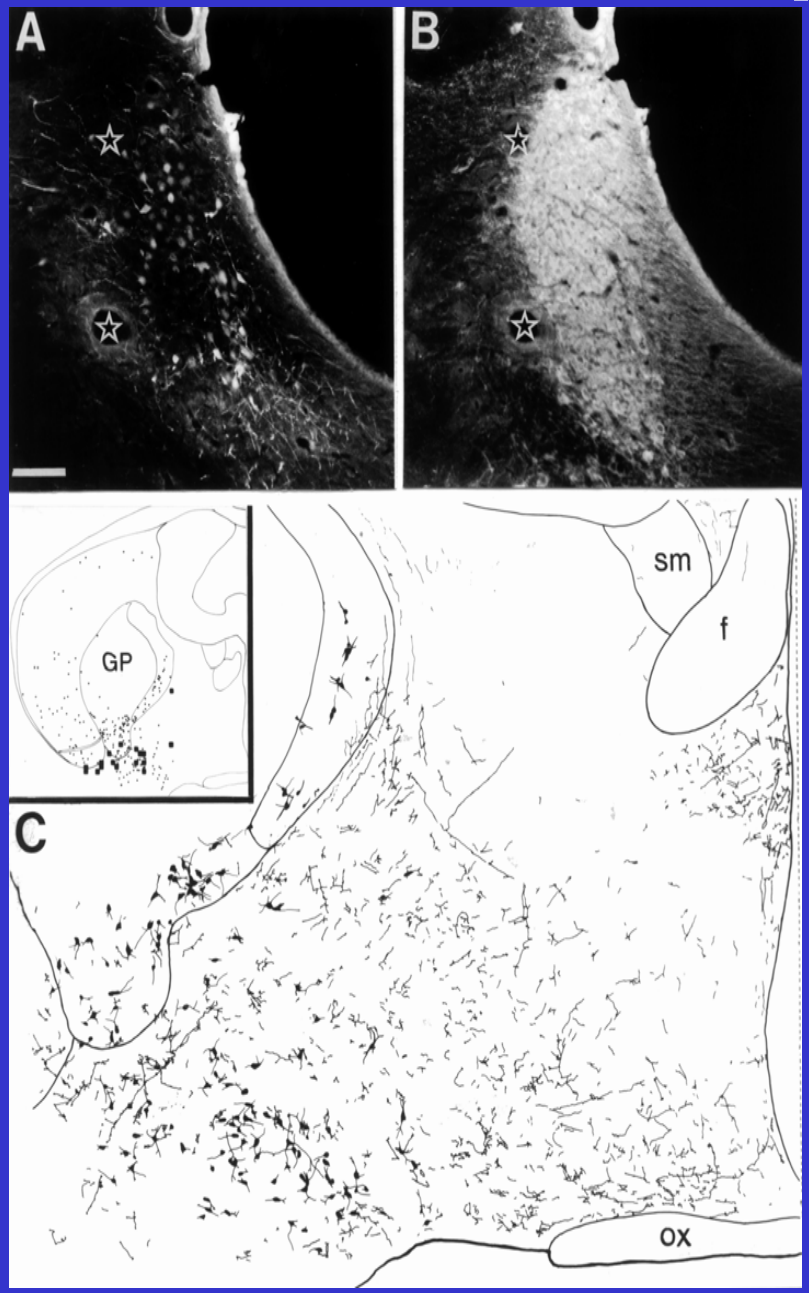

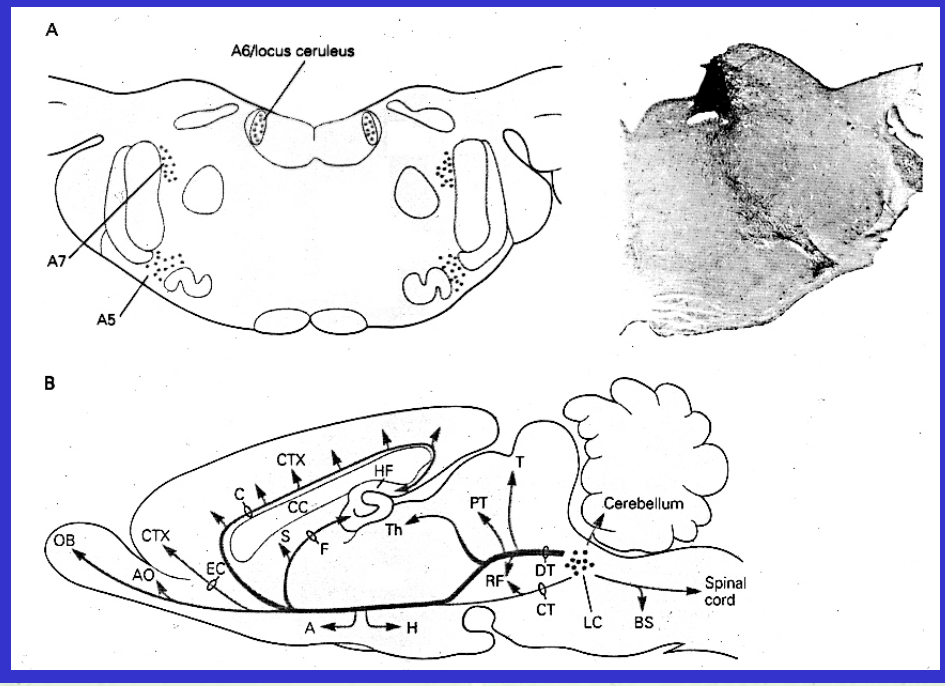

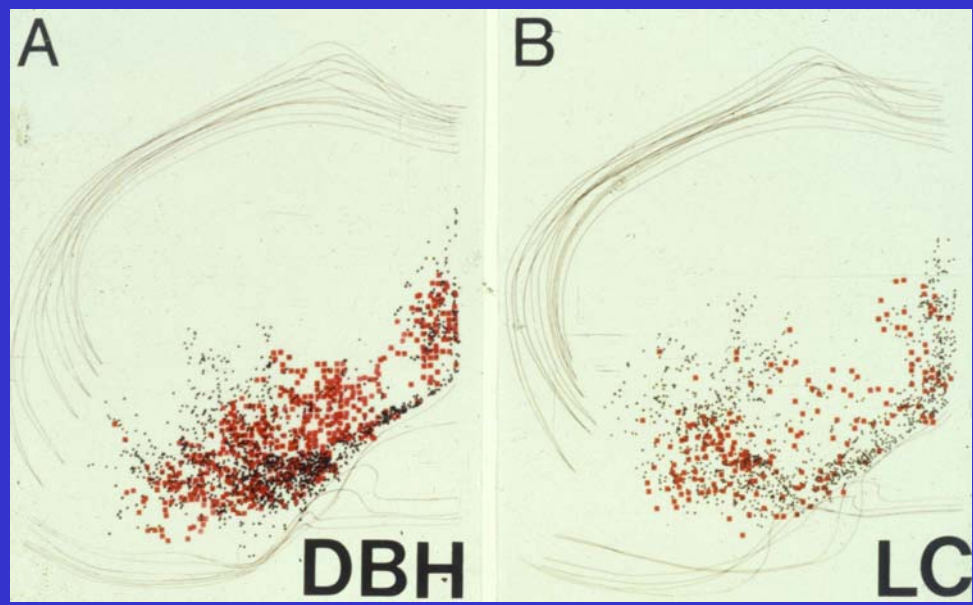

LC can affect the cortex via the BF

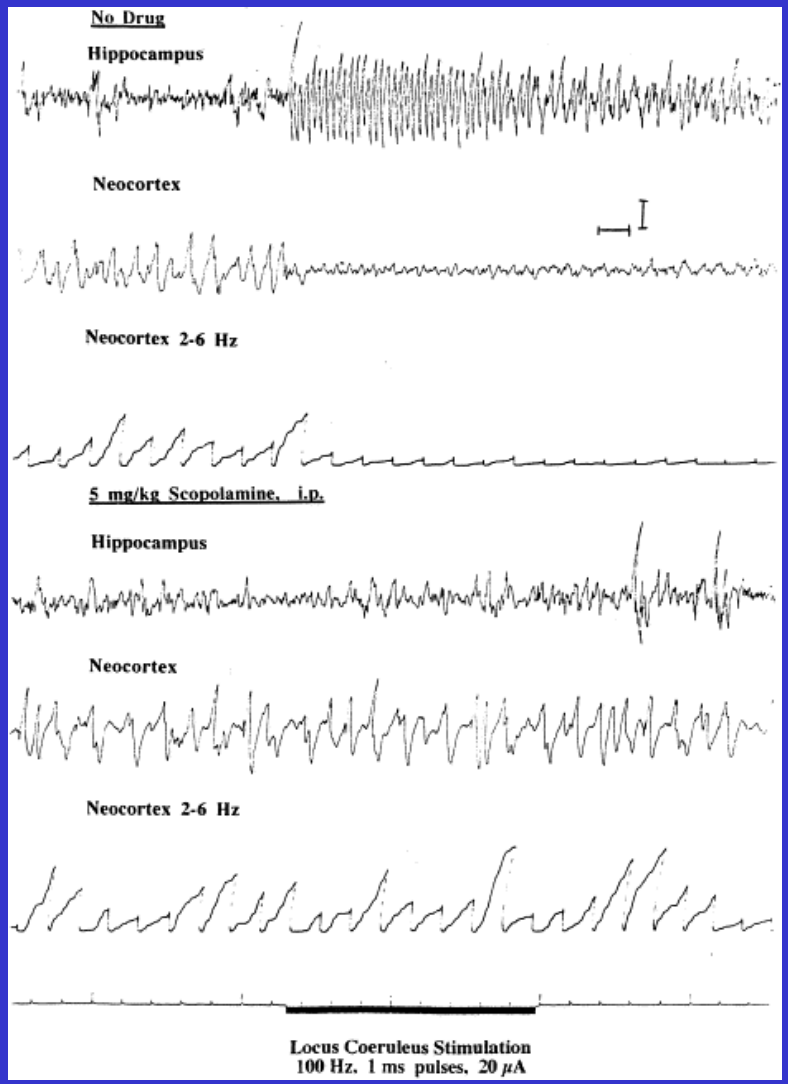

Dringenberg and Vanderwolf, 1998

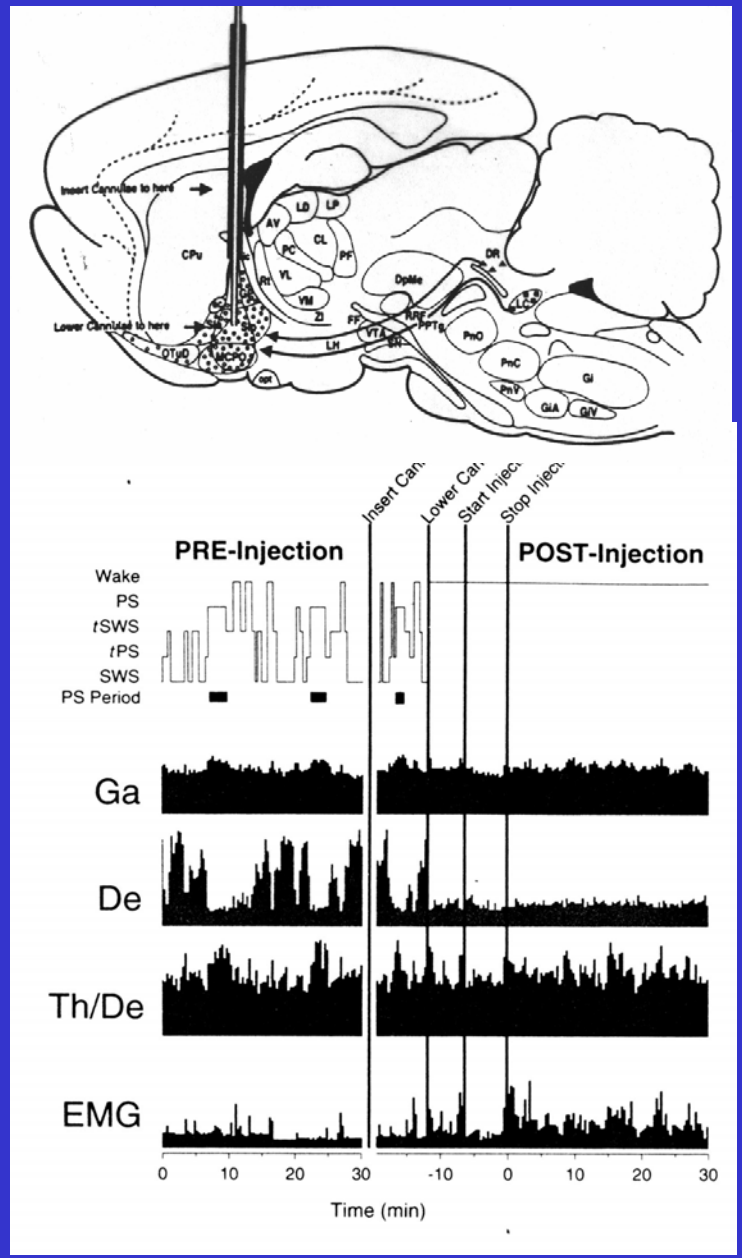

Cape and Jones, 1998

CHOLINERGIC NEURONS RECEIVE SYNAPSES FROM THE MIDBRAIN DOPAMINERGIC AREA

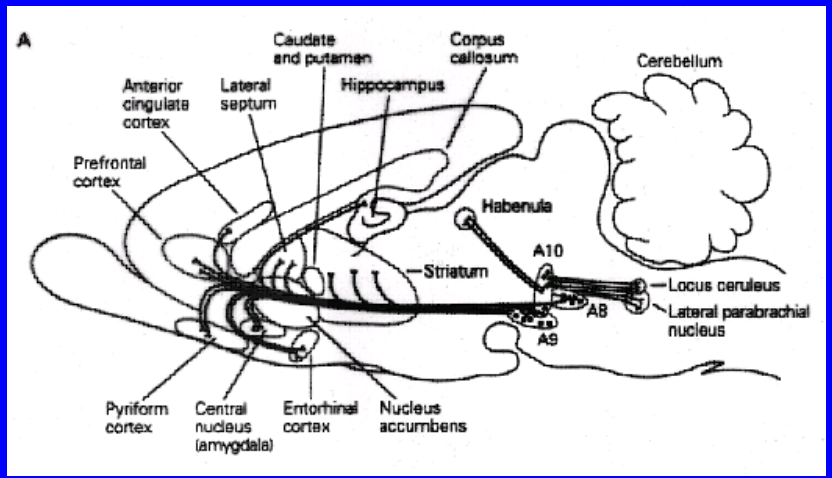

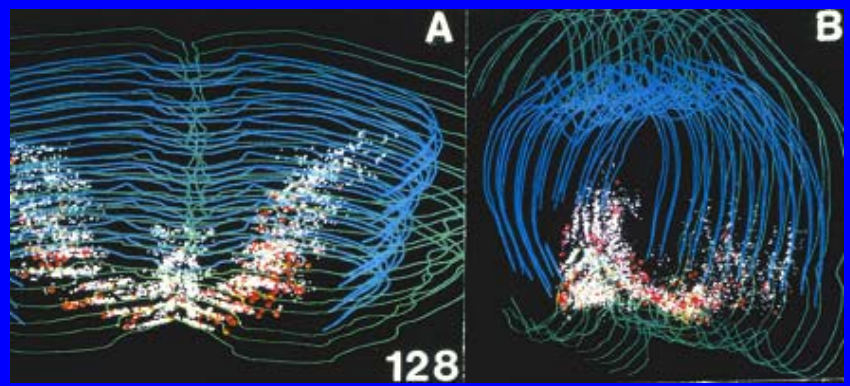

Ventral midbrain axons contact CH and PV cells in the BF

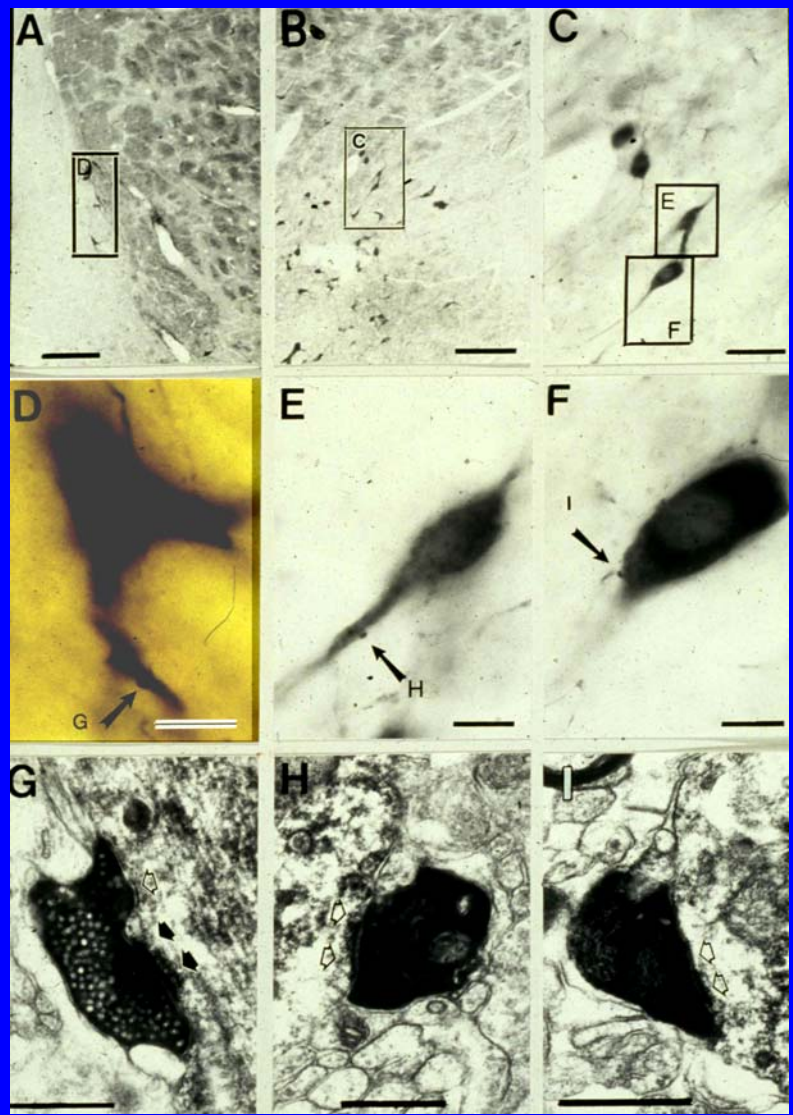

Gaykema and Zaborszky, 1996

Diffuse input to the BF: histaminergic axons in close proximity to ChAT neurons

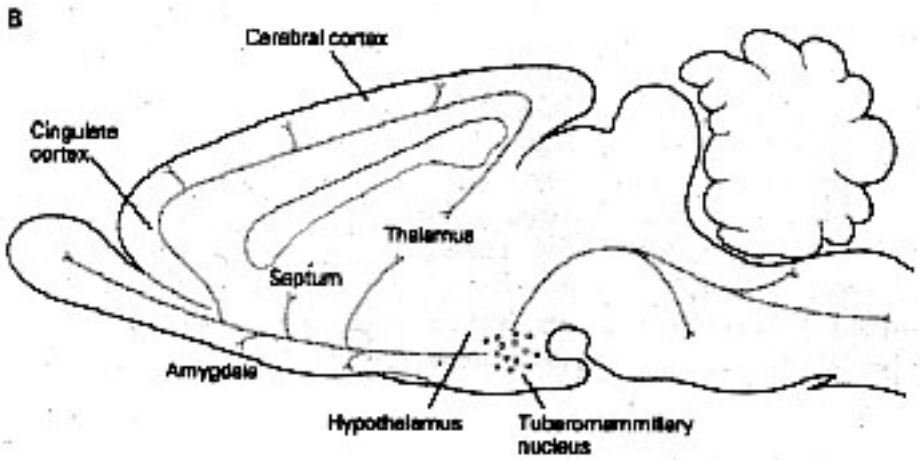

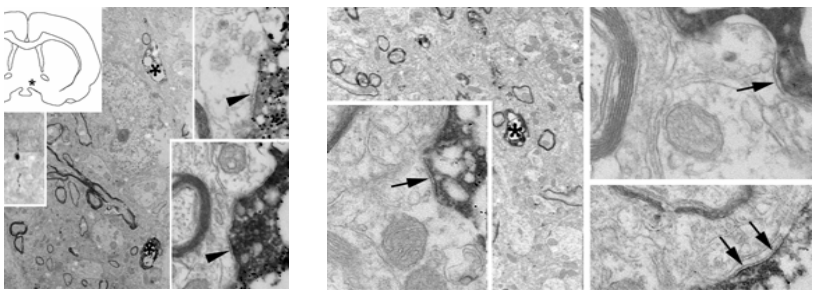

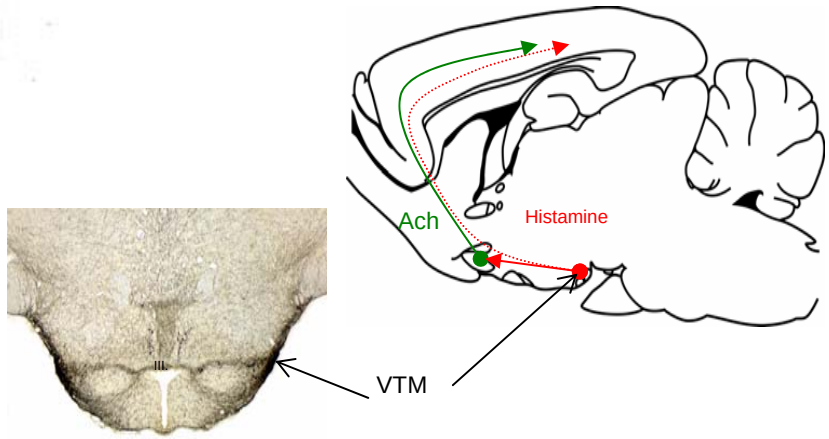

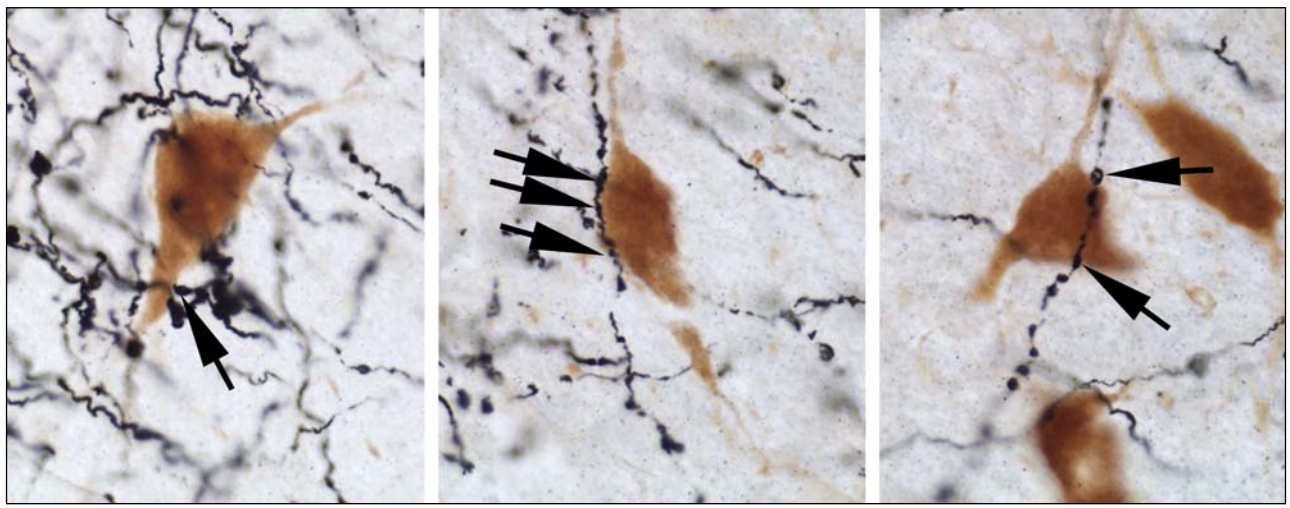

Turi, Zaborszky et al.: SFN 2004

The brainstem monoaminergic cell groups send projections to the bbasal forebrain cholinergic and non-cholinergic neurons

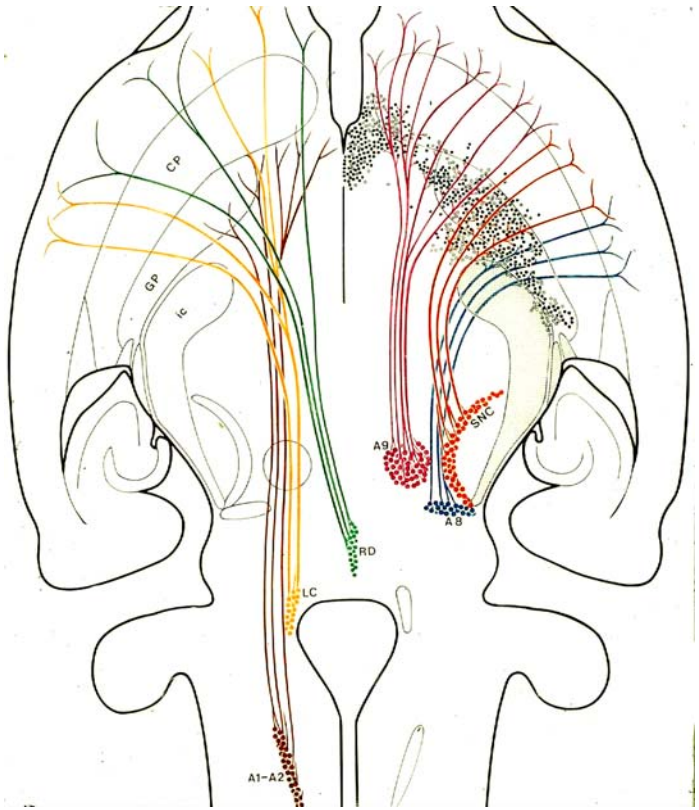

Mesopontine projections to PV (and CH) neurons in the BF

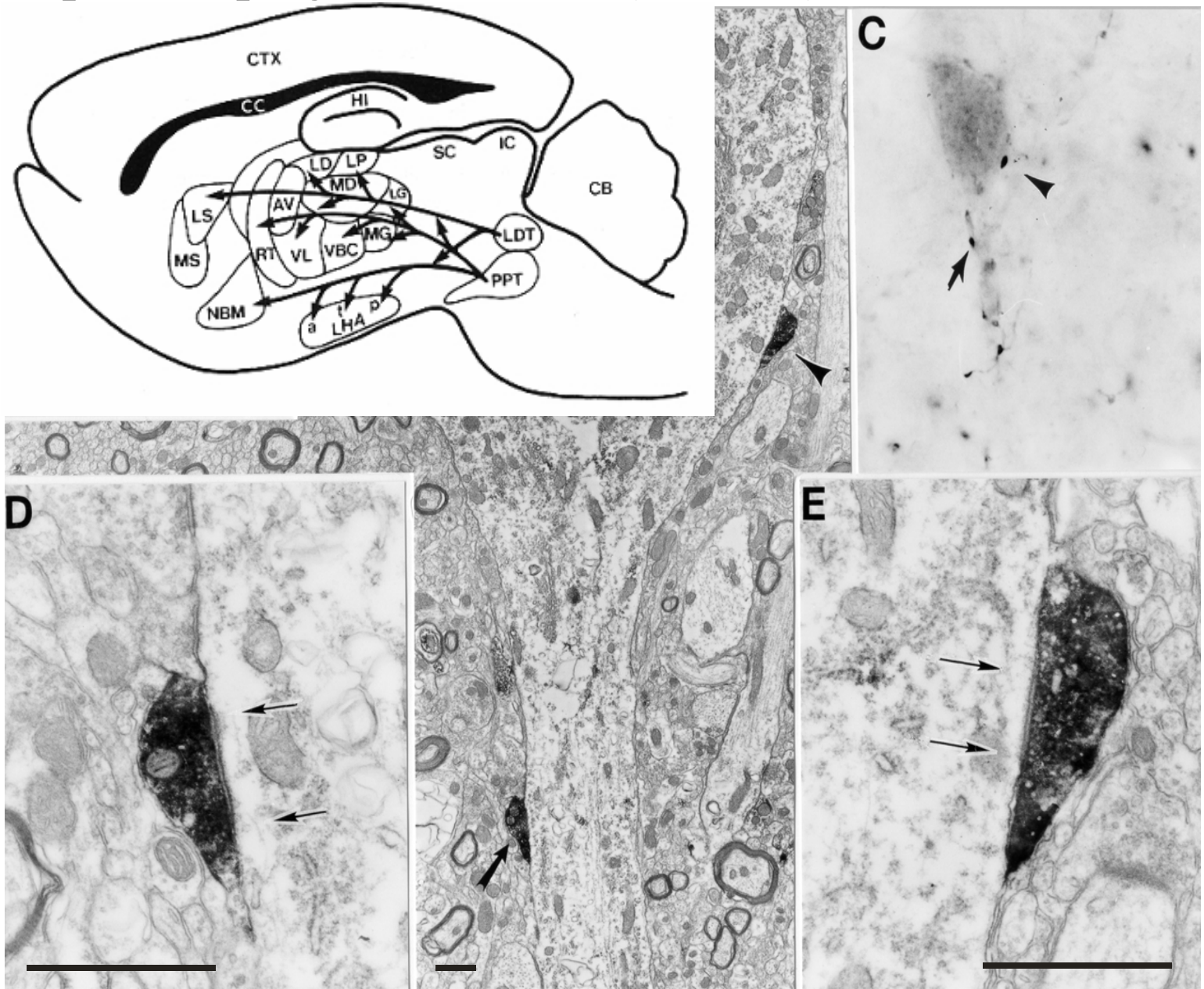

Corticopetal Vglut2 cells in the brain

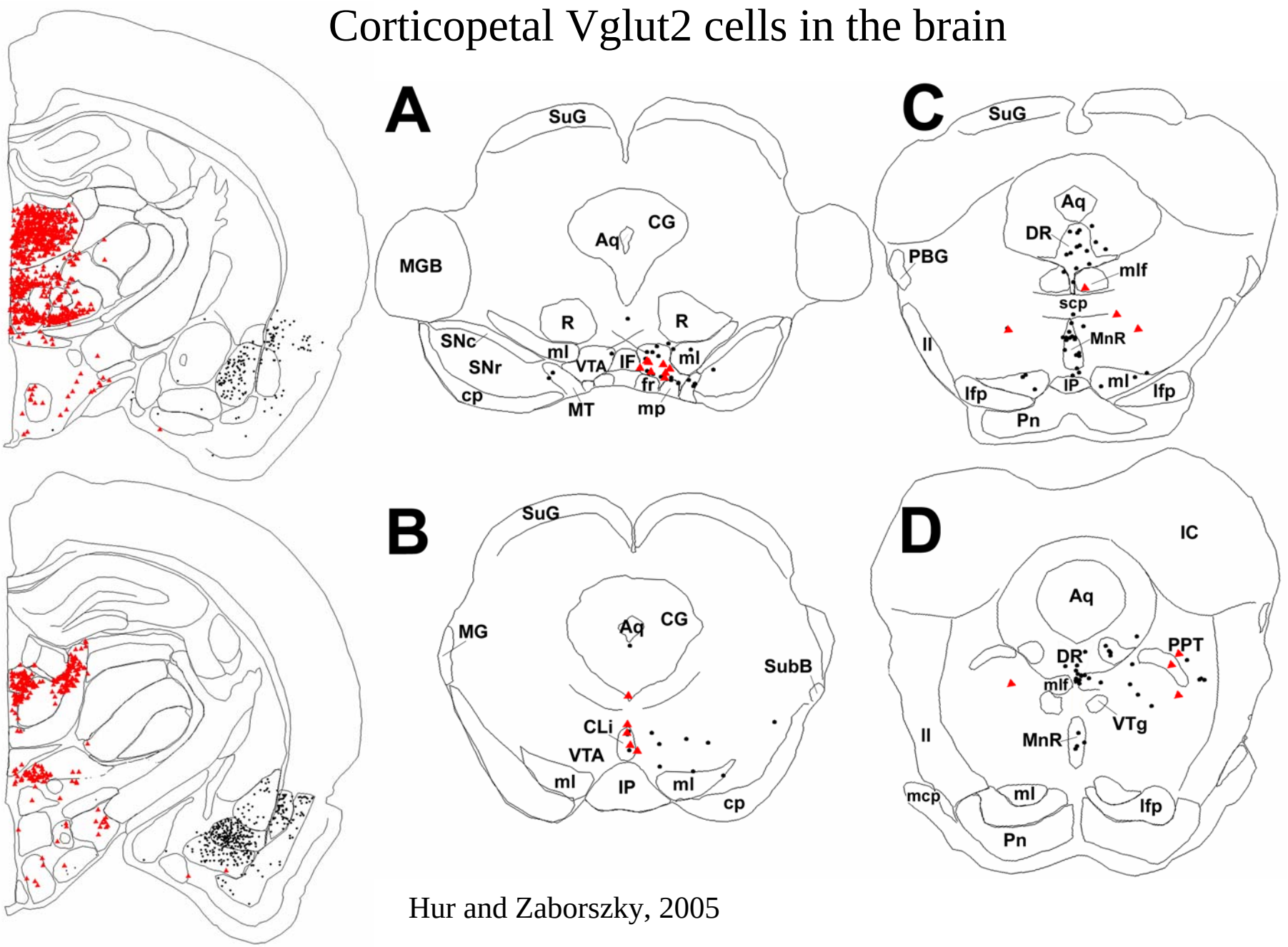

Hur and Zaborszky, 2005

Diffuse input: Vglut 2 synapses on CH dendrites

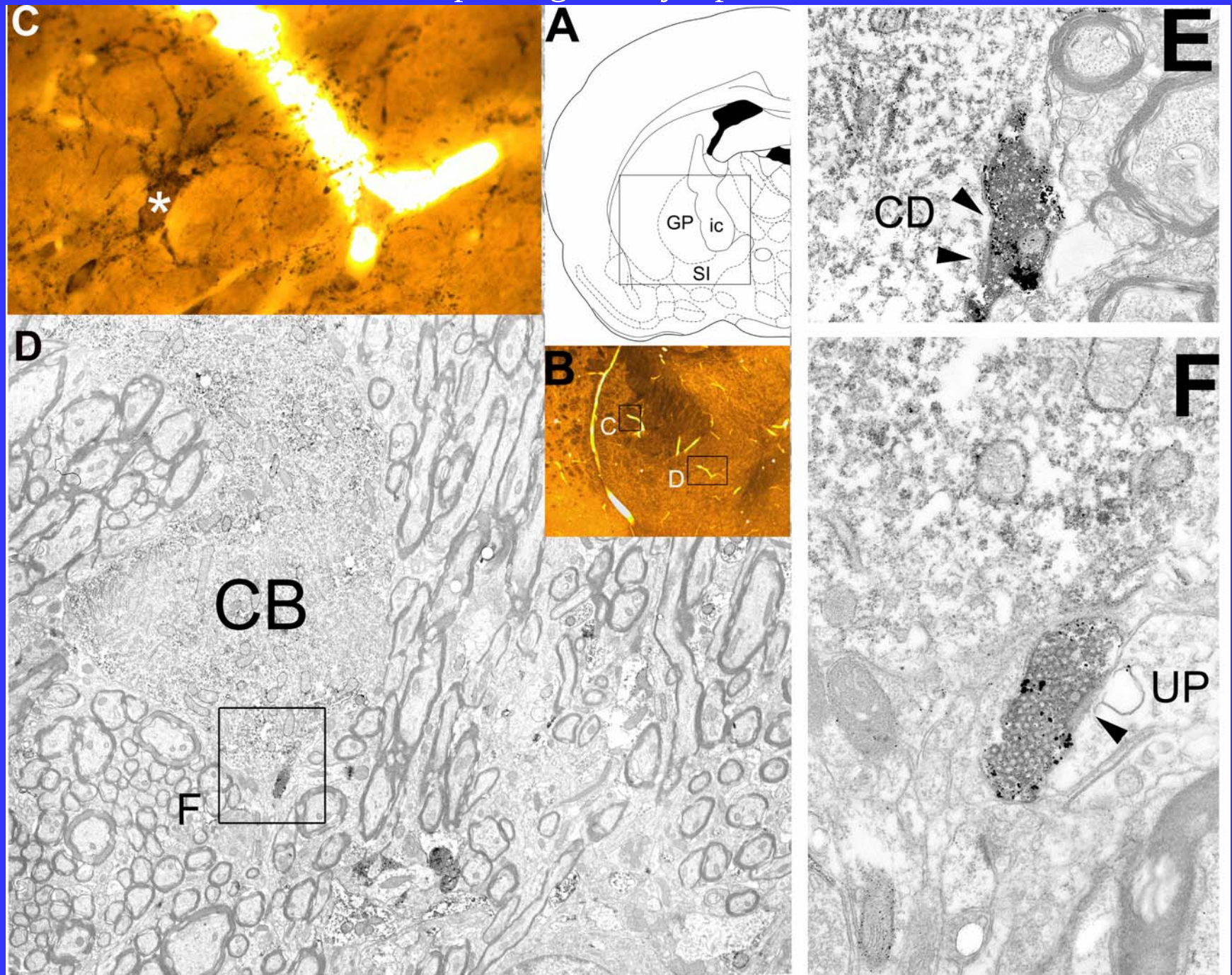

Diffuse input to BF: hypocretin axons

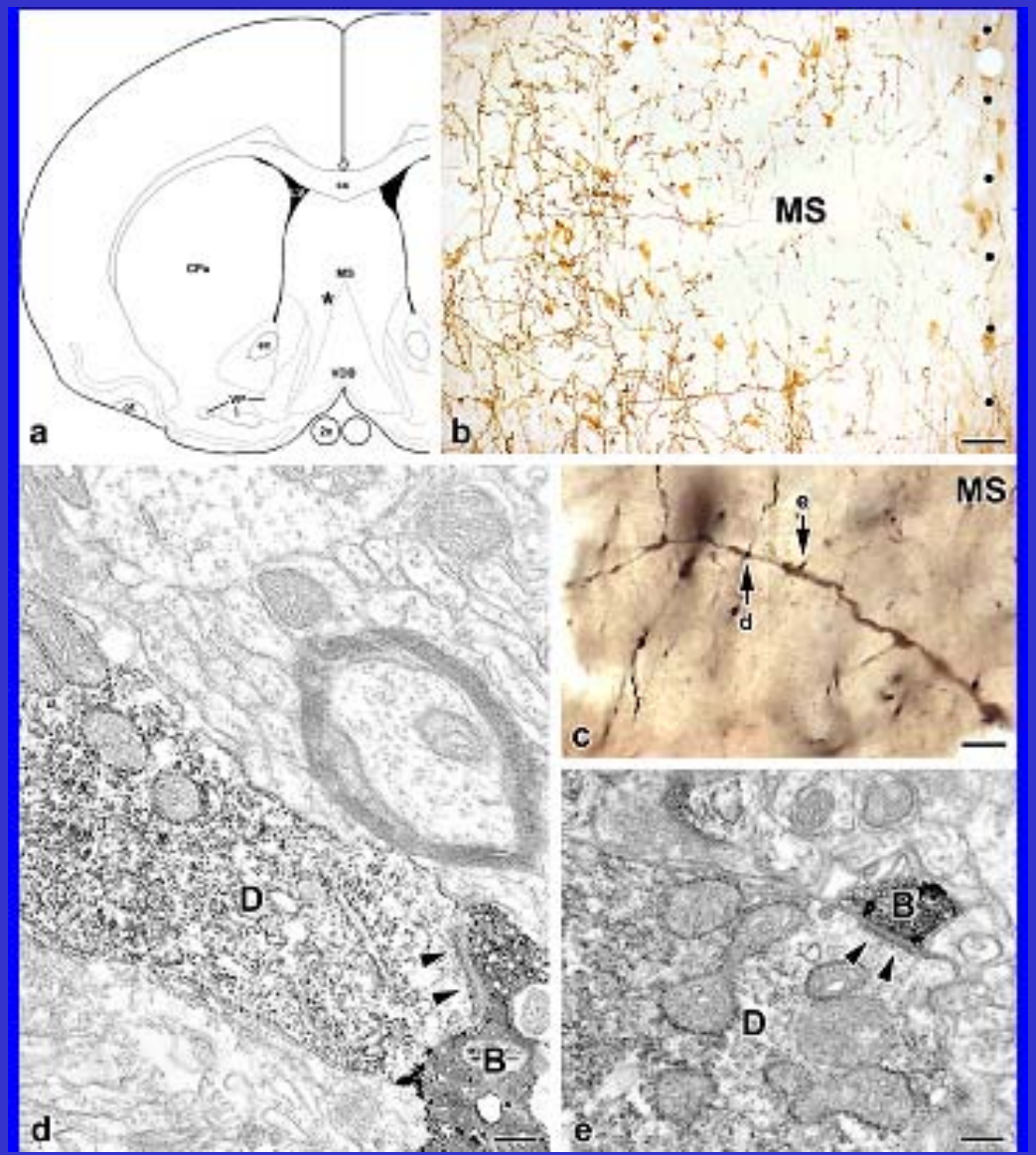

Wu, Zaborszky, Hajszan, van den Pol, Alreja, 2004

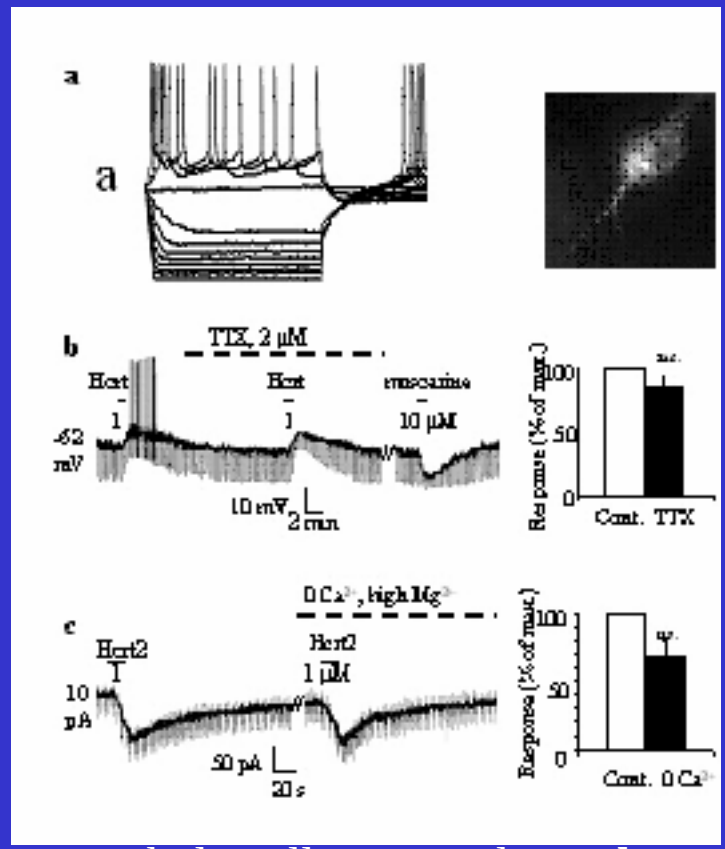

a: whole-cell current clamp; **b**: current clamp showing the depolarizing effect of Hcrt. **c**: voltage clamp (-65 mV) in which Hcrt2 induced an inward current that persisted in zero Ca2+, high Mg2+ ACSF.

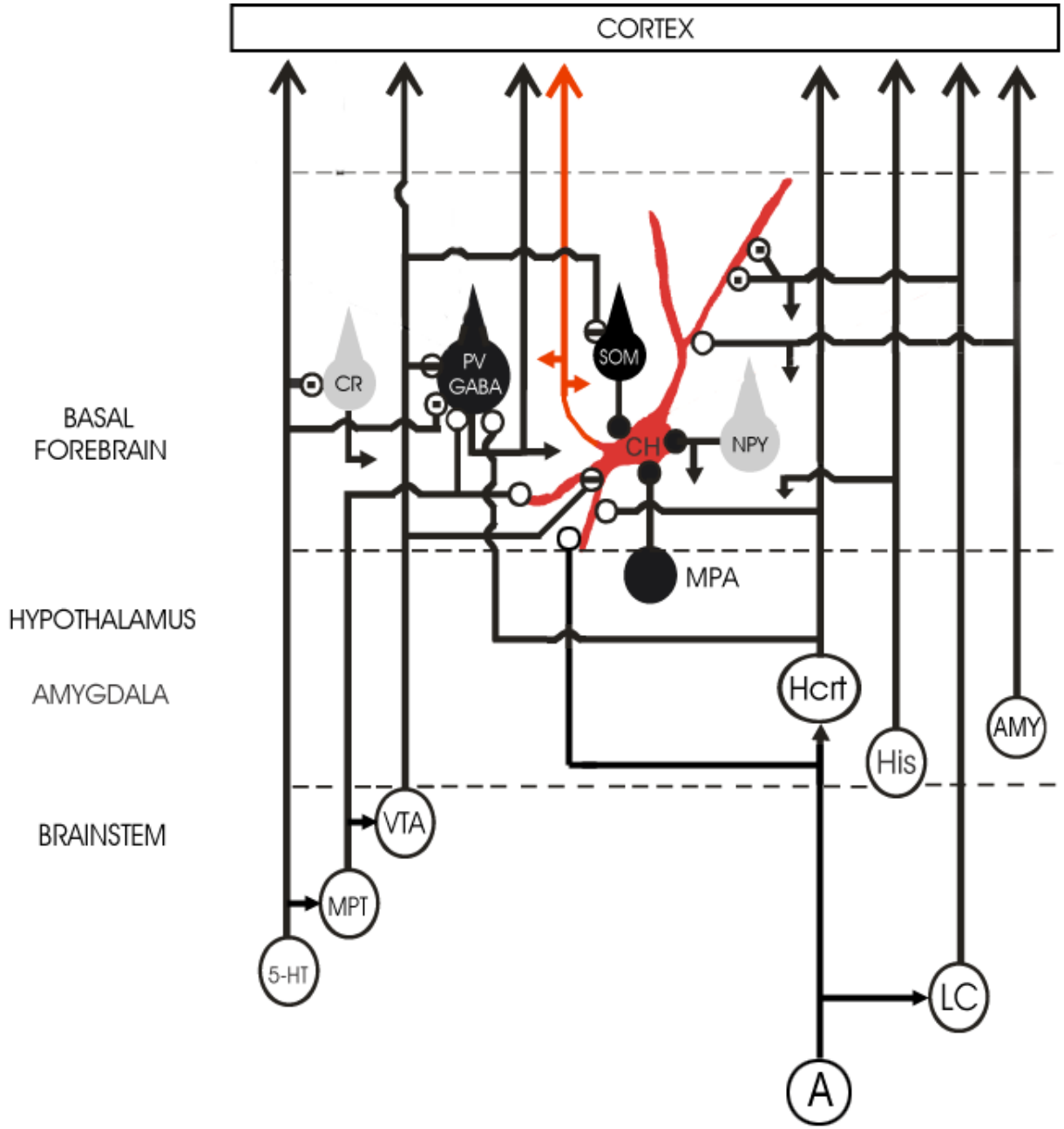
CORTEX
BASAL FOREBRAIN
HYPOTHALAMUS
AMYGDALA
BRAINSTEM
CR
PV GABA
SOM
CH
NPY
MPA
Hcrt
His
AMY
VTA
MPT
5-HT
LC
A

SLEEP SWITCH, FLIP-FLOP SWITCH

Sleep-active neurons in the VLPO

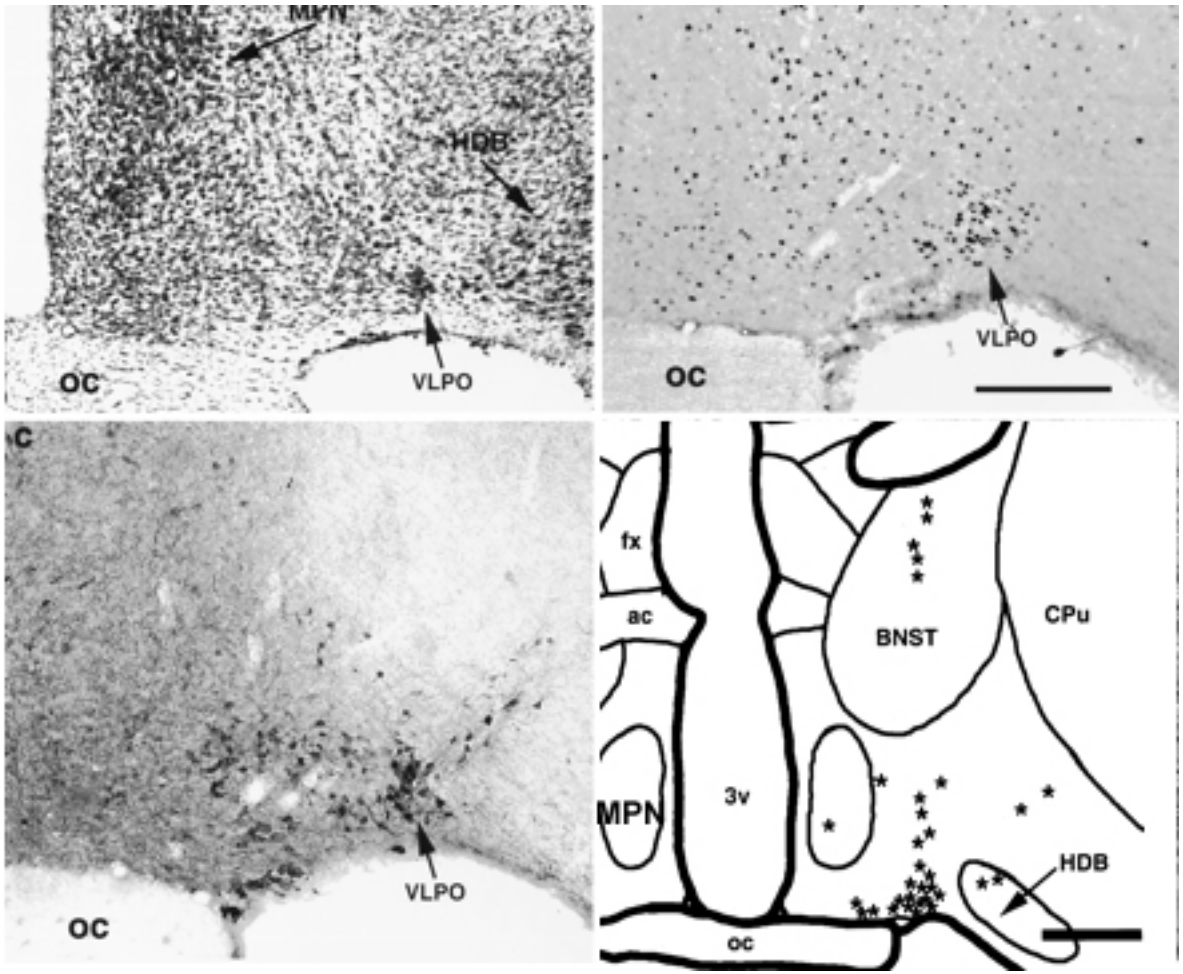

A: Giemsa-stained section showing a small triangular cluster of cells (ventrolateral preoptic nucleus).b: Fos-ir neuronal nuclei in the VLPO after 1 hr period spent predominantly asleep. C: the VLPO is demarcated as a galanin/GABA positive cell group. Lower right: retrogradely labeled neurons that project to the tuberomammilary nucleus(Sherin et al., 1998).

Projections from the VLPO

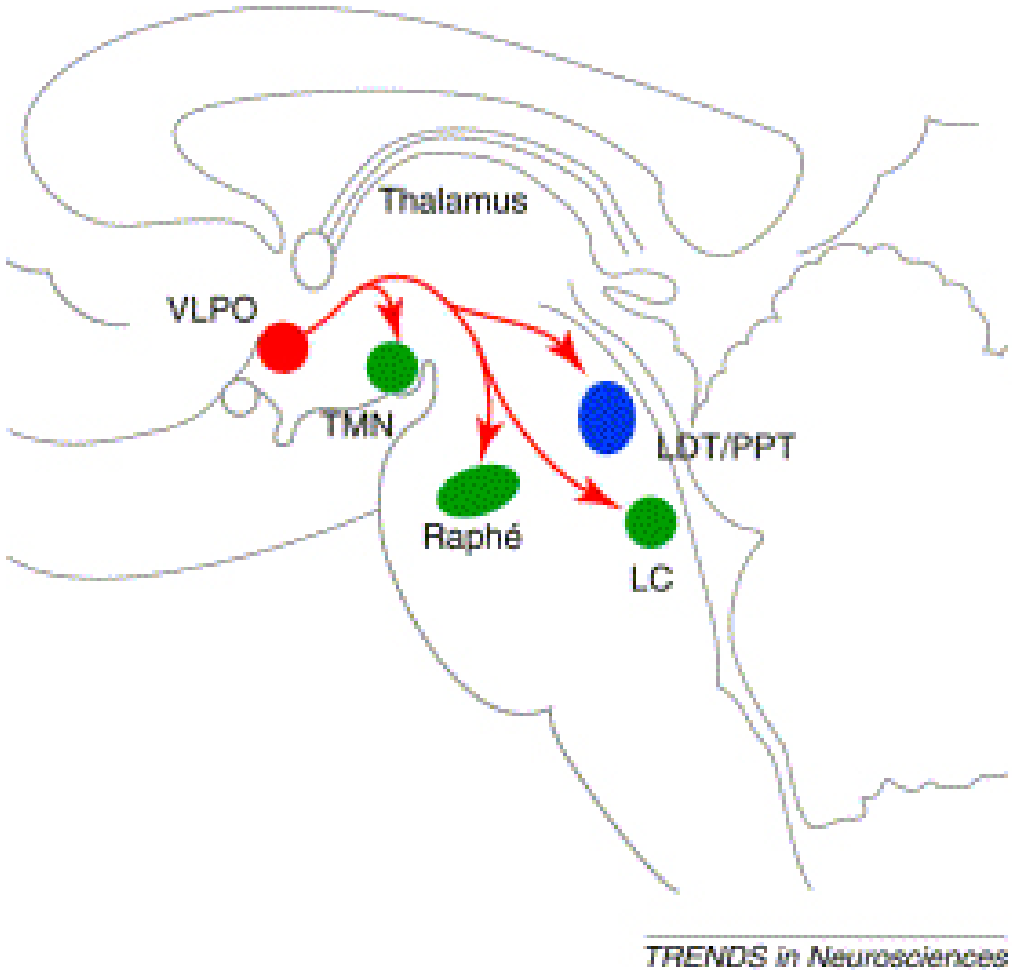

Saper et al., 2001

GABA release in the DR during REM

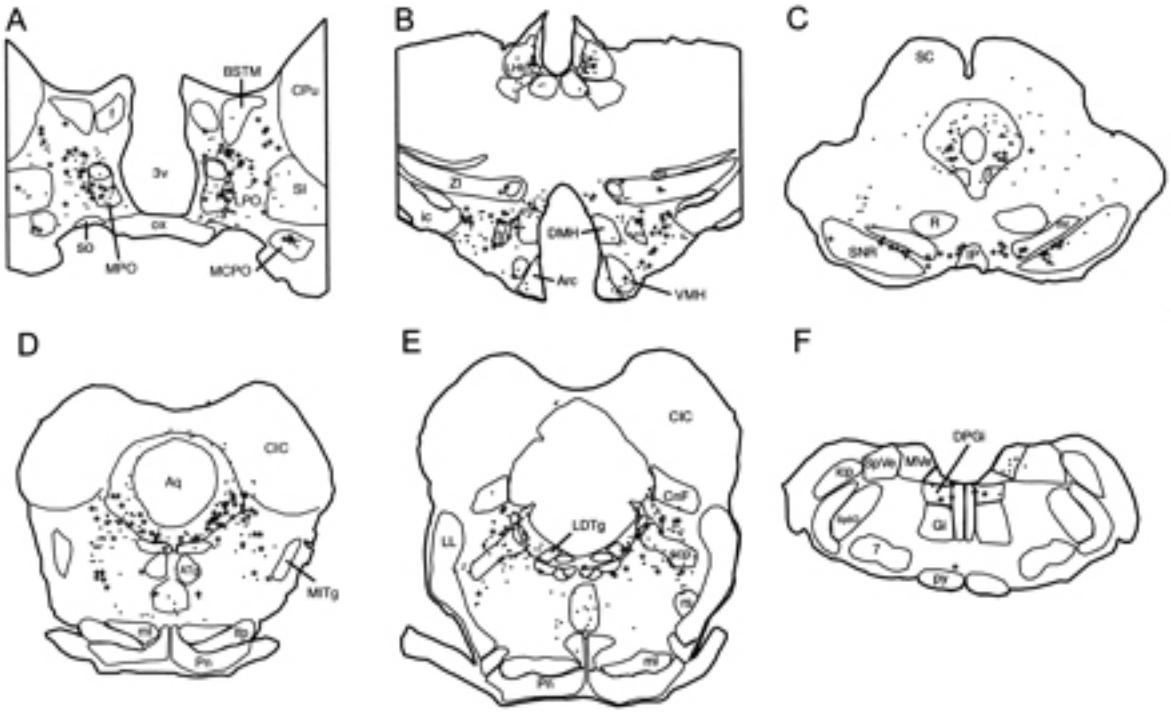

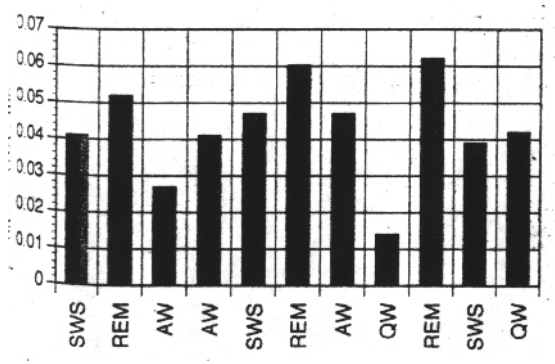

GABAergic afferents to the DRNm using retrograde tracing with cholera toxin B and glutamic acid decarboxylase immunohistochemistry. Stars corresponds to double-labeled cells. Note abundant projection from the medial (MPO) and lateral preoptic area (LPO) and pontine ventarl periaqueductal gray (Gervasoni et al., 2000).

The cessation of firing of 5-HT raphe neurons is a key controlling event of REM. REM sleep is accompanied by a selective increase in GABA release, but not glutamate in the DRN in naturally sleeping cats (Nitz and Siegel, 1997).

The flip-flop switch

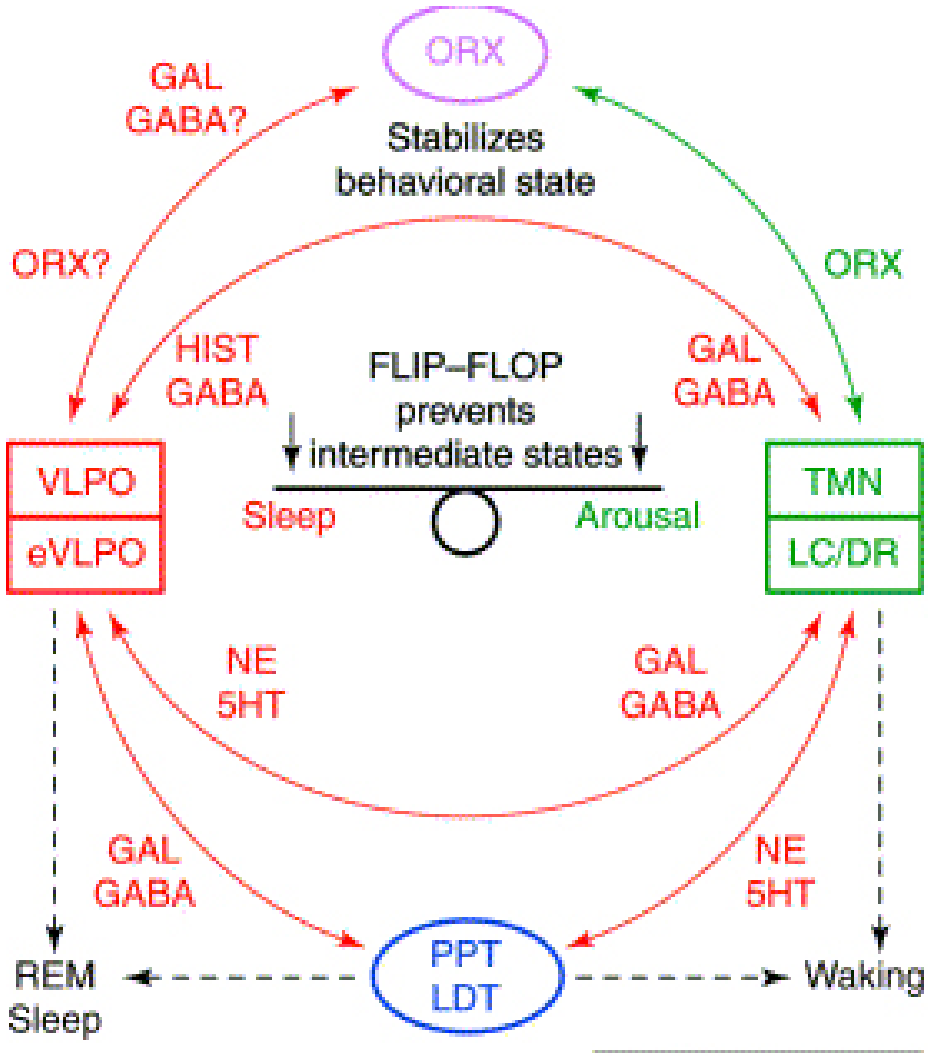

A model for reciprocal interactions between sleep- and wake-promoting brain regions, which produces a flip–flop switch. Aminergic regions such as the TMN, LC and DR promote wakefulness by direct excitatory effects on the cortex and by inhibition of sleep-promoting neurons of the VLPO. During NREM sleep, the VLPO inhibits amine-mediated arousal regions through GABAergic and galaninergic (GAL) projections. The inhibition of the amine-mediated arousal system disinhibits VLPO neurons, further stabilizing the production of sleep. Orexin/ (ORX) neurons in the lateral hypothalamic area might further stabilize behavioral state by increasing the activity of aminergic neurons, thus maintaining consistent inhibition of sleep-promoting neurons in the VLPO and REM-promoting neurons in the PPT–LDT (Saper et al., 2001).

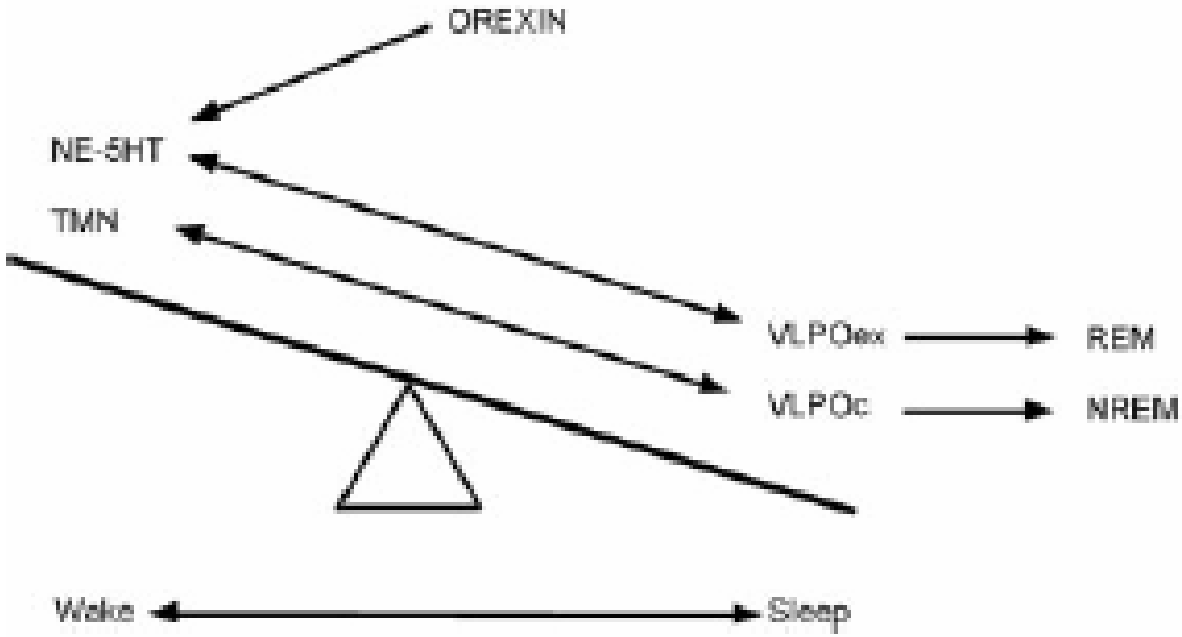

Diagram to illustrate the relationship of the flip-flop switch between the VLPO and components of the ascending arousal system (Saper et al, 2005) The VLPO cluster (VLPOc) primarily inhibits the histaminergic tuberomammillary nucleus (TMN), whereas the extended VLPO (VLPOex) preferentially inhibits the noradrenergic (NE) locus coeruleus and the serotoninergic (5HT) dorsal and median raphe nuclei. In return, the VLPOex is inhibited by serotoninergic inputs from the dorsal raphe nucleus and noradrenergic inputs from the ventrolateral medulla and the locus coeruleus. The VLPOc is heavily innervated by the TMN, but has no histamine receptors; however, TMN cells also contain galanin, GABA, and endomorphin, which can inhibit the VLPOc neurons. The VLPOc and the TMN are thought to play important but opposing roles in regulating NREM sleep, whereas the VLPOex and the locus coeruleus and dorsal raphe nuclei are thought to be opposing forces in regulating REM sleep. The mutually inhibitory interactions of the VLPO and the monoaminergic neurons produces a state similar to a ".ip-.op switch" in an electrical circuit. Such switches have sharp transitions, but may be unstable. The orexin neurons, which reinforce the monoaminergic systems by activating them, act to stabilize the .ip-.op switch and prevent unwanted transitions.

THALAMO-CORTICAL INTERACTIONS AND THEIR MODULATIONS BY ASCENDING BRAINSTEM AND FOREBRAIN PATHWAYS

Synaptic organization of the thalamus

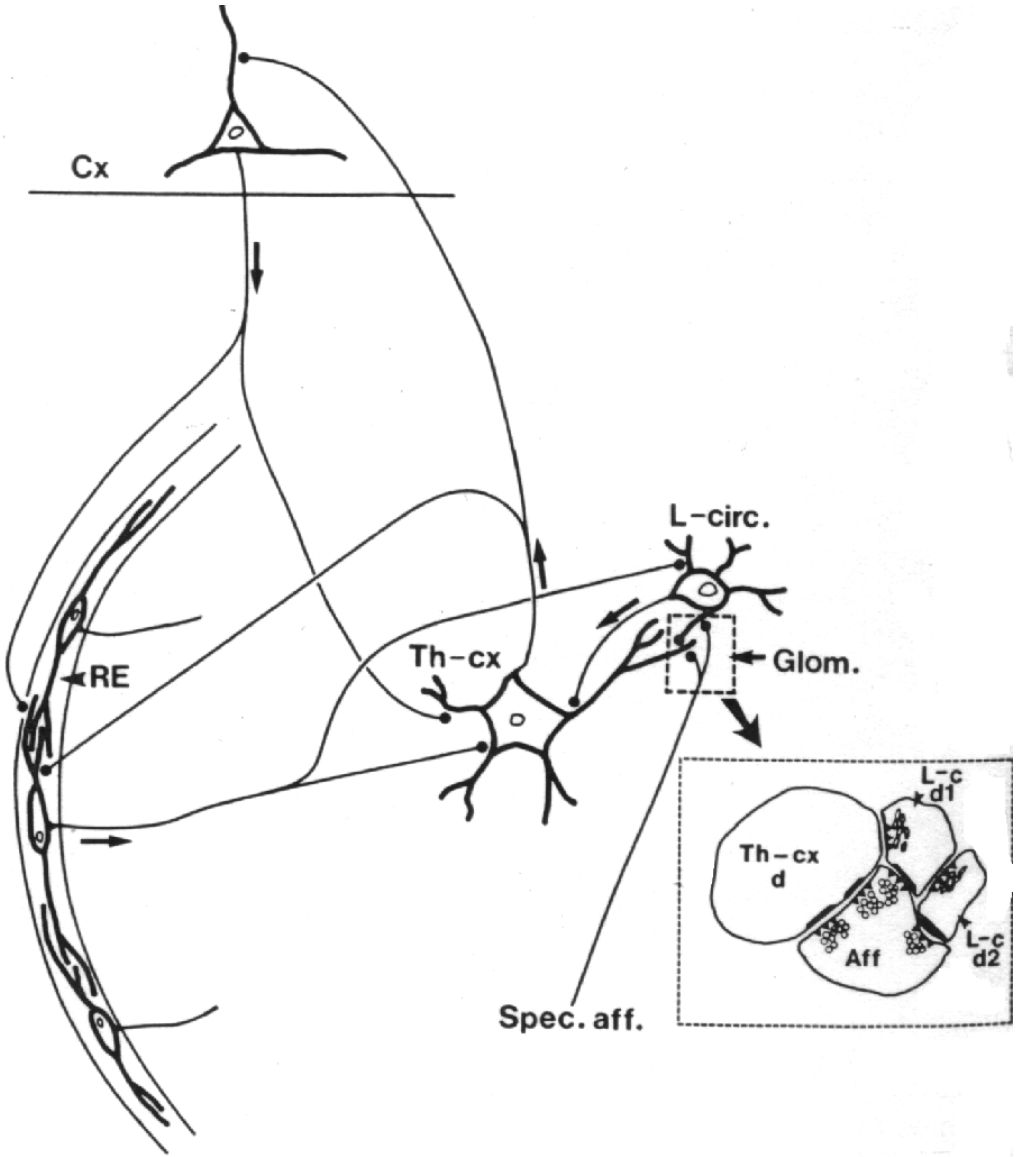

RE: reticular thalamic nucleus; Th-cx: thalamocortical n.; Cx: pyramidal n.; L-circ: local circuit n.; Inset: synaptic contacts within a glomerulus

(Llinas and Steriade, 1988)

Cholinergic innervation of the thalamus

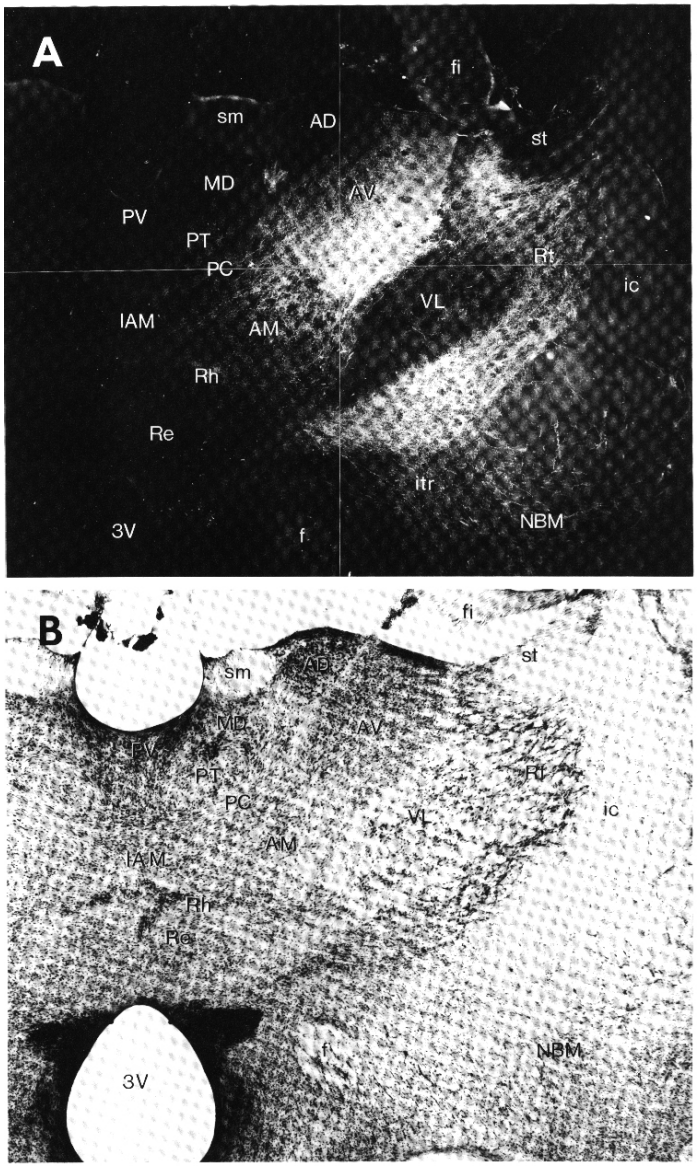

Cholinergic innervation of the thalamus. A: Choline acetyltransferase staining, B: Adjacent Nissl-stained section (Levey et al., 1987)

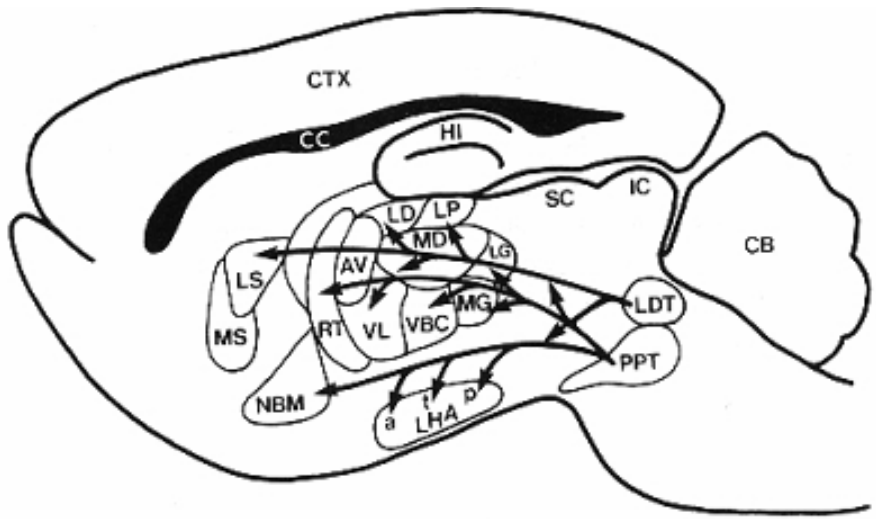

Histaminergic innervation of the forebrain, including the thalamus

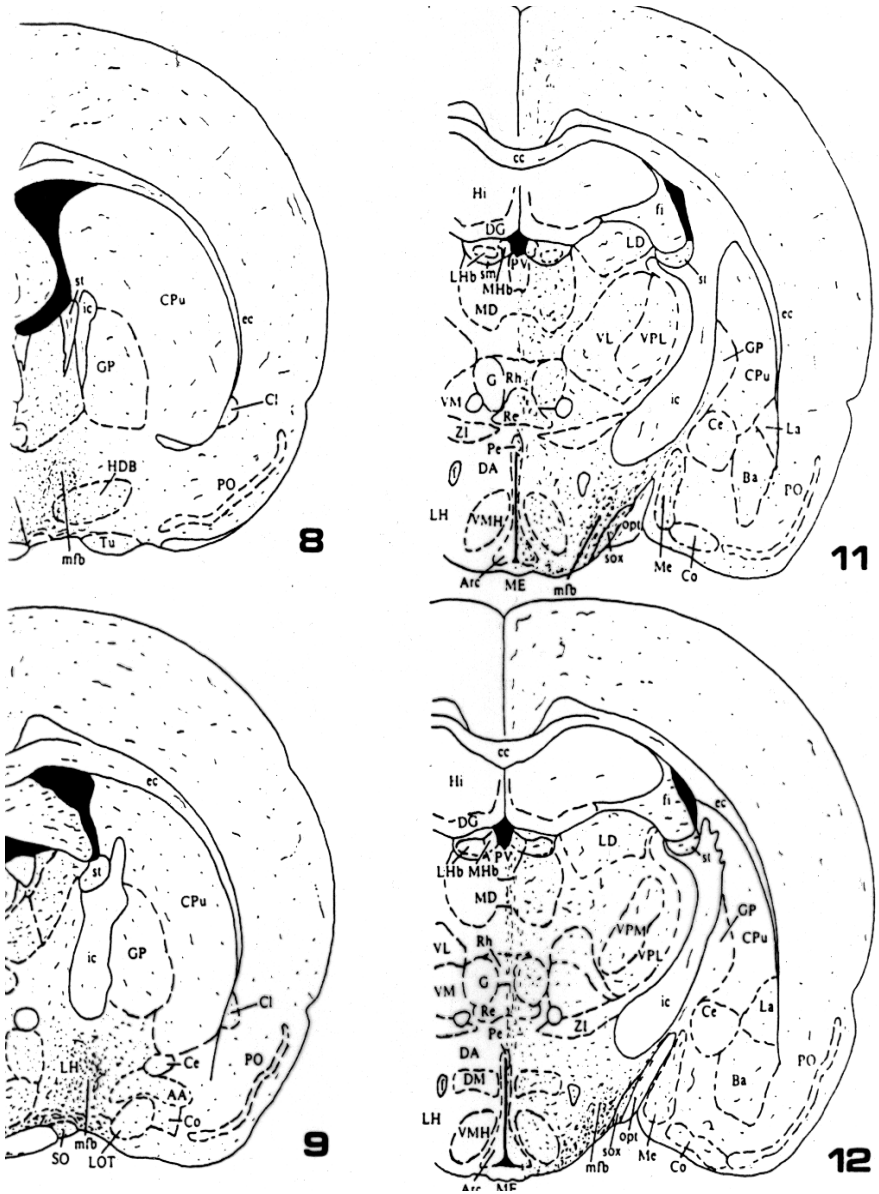

Distribution of histidine decarboxylase-positive fibers at four level in the forebrain (Inakagi et al., 1988).

NE and /or E innervation of the forebrain

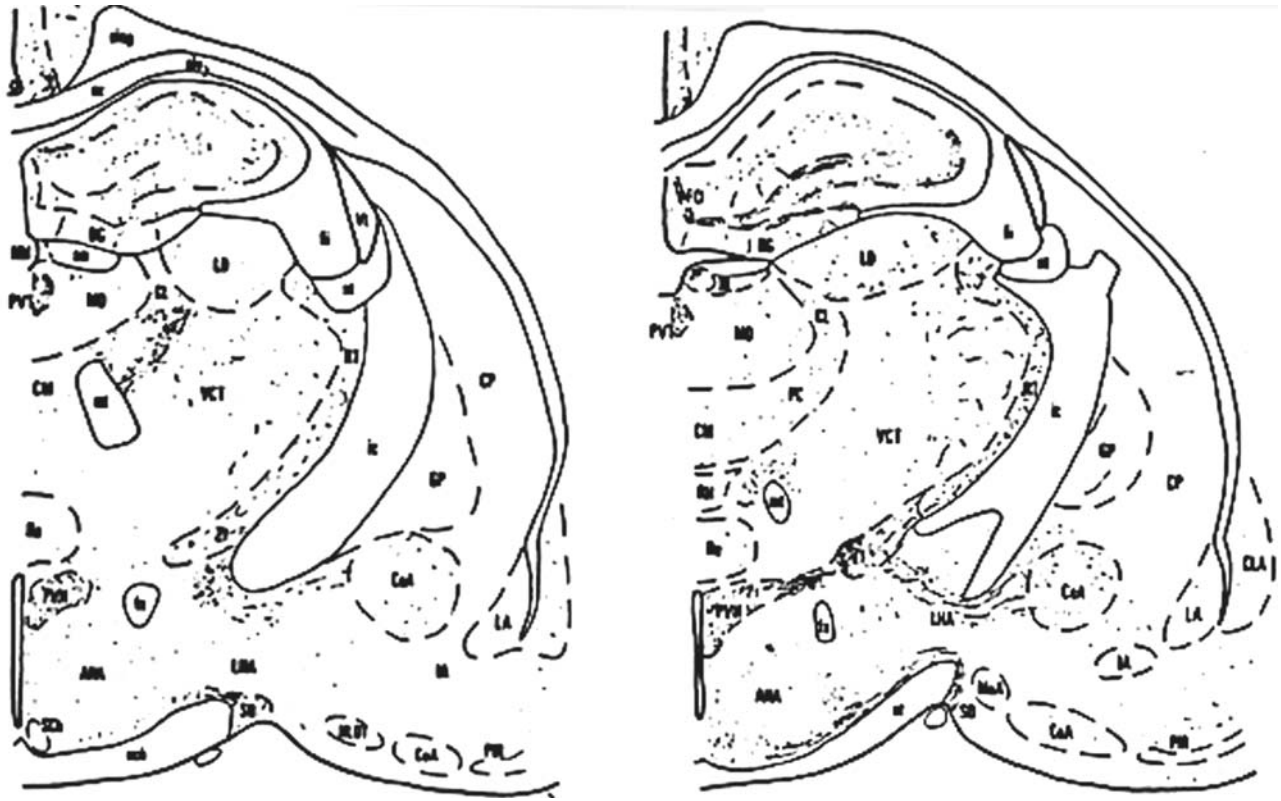

Distribution of dopamine-Beta-hydroxylase immunoreactivity at mid-thalamic level (Swanson and Hartman, 1997).

Different types of NREM sleep oscillations in the thalamocortical circuit

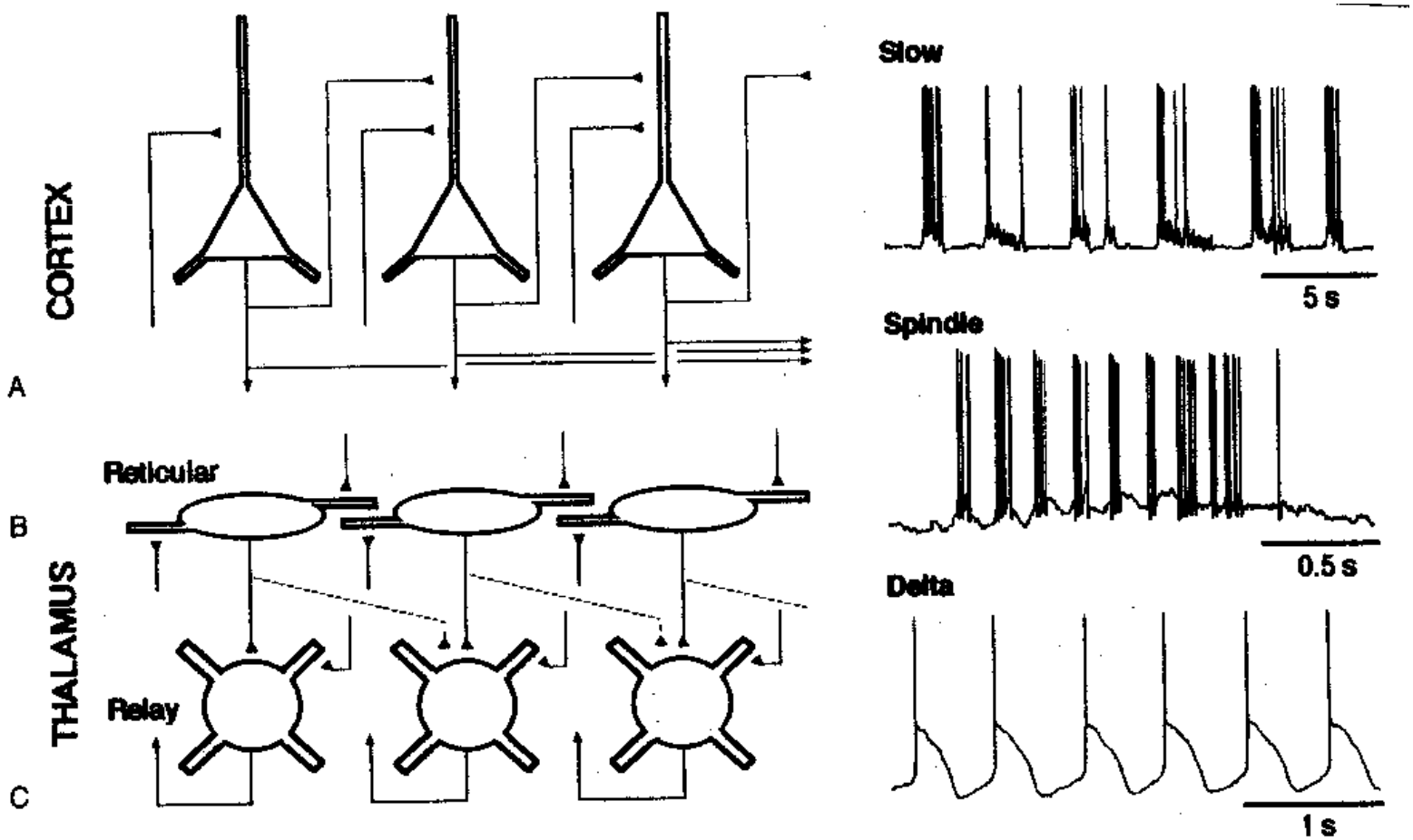

Three rhythmic electrical activities characterizes SWS: spindles (7-15 Hz) that are generated in the GABAergic RE neurons , delta waves (1-4Hz), that are generated in the cortex and thalamus and slow oscillation (0.5-1Hz) that is generated intracortically. Note the different time calibrations. (Steriade, 2000). Each of them is blocked by brainstem or forebrain cholinergic system.

Fig. 55. Coherence of cortical and thalamic spindles

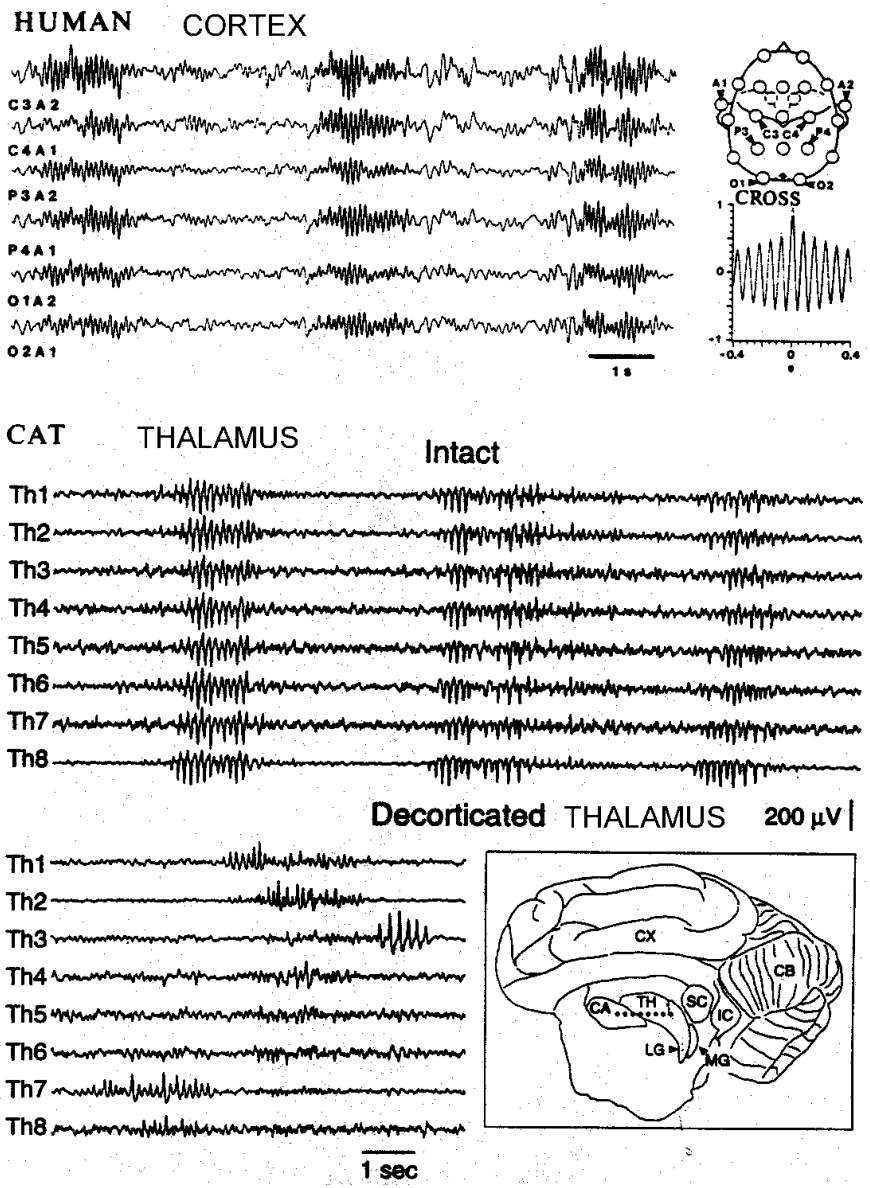

Cortical spindle sequences occur nearly simultaneously during natural sleep of humans and cats but decorticltion disorganizes the widespread coherence of thalamic spindles. Averaged correlations shows rhythmicity at 14 Hz . After decortication, recordings from virtually same thalamic sites showed disorganization of spindle simultaneity (Steriade, 2000).

Intracellular aspects of spindling in the thalamocortical system

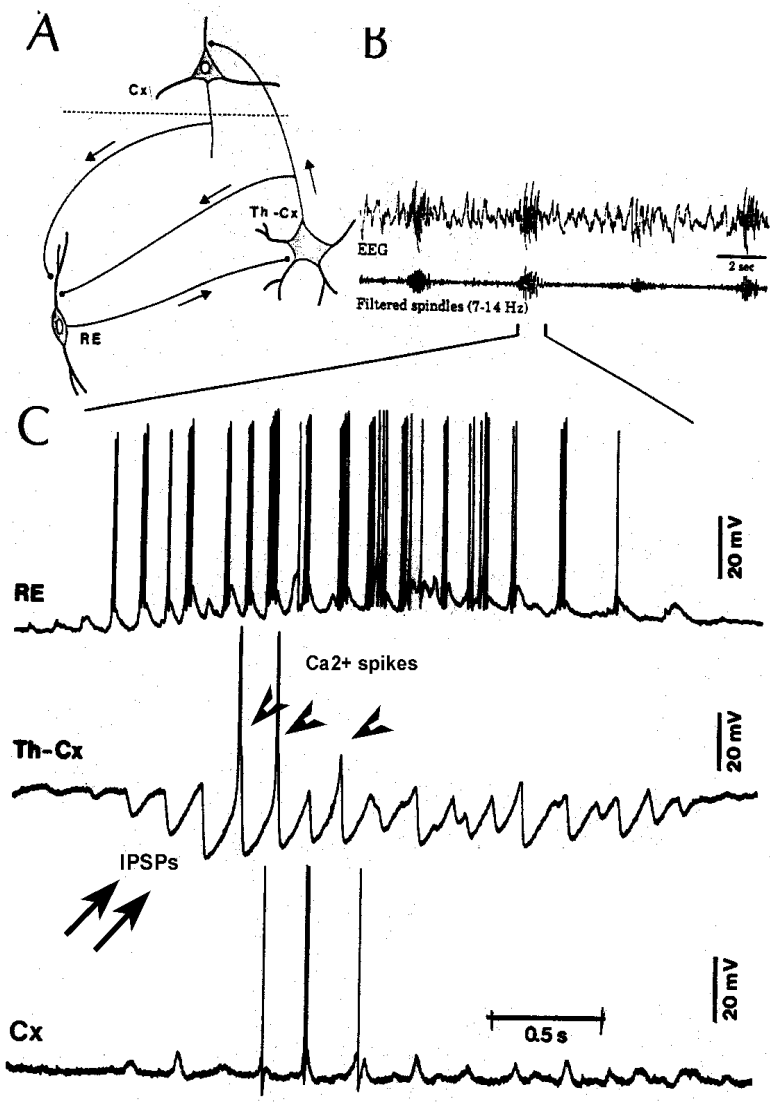

Spindle oscillations in reticular (RE), thalamocortical(Th-Cx, VL) and cortical (Cx, motor) neurons. **A**: Circuit of 3 neurons. **B**: Two rhythms (7-14 Hz and 0.1-0.2 Hz) of spindle oscillations in cortical EEG. **C**: Intracellular recording in cats under barbiturate anesthesia. Note rhythmic spike-bursts of RE neuron during a spindle sequence and concomitant IPSPs leading to post-inhibitory rebound bursts in Th-Cx and Cx neurons. (Steriade, 2002). The spikes in cortical cells is evident in the EEG as spindles.

Blockage of thalamic spindle oscillation by peribrachial stimulation

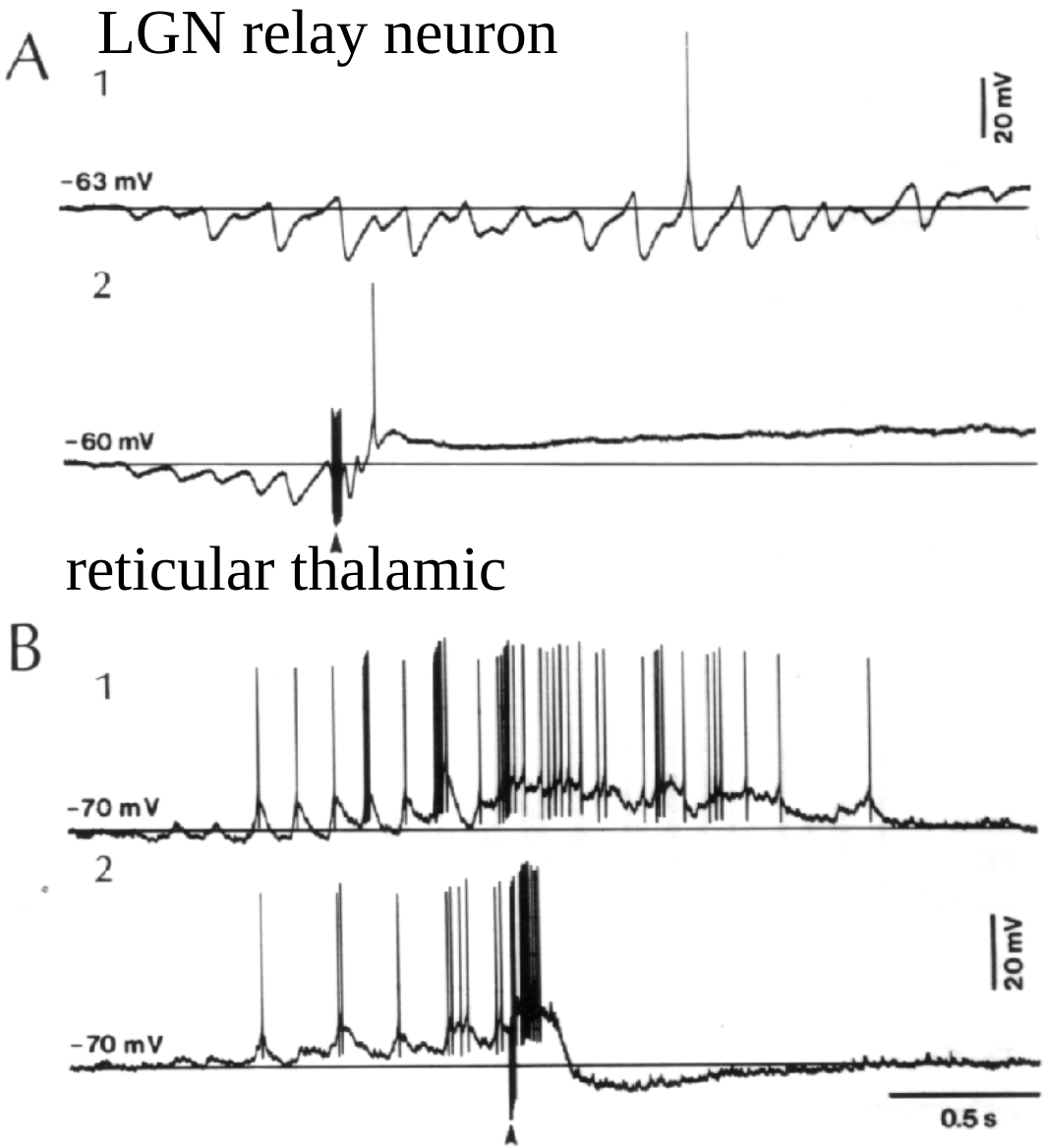

Blockage of spindle oscillations in intracellularly recorded thalamocortical and reticular thalamic (RE) neurons of unanasthetized encephale isole cats with deafferentation of trigeminothalamic pain pathways. **A**: an Lateral geniculate relay neuron.**B**: a neuron recorded in the perigeniculate sector of the RE. Arrowhead: brainstem mesopontine cholinergic (peribrachial) area stimulation. The disruption of spindles occur in the RE where sleep oscillation is generated (Hu, Steriade, Deschenes, 1989).

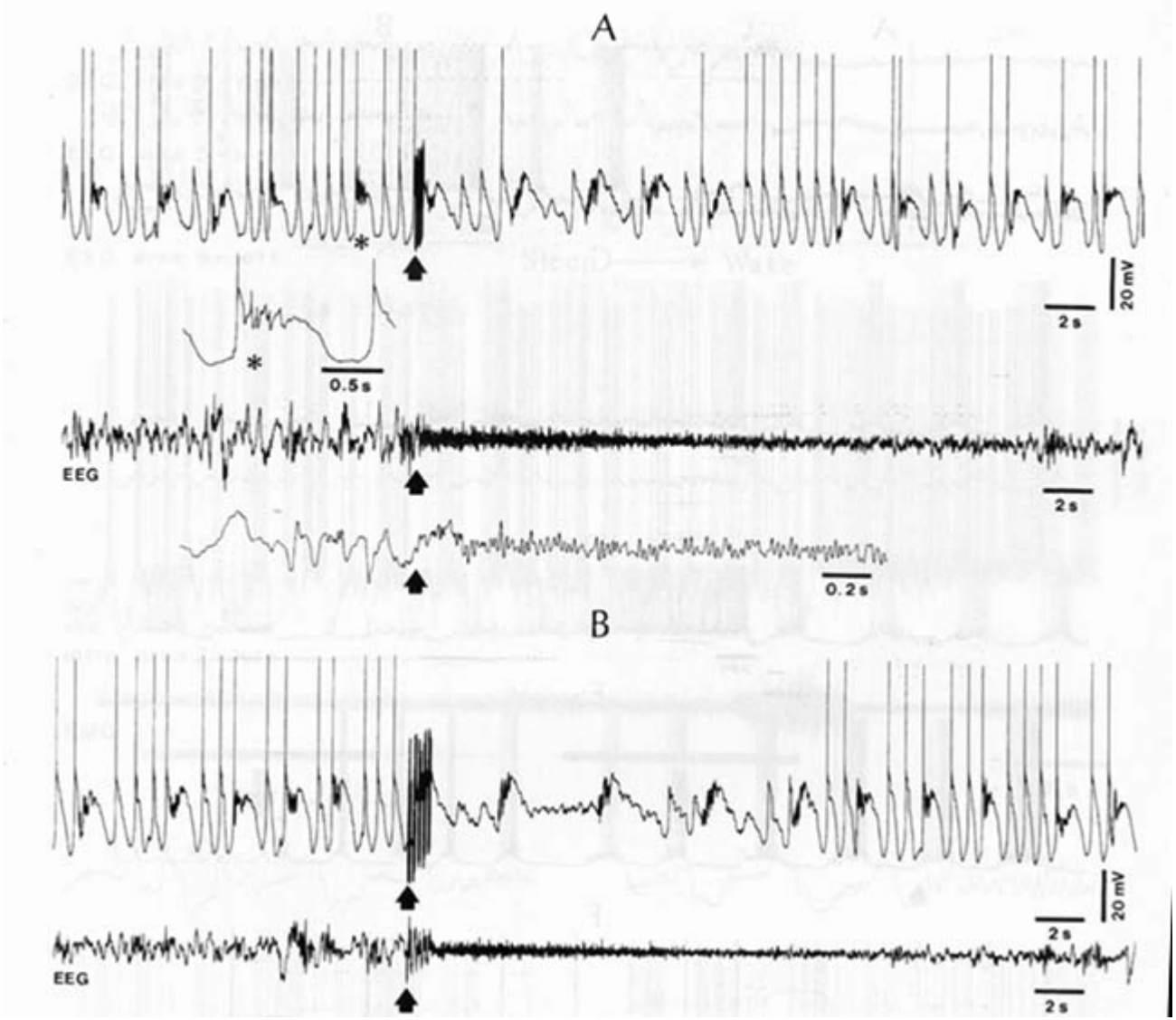

Supression of the clock-like delta oscillation in a thalamocortical cell by stimulation of the PPT and simultaneous activation of the appearance of fast (40Hz) activity. Cat, urethane anaesthesia.Intracellular recording from thalamocortical cell in the LP thalamus together with EEG from postcruciate gyrus. A: a pulse-train to PPT; B: 5 pulse trains to PPT.

State-dependent activities in cortical and thalamic neurons

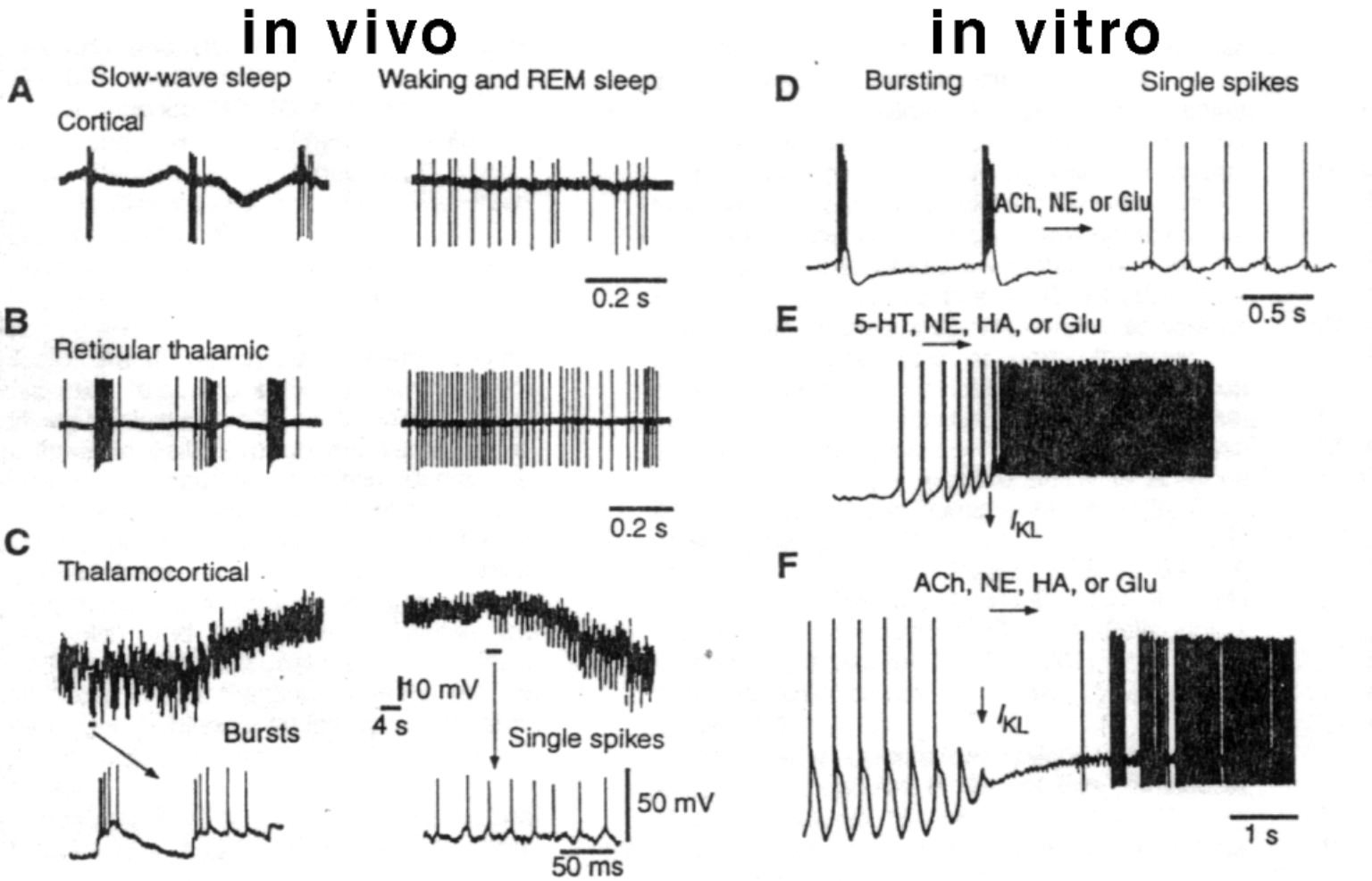

Neurons in the cerebral cortex (A), thalamic reticular nucleus (B) and thalamic relay nuclei (C) change their activities in vivo from periodic and rhythmic spike bursts during natural, SWS to tonic firing of trains of single spikes during waking and REM-sleep in behaving cats with chronic implants (D-F). Similar changes in firing pattern occur in vitro in these neurons in response to various neurotransmitters released by brainstem modulatory systems (Steriade et al., 1993).

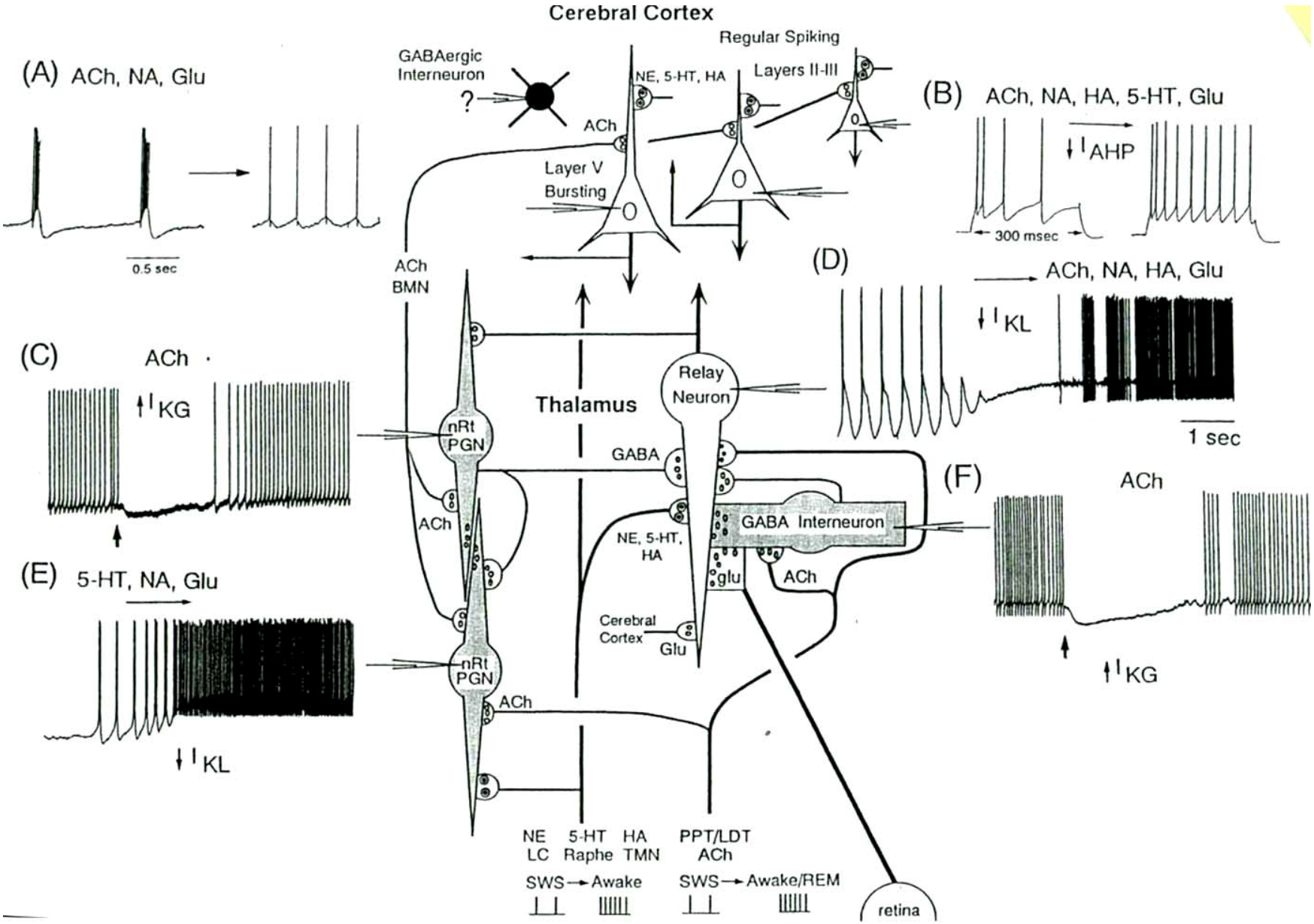

McCormick, 1997

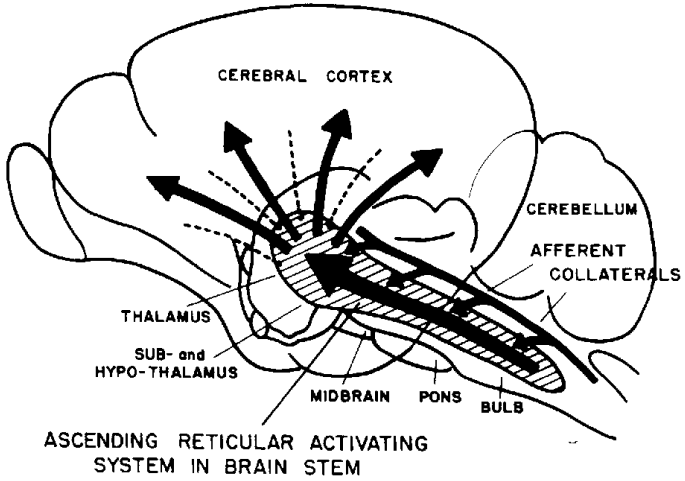

The brainstem activate thalamocortical and neocortical neurons via two routes. Thus, in contrast to the original idea of M-M, either a cholinergic-PPT/LDT –thalamocortical glutamatergic or the mesopontine-glutamate- basal forebrain cholinergic neurons are sufficient to activate the cerebral cortex.

1.Thalamocortical cells and thalamic reticular cells can generate action potentials either as rhythmic bursts or as tonic, single-spike acticvity, depending upon the membrane potential of the cell. Activation of muscarinic, alfa1-adrenergic, H1-histaminergic or metabotropic glutamate receptors (mGluR)results in depolarization of relay neurons through reduction of I_{KL}. This depolarization subsequently shifts these neurons to the single-spike mode of action potential generation. Similarly, activation of alfa1-adrenergic, 5-HT2 receptors, mGluR receptors has similar effect in the thalamic reticular neurons (McCormick, 1997).

2. In contrast, activation of muscarinic receptors in the thalamic reticular neurons or local GABAergic neurons results in inhibition of their output through an increase in potassium conductance (I_{KG}) (McCormick).

3. In the cerebral cortex, activation of muscarinic, alfa1-adrenergic, or mGluR results in abolition of burst firing of layer V burst generating neurons and a switch to tonic, single-spike mod of action potential generation. In regular spiking cells, activation of muscarinic, beta-adrenergic, Hz-histaminergic, serotoninergic and mGluR receptors results in a decrease in spike frequency adaptation by blocking I_{AHP} (and I_M for Ach and 5HT). These responses allow ascending modulatory transmitter systems to prepare thalamocortical systems for sensory transmission, processing (McCormick).

4.The three brain rhythms (spindle, delta and slow oscillation) are obliterated by brainstem cholinergic and n. basalis cholinergic and GABAergic actions exerted on thalamocortical,, thalamic reticular and neocortical neurons. The blockade of low-frequency (<15 Hz) sleep oscillations, which are widely synchronized, is accompanied by the occurrence of fast (20-60Hz) rhythms, which are synchronized over restricted cortical territories and well defined corticothalamic systems. The fast rhythms appear during the sustained depolarization of thalamic and neocortical neurons in wakefulness and REM sleep, as well as during the depolarizing phases of the slow oscillation in non-REM sleep. Thus, fast rhythm are voltage dependent and do not necessarily reflect high cognitive and conscious processes (Steriade, 2004).

THE REM SLEEP

REM sleep phenomenon

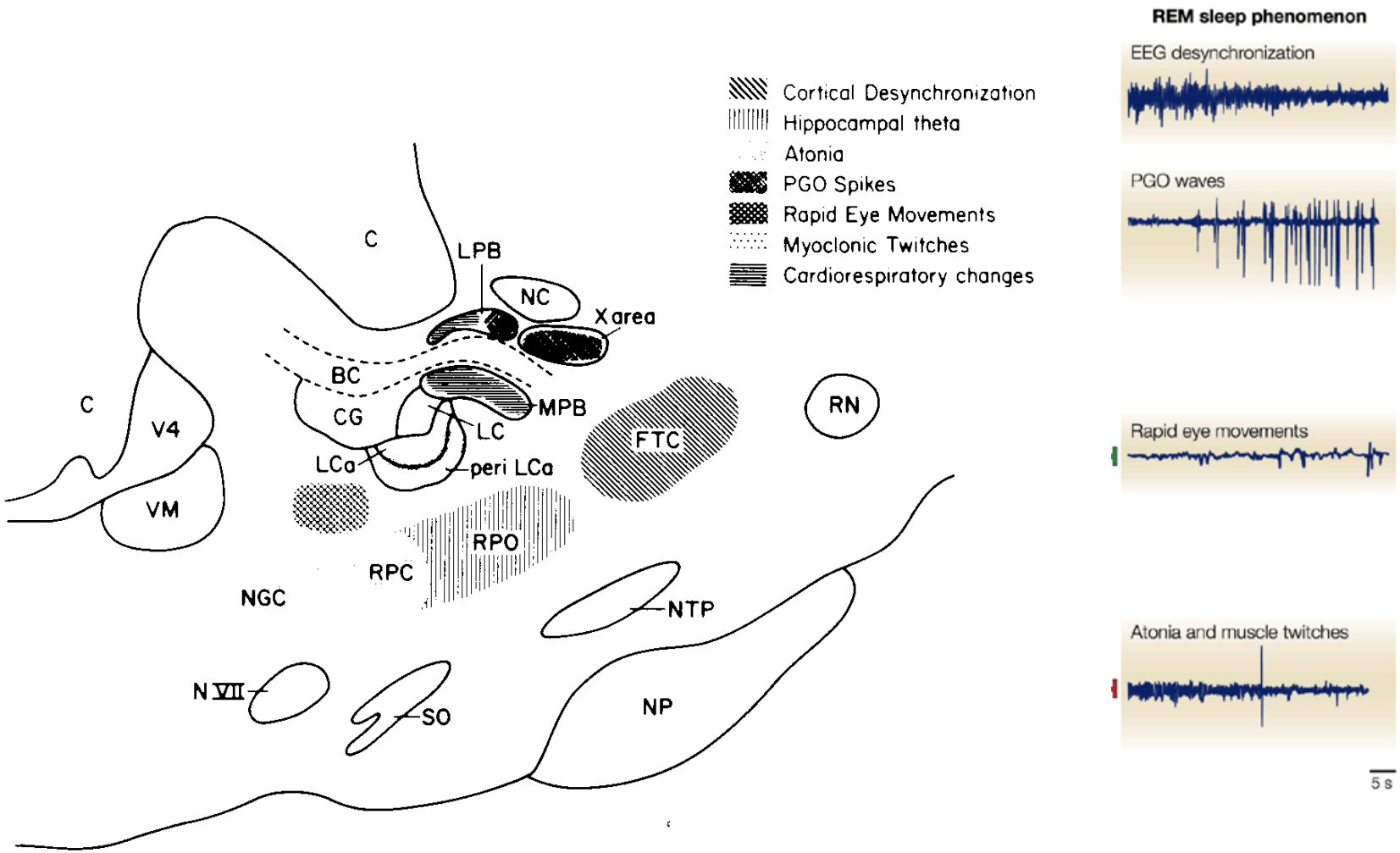

EEG desynchronization results from a net tonic increase in reticular (cholinergic) ascending, thalamocortical and cortical neuronal firing rates. PGO wawes are the results of tonic disinhibition and phasic excitation of burst cells in the lateral pontomesencephalic tegmentum. Rapid eye movements are the consequence of phasic firing of vestibular cells; the latter excite ocolomotor neurons.

Circuitry involved in muscle paralysis that occurs during REM sleep

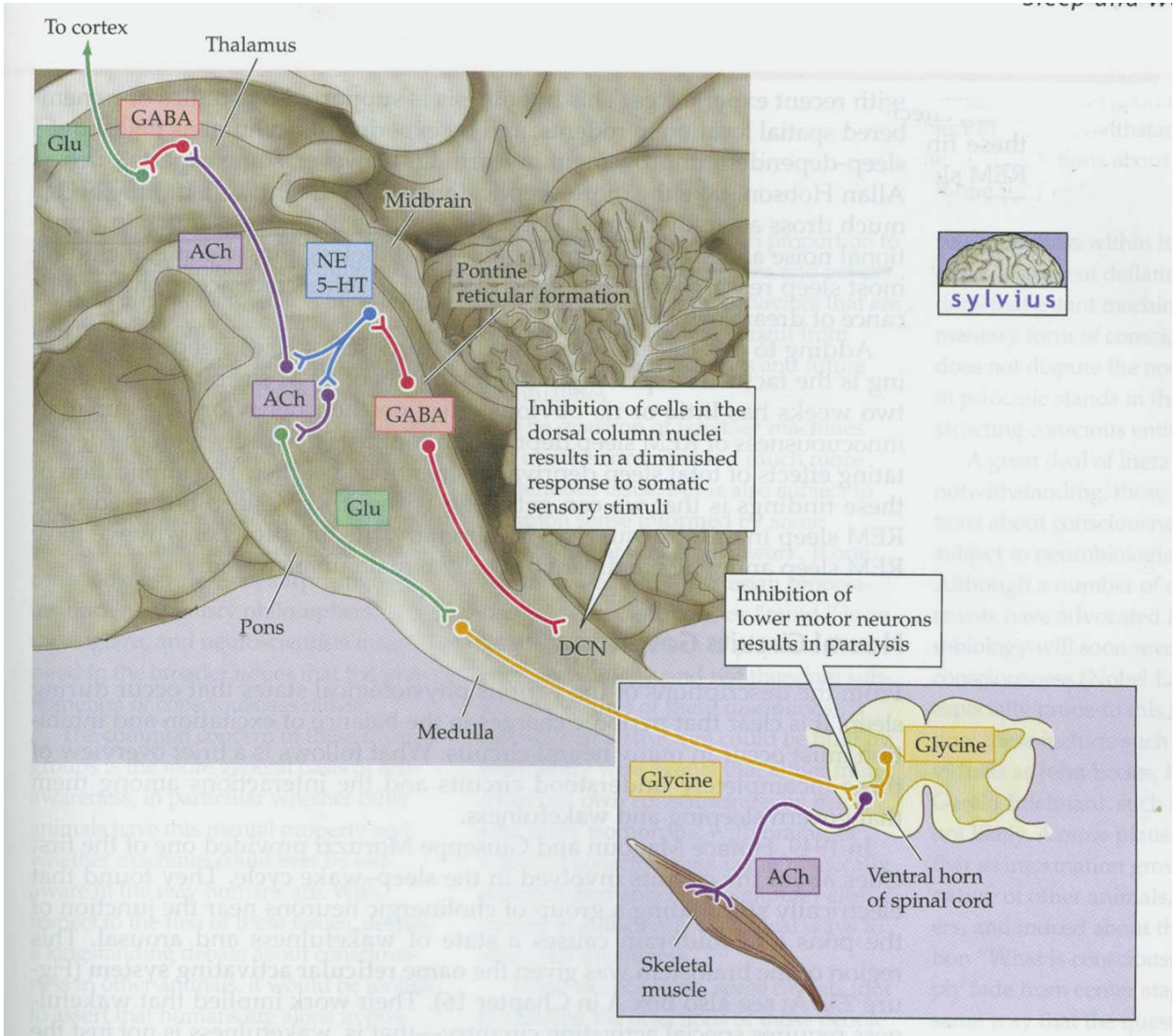

Purves et al., 2004

Muscle atonia is the consequence of tonic postsynaptic inhibition of spinal anterior horn cells by the pontomedullary reticular formation. Muscle twitches occur when excitation by reticular and pyramidal tract motorneurons phasically overcomes the tonic inhibition of the anterior horn cells.

REM –non-REM oscillation I

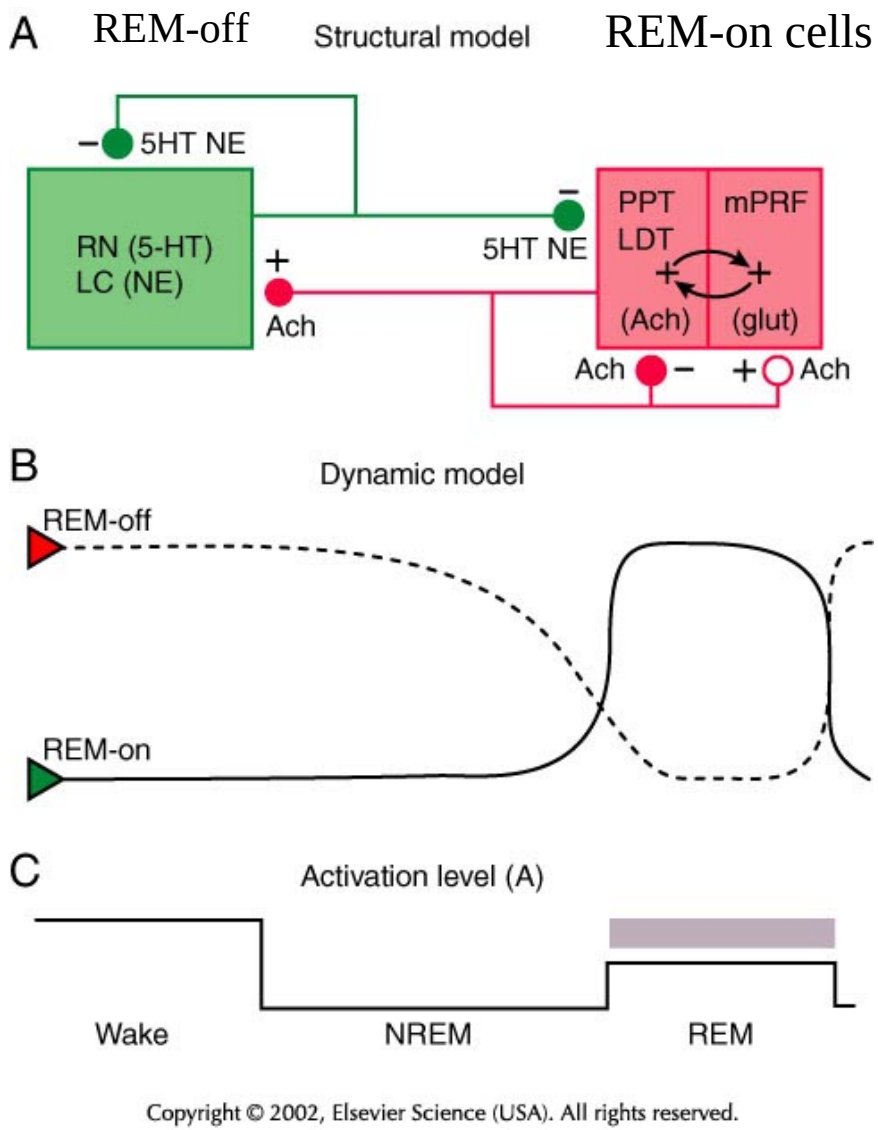

5HT inhibition in the PPT

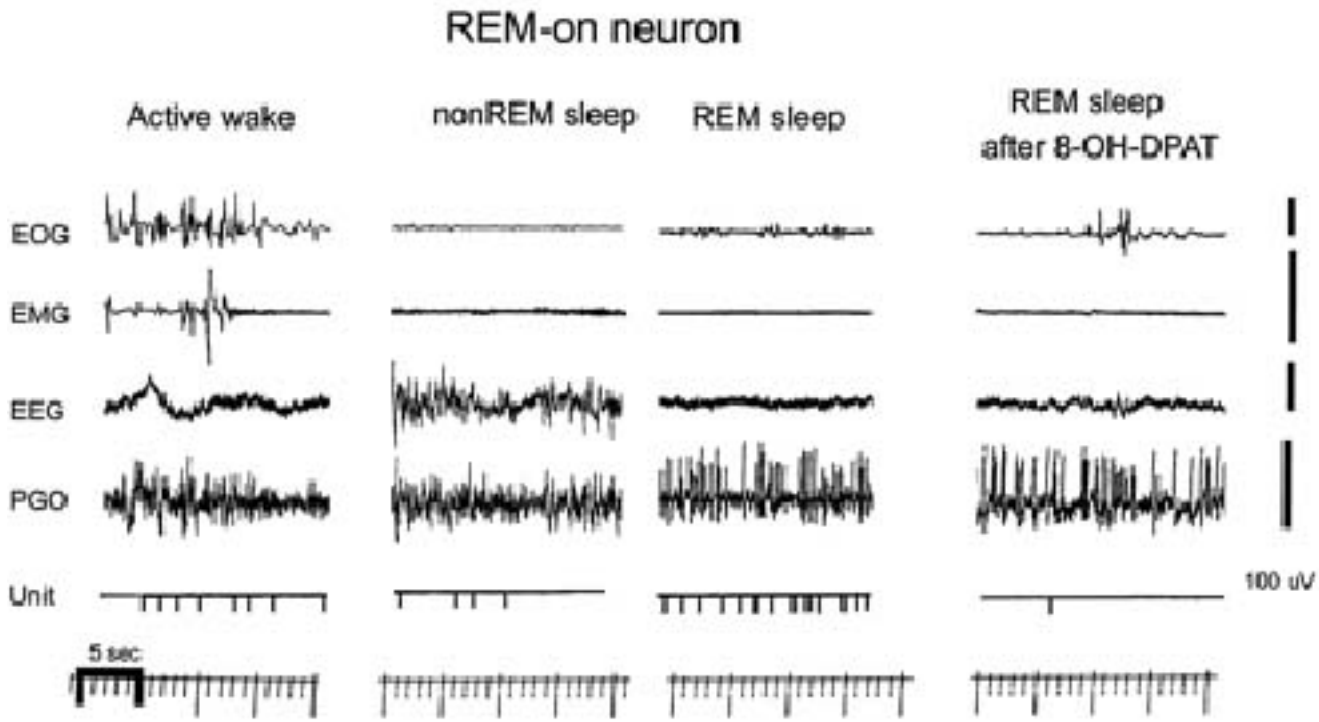

Digitized inkwriter record of **REM-on** unit discharge in the PPT area of naturally sleeping cats. Note the low level of unit activity in active wakefulness, which continues in non-REM sleep, but increases more than two-fold in REM sleep. 8-OH-DPAT, a selective 5-HT1A agonist dramatically suppressed unit activity in the same REM-period. (Thakkar et al., 1998).

REM-non-REM oscillation I I

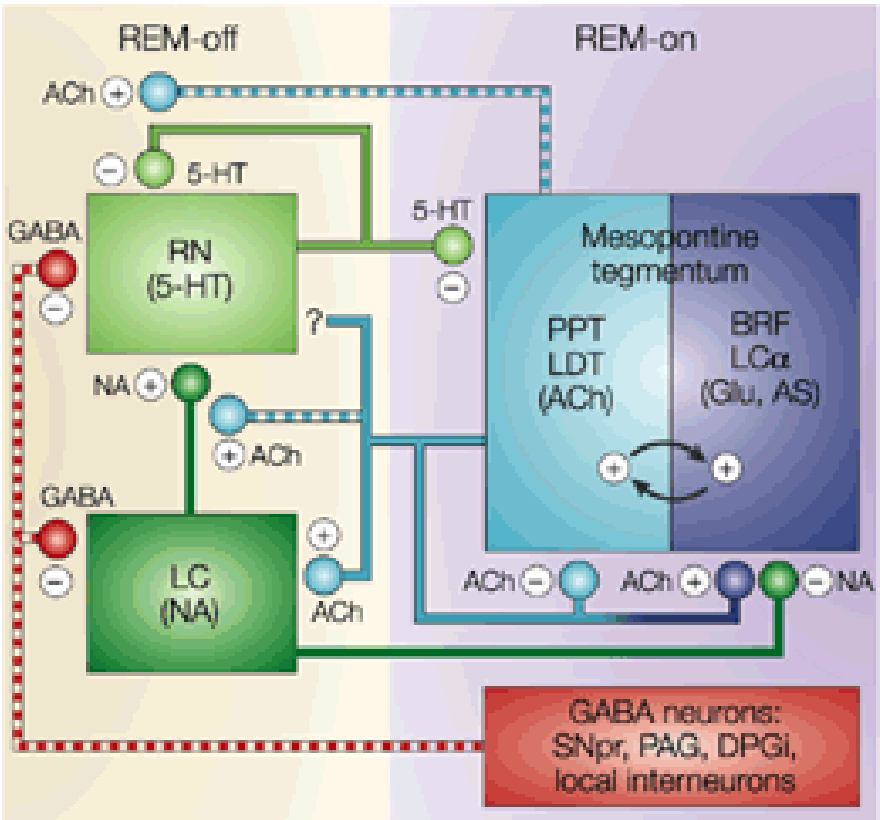

The reciprocal-interaction model of REM-NREM alternation. **REM-on cells** are the cholinergic cells in the PPT/LDT area, GABAergic local or projection neurons neurons in the ponto-medullar reticular formation (DPGi), periaqueductal gray (PAG), and in the substantia nigra pars reticularis. There are also putative glutamatergic REM-on neurons in the reticular formation. **REM-off** cells are the noradrenergic locus coeruleus (LC) and the serotoninergic (5-HT) raphe (RN) neurons. Note that there are self-inhibitory cholinergic autoreceptors in the mesopontine cholinergic nuclei. Also, the noradrenergic (NA) and 5-HT fibers inhibit the wake-REM-on neurons (Pace-Schott and Hobson, 2002).

THE HOMEOSTATIC REGULATION OF SLEEP-WAKE CYCLE

Adenosine as the homeostatic drive for sleep

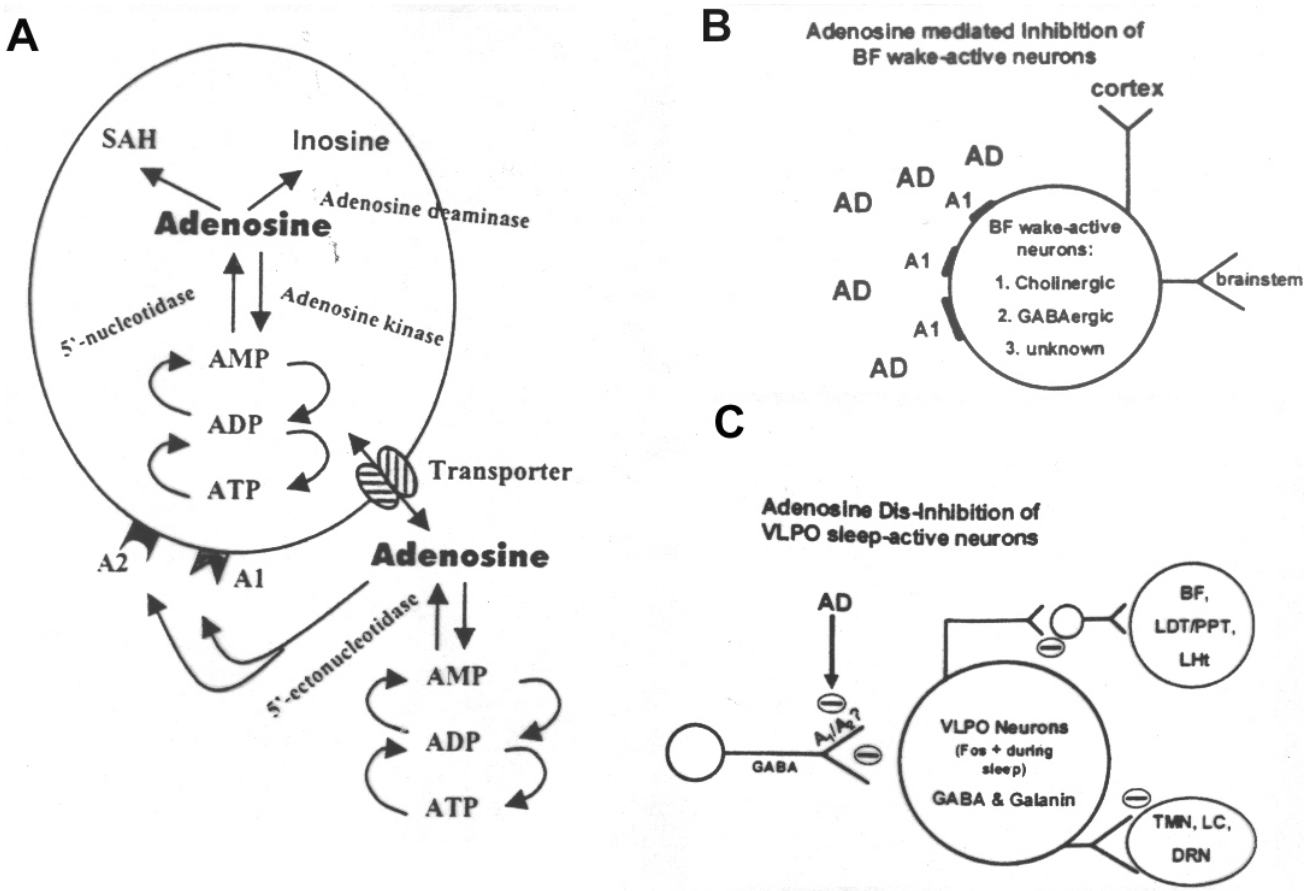

A: Schematic of the main intra- and extracellular metabolic pathways of adenosine. A1, A2 adenosine receptor subtypes. **B**: The BF region contains numerous cholinergic and non-cholinergic wake-active neurons that project to the cortex and thalamus and whose activity is thought to promote cortical activation. Adenosine is proposed to inhibit the activity of these neurons possibly via A1 receptor mediated hyperpolarization.

C: The hypothalamic preoptic area (POA/VLPO) contains sleep-active neurons and send inhibitory projections directly to all major monoaminergic cell groups and indirectly to the cholinergic (PPT,LDT,BF) and lateral hypothalamic neurons. AD can activate neurons in the POA via an inhibition of presynaptic GABA release onto the putative sleep-active neurons.Functionally, these two mechanisms are complementary, ie. Increased AD levels in either area is predicted to reduce W and promote the transition to sleep (Strecker et al., 2000).

Intracellular pathways of adenosine

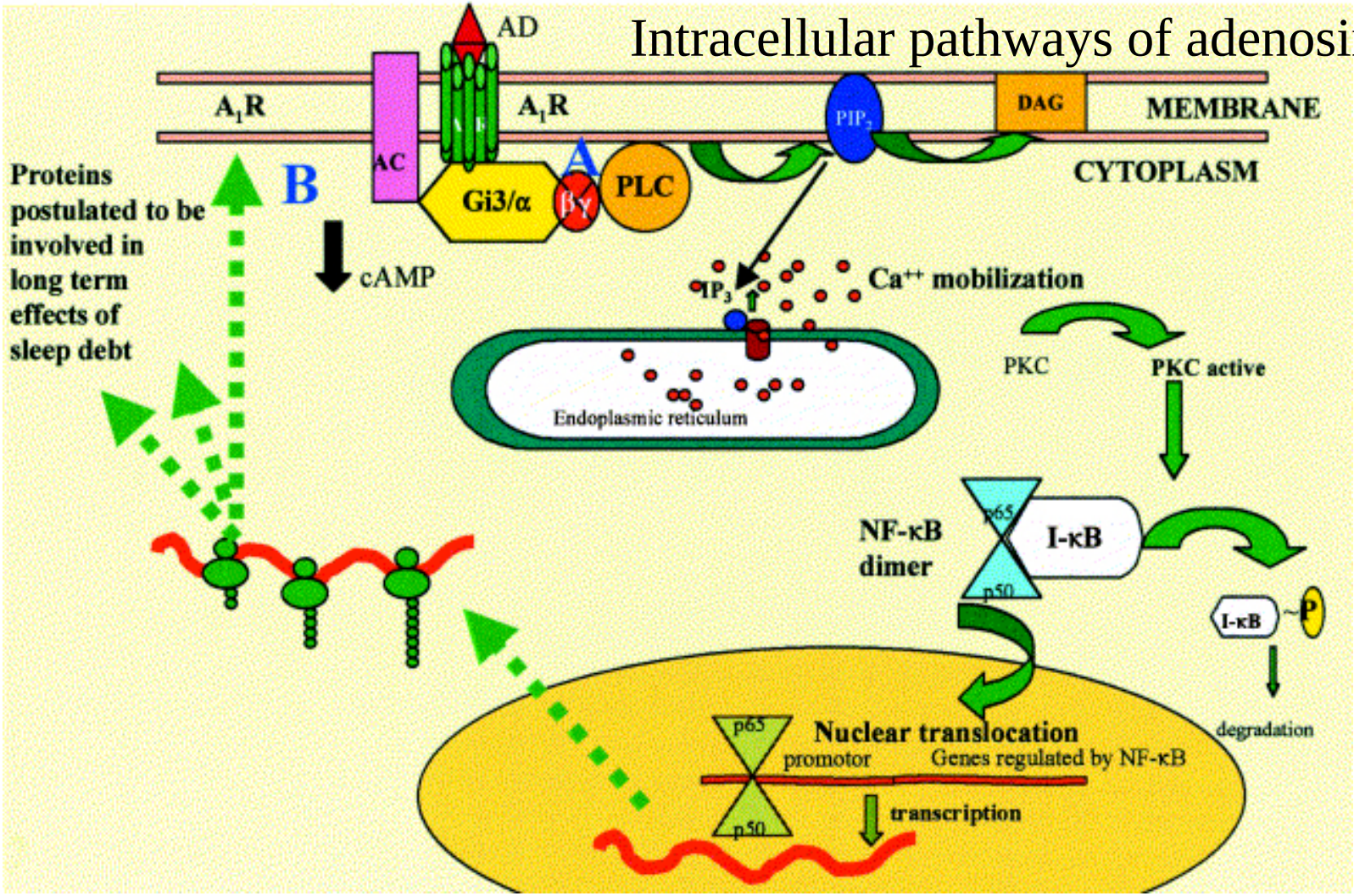

The A1 adenosine receptor (A1 R) is coupled to Gi3 protein that can either activate the pathway B, by inhibiting adenylate cyclase (AC), or increase in adenosine levels might activate another pathway A by activating PLC, resulting in the activation of PKC due to the mobilization of internal Ca2+ by IP3. PKC can phosphorylate I-B, releasing NF-B dimer to be translocated into the nucleus. The phosphorylated I-B is degraded in the cytoplasm. The NF-B dimer regulates transcription of several genes that have the NF-B consensus sequence upstream from their promoter. This pathway may result in the production of proteins, including the A1 adenosine receptor, that may play a role in producing the long-term effects known as sleep debt (Basheer et al., 2001).

Wake-sleep switch and adenosine

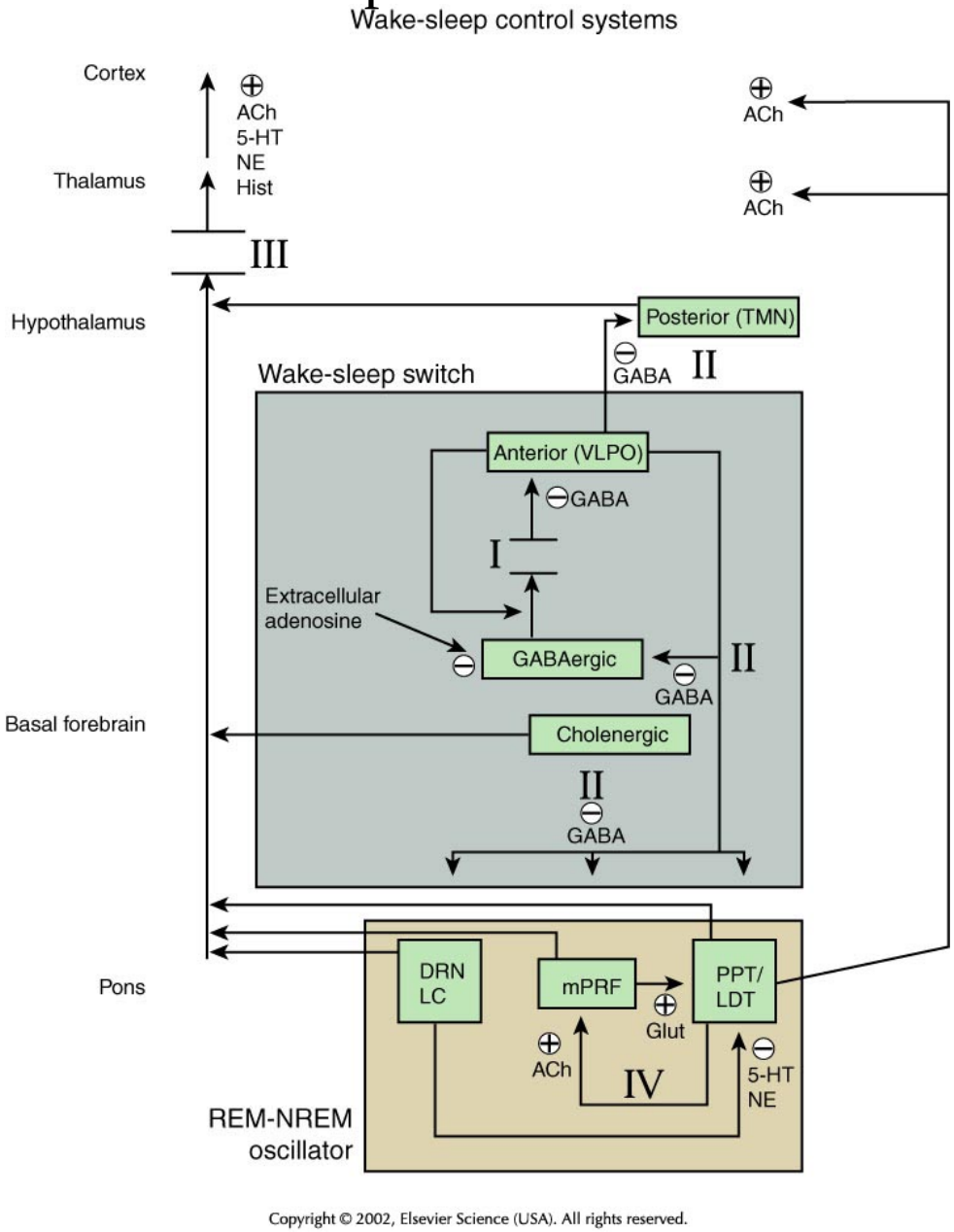

I. During prolonged wakefulness, accumulating adenosine inhibit specific GABAergic anterior hypothalamic neurons that innervate the sleep-active VLPO neurons during waking.

II: Disinhibited sleep-active GABAergic neurons of the VLPO then inhibit the wake active histaminergic neurons of the TMN, and the serotoninergic DRN and noradrenergic LC and cholinergic PPT/LDT neurons, thereby initiating NREM sleep.

III: Forebrain activation by ascending aminergic and orexinergic arousal systems is disfacilitated.

IV: Once NREM sleep is thus established, the executive networks of the pons initiate and maintain the ultradian REM/NREM cycle.

THE CIRCADIAN REGULATION OF SLEEP-WAKE CYCLE

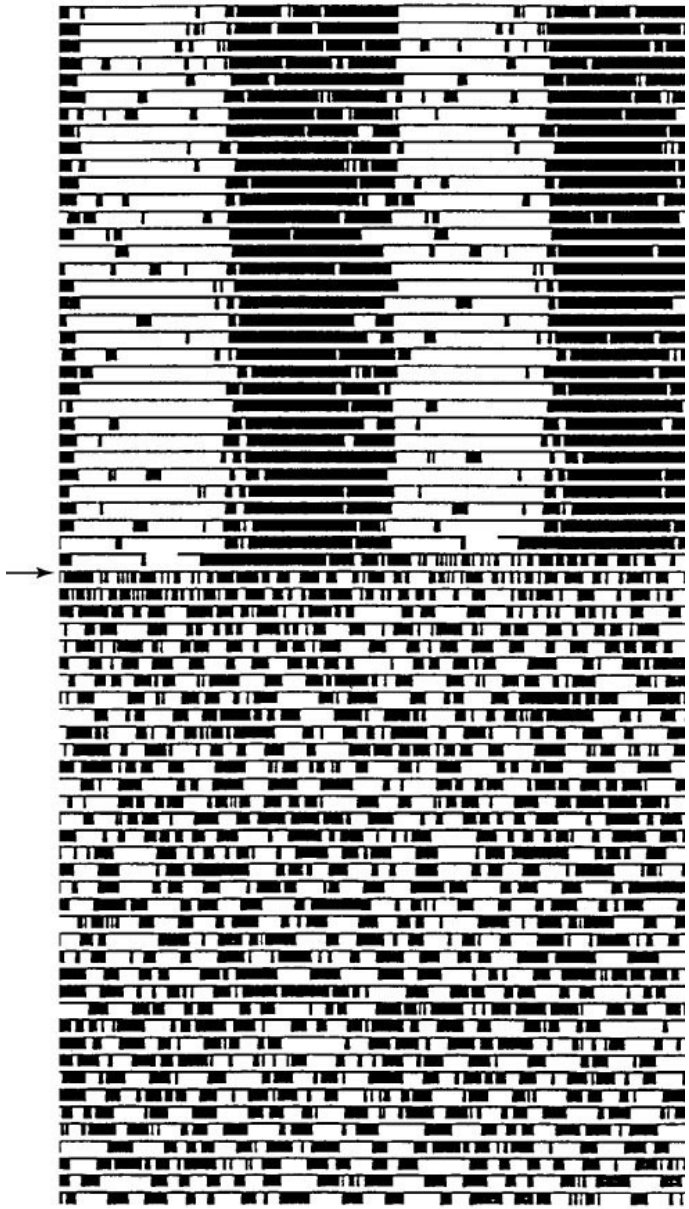

This is a record of activity of an albino rat maintained in a light-dark cycle. From the top of the record to the arrow, the animal exhibits a normal rhythm of activity, indicated by dark areas. The record is double plotted, which means that each line shows the preceding day and the new day to ease evaluation of the record. At the arrow, a bilateral SCN lesion was performed. Activity is distributed randomly thereafter, meaning circadian organization of rest-activity has been lost (Moore, 2002). In the absence of the SCN the total amount of sleep is unchanged, but there is no day/light variation (timing) in sleep

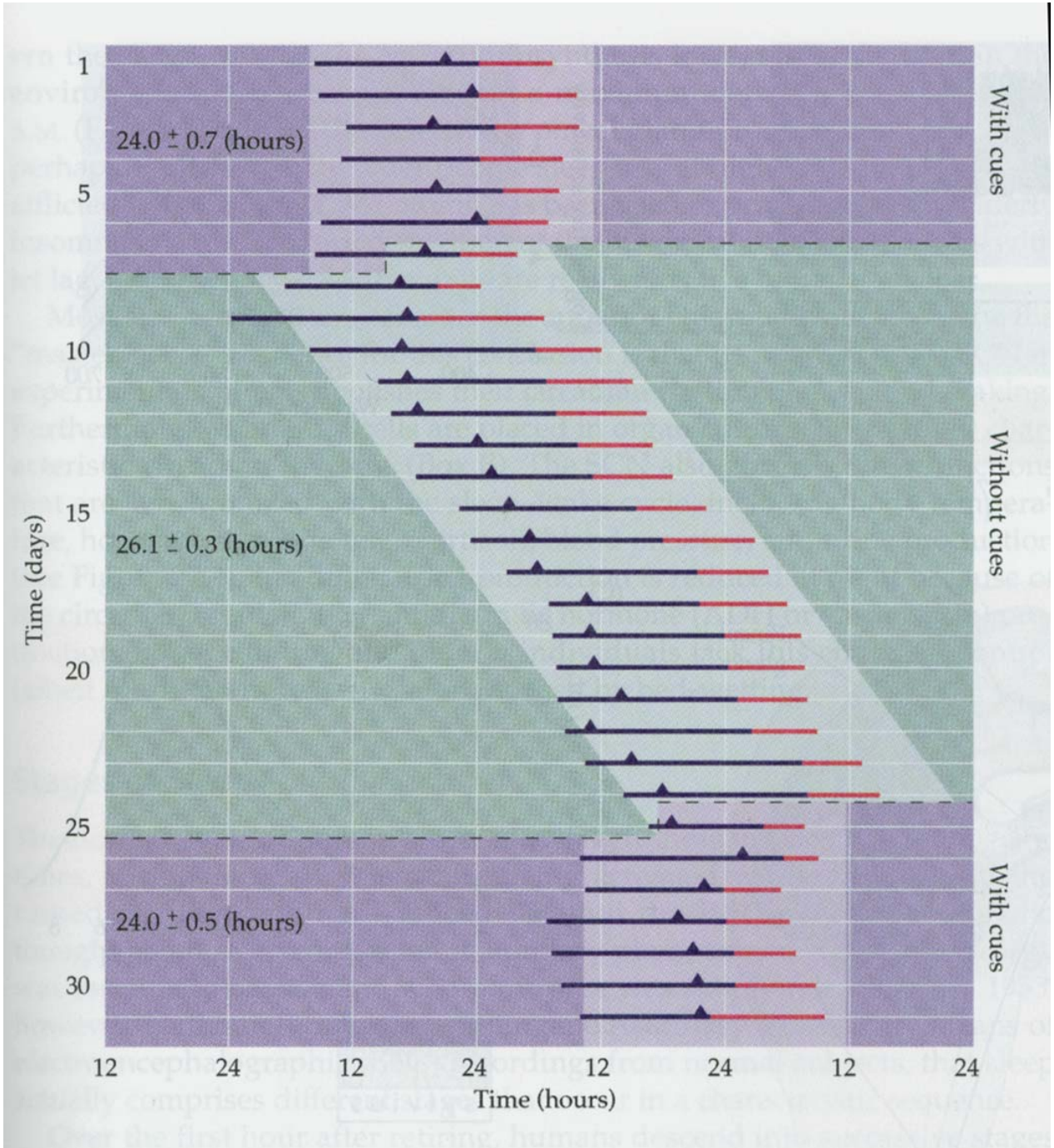

Rhythm of waking (blue lines) and sleeping (red) of a volunteer in an isolation chamber with and without cues about the day-night cycle. Numbers represent the mean+SD of a complete w-s cycle in each condition (Scchmidt et al., 1983)

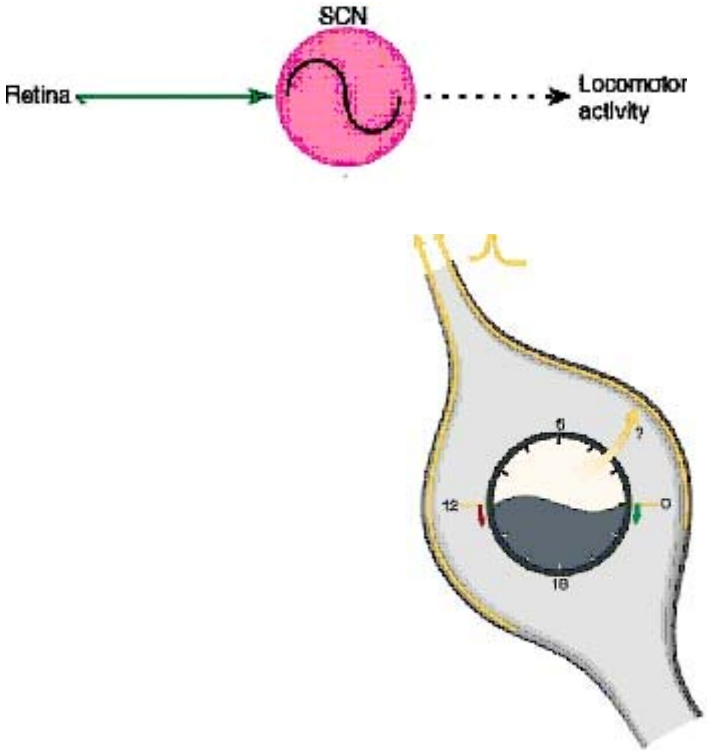

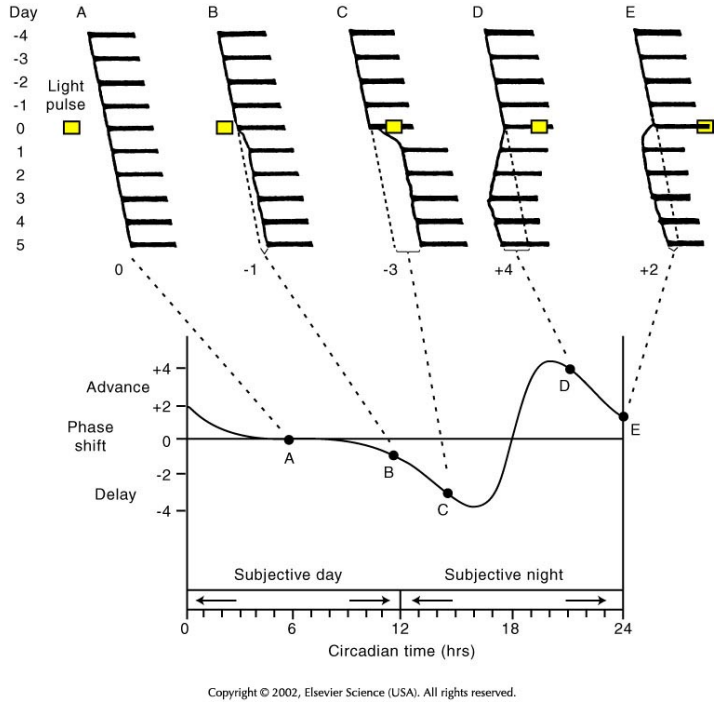

The light phase response curve (PRC). With animals maintained in constant dark, activity is recorded (horizontal bars) and light pulses are given as indicated. Light establishes both the phase and the period of the pacemaker and thus, is the dominant entraining stimulus of the circadian system. The pacemaker can be viewed as a somewhat inaccurate clock, which must be reset repeatedly. It free runs with a period that is slightly off 24 h in the absence of light-dark cycle. The light-dark cycle sets the exact timing of the pacemaker. The PRC shows that the pacemaker responds differently to light at different times of the day (Moore, 2002). The left side of the figure provides a schematic illustration of how individual SCN neuron is able to mimic the day (L) signal with its molecular clock, resulting in membrane depolarization. This membrane depolarization results in propogation of the light signal to target neurons of the SCN and to phase shift of the molecular clock: phase delay (red arrow) or phase advance (green). Without the molecular clock, the light signal will still be transmitted to SCN targets. However, without the SCN, no signal will activate SCN target structures,(Buis and Kalsbeek, 2001).

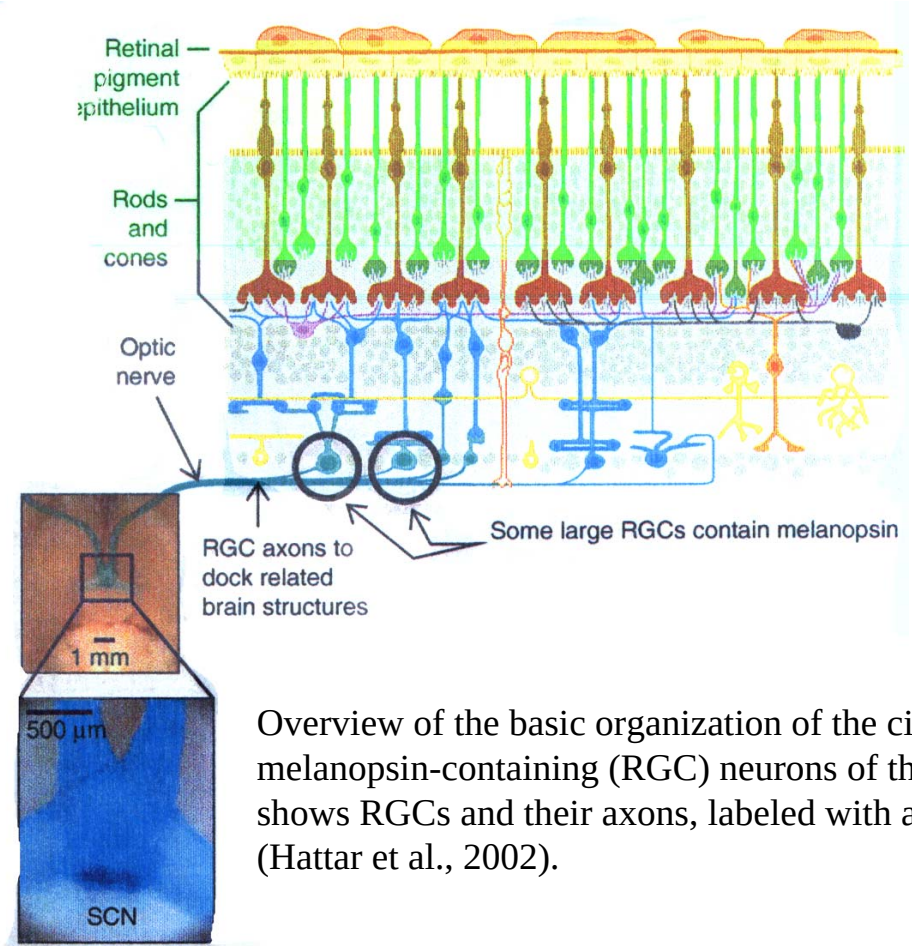

Overview of the basic organization of the circadian timing system. Information from the light-sensitive, melanopsin-containing (RGC) neurons of the retina reach the SCN, the circadian pacemaker. Inset shows RGCs and their axons, labeled with a tau-lacZ marker, connecting with the SCN in mouse brain (Hattar et al., 2002).

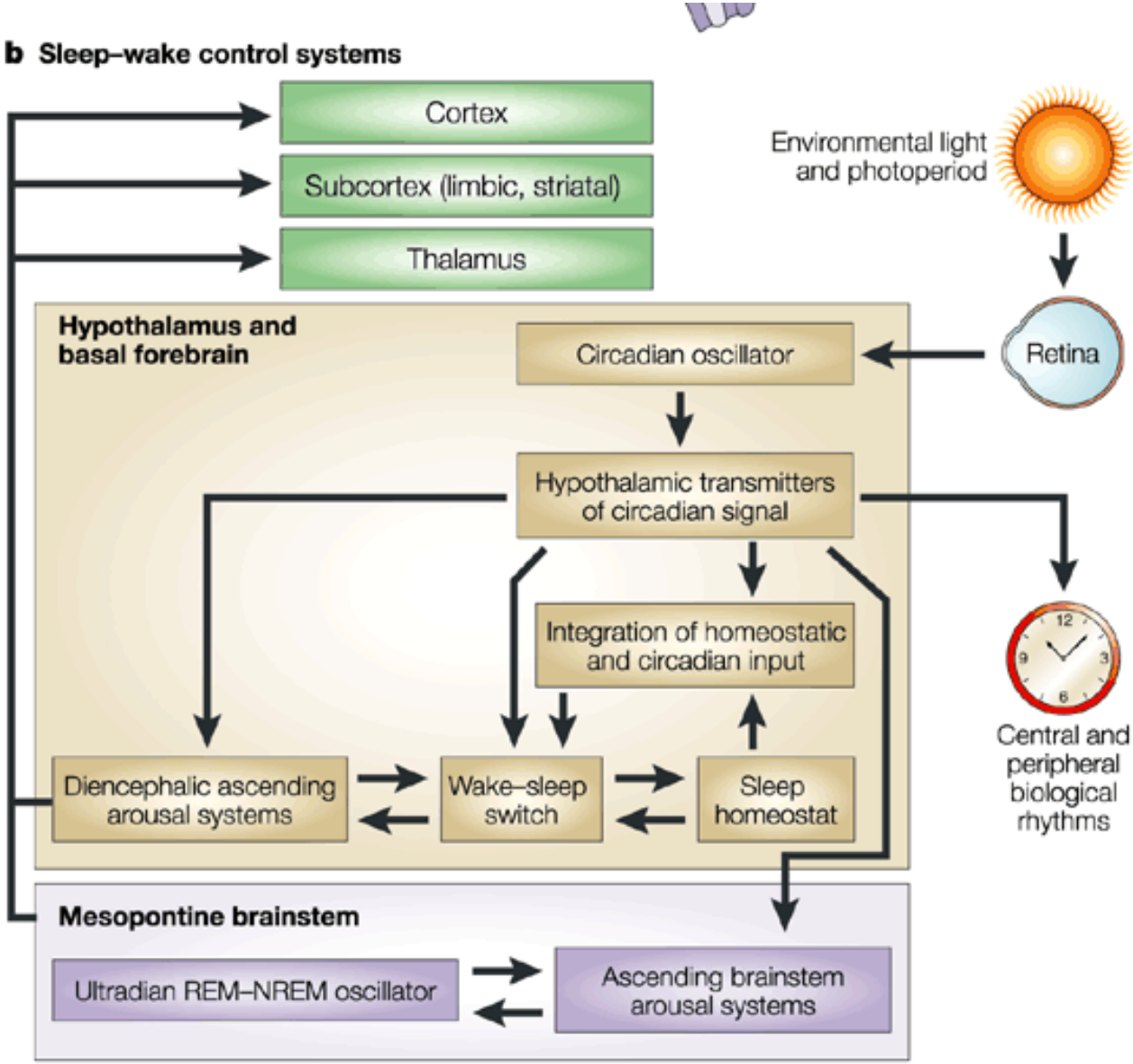

Nature Reviews | Neuroscience

Lesion of the hypothalamic n. DM eliminate the circadian firing of the LC

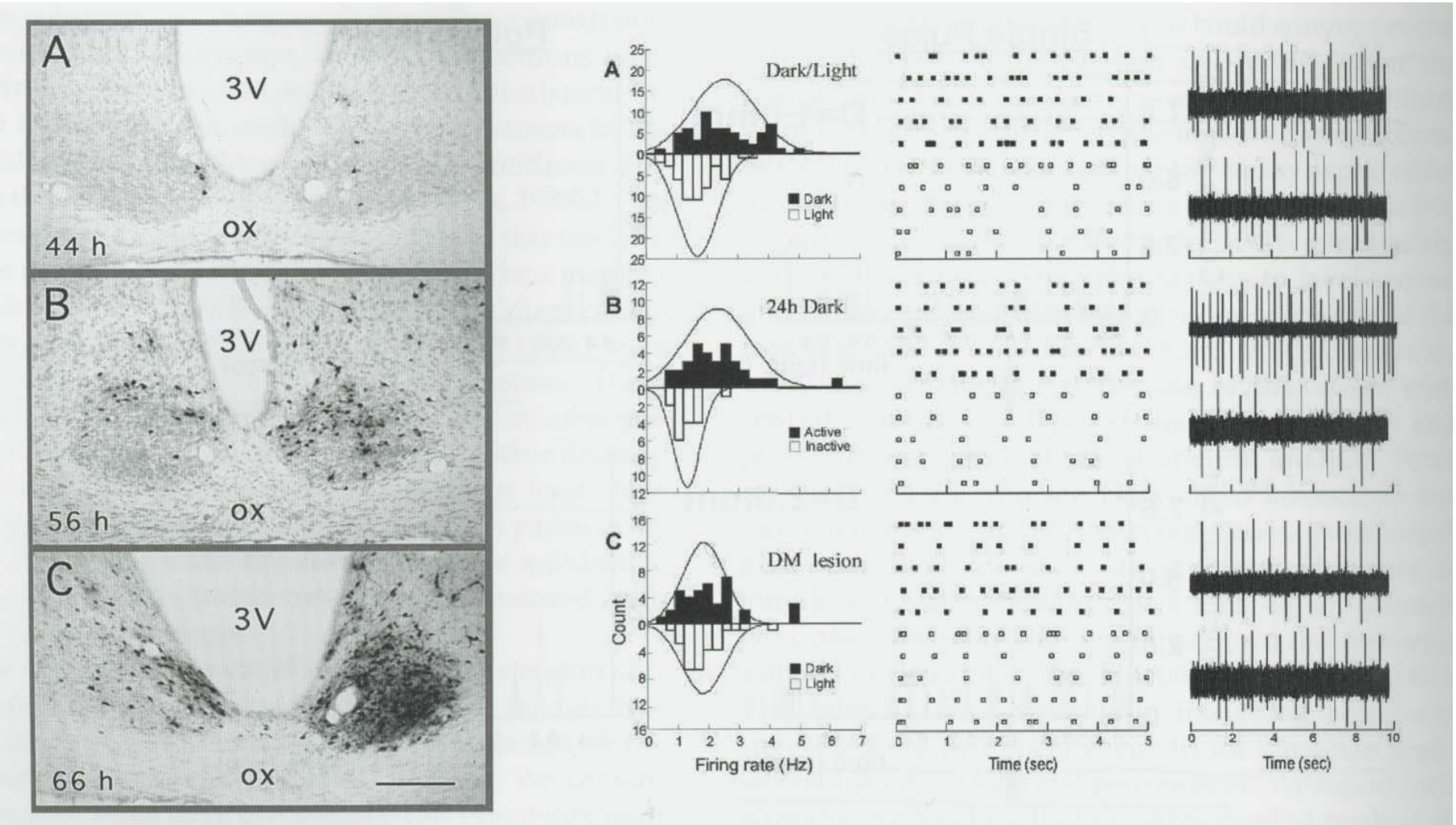

A-B-C herpes virus retrograde tracing from the locus coerules. Lesion in the DM eliminate labeling in suprachiasmatic nucleus and stop circadian firing of the LC (From Aston-Jones, 2004)

POSSIBLE CONENCTIONS BETWEEN TH E CIRCADIAN PACEMAKER AND THE SLEEP-WAKE CONTROL SYSTEMS

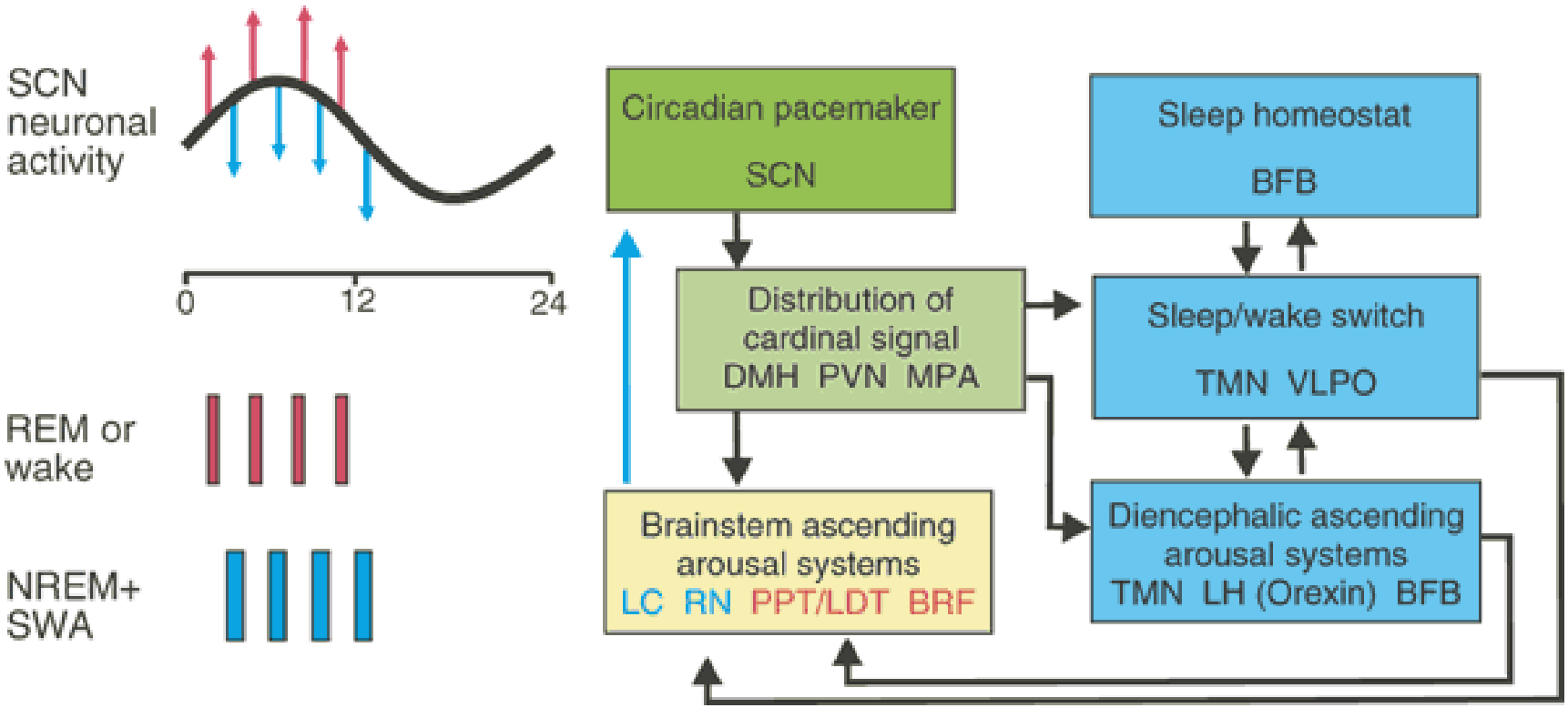

The circadian timing signal generated in the SCN is transmitted through nuclei in the anterior hypothalamus to sleep/wake control systems of the diencephalon (blue) and then to structures in the brainstem controlling REM-NREM cycling (yellow). BFB=basal forebrain. BRF=brainstem reticular formation. Circadian influence can reach the VLPO either directly from the SCN or through the dorsomedial hypothalamic nucleus that receive dense projections from the SCN (Pace-Schott and Hobson, 2002; Colwell and Michael, Nature Neurosci, 6, 1005, 2003).

Coordination of sleep, feeding, thermoregulation, etc by the circadian signal

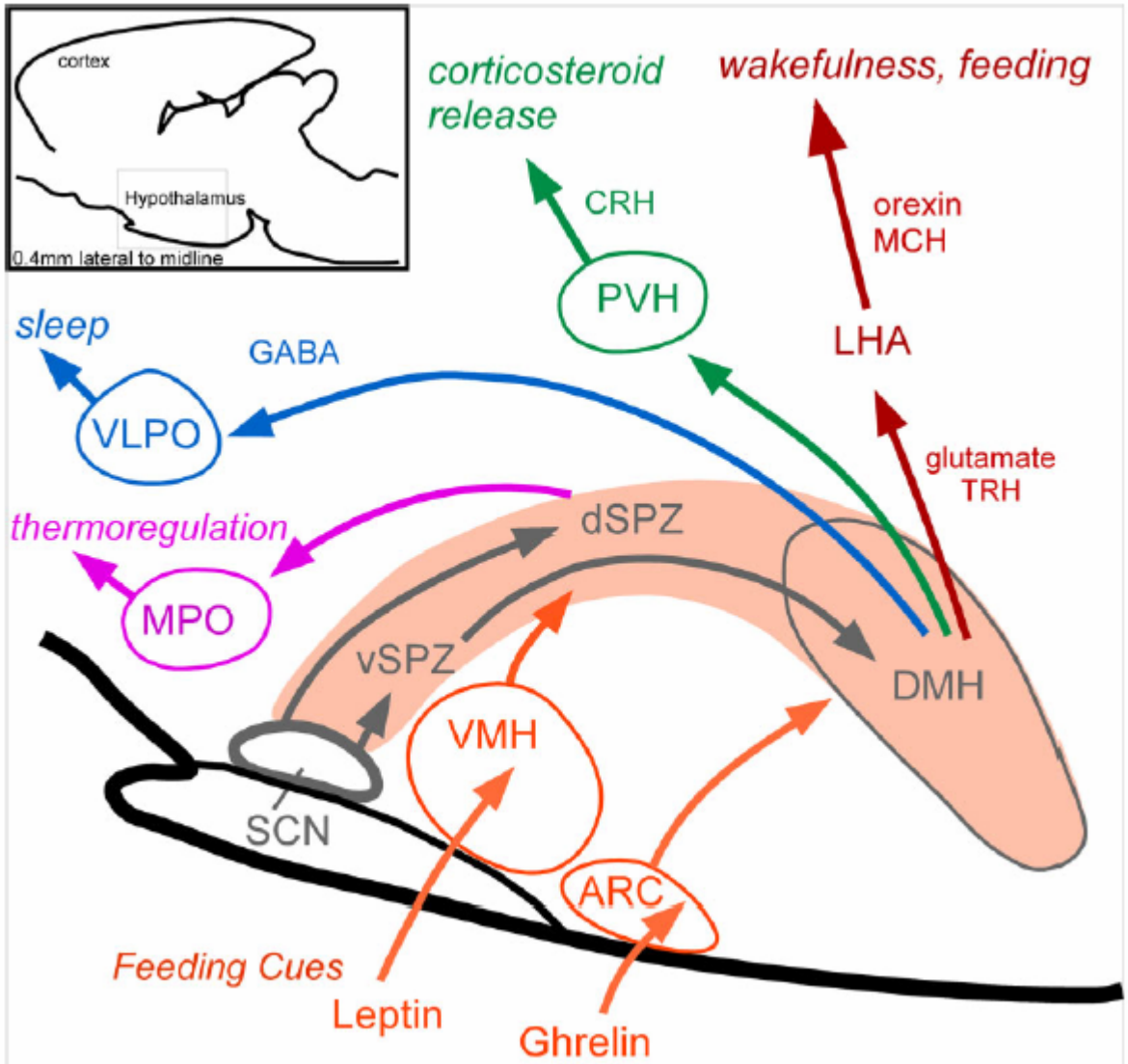

A summary diagram to illustrate the major pathways that translate the output from the brain's biological clock (the suprachiasmatic nucleus) into circadian rhythms of sleep, feeding, corticosteroid secretion, and body temperature. The suprachiasmatic nucleus sends the bulk of its output into a column (the orange shaded area) that consists of the subparaventricular zone and the dorsomedial nucleus of the hypothalamus. The purpose of this three-stage integrator for regulating circadian rhythms may be that it allows flexibility in organizing daily schedules. For example, animals that are given food only during the normal sleep cycle soon invert their circadian cycle to be awake when the food is presented. Feeding-related signals such as leptin or ghrelin may enter the hypothalamus and be relayed by the ventromedial nucleus and arcuate nucleus to the subparaventricular zone and dorsomedial nucleus, to influence circadian rhythm organization.

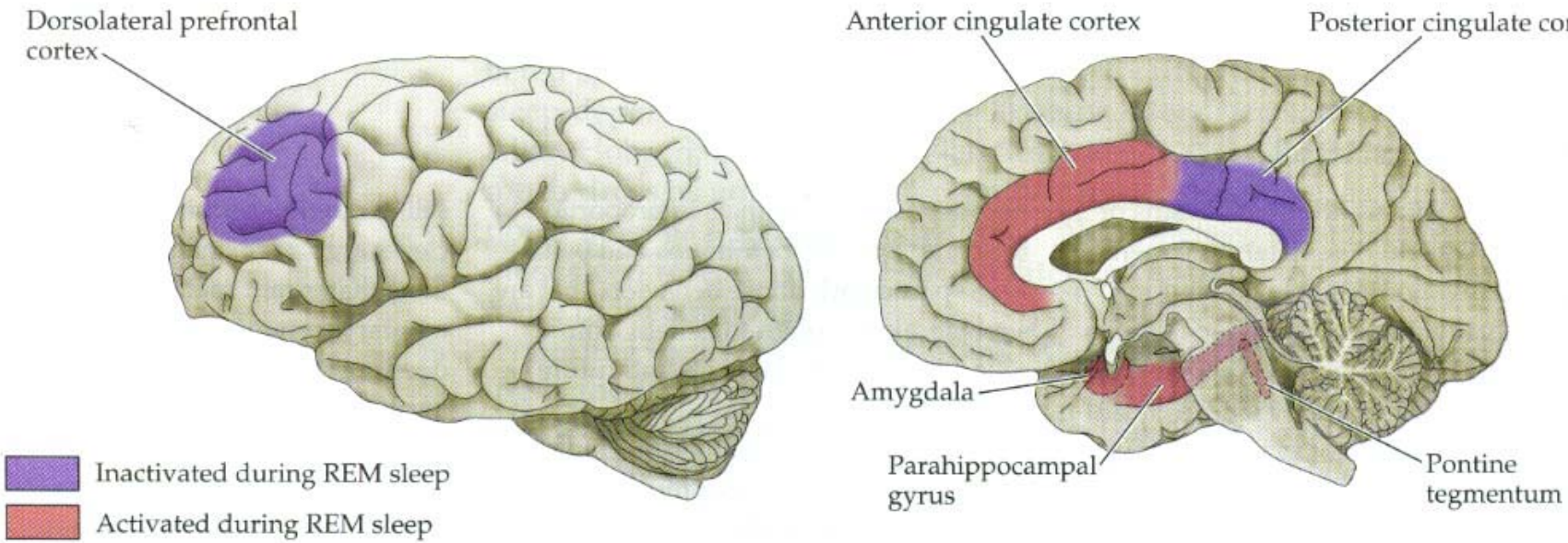

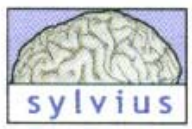

Figure 27.10 Diagram showing cortical regions whose activity is increased or decreased during REM sleep. (After Hobson et al., 1989.)

OREXIN AND NARCOLEPSY

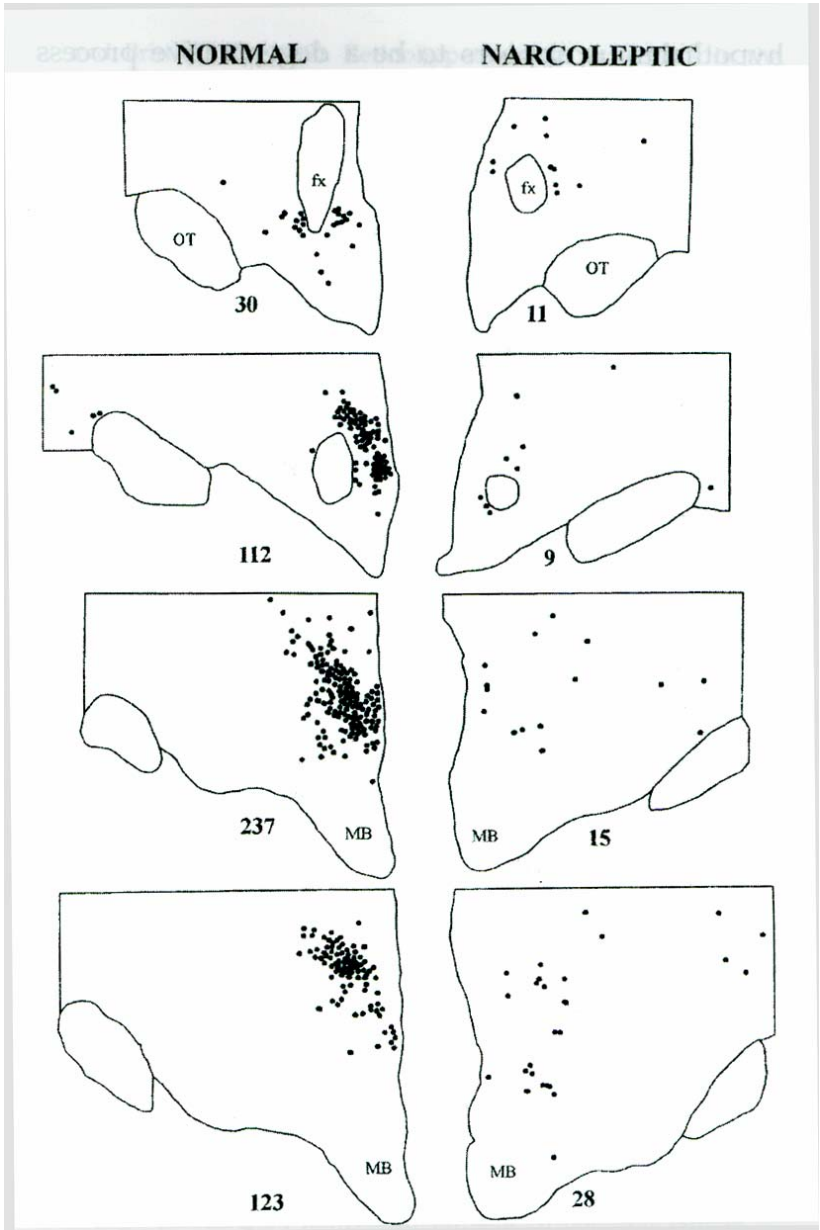

Orexin neurons in the human hypothalamus (From Saper, 2004)

Sleep disturbances in degenerative disorders

1) During aging, there is a progressive loss of neurons in VLPO, associated with difficulty falling a sleep

2) Narcolepsy (degeneration of orexin neurons), unwanted transitions to sleep while awake, as well as more frequent transitions to wake while asleep; cataplexy: sudden onset of atonia

3) REM behavior disorder (dopaminergic deficiency, often in PD patients), they fail to engage atonia during REM sleep and may act out their dreams. Many of these patients also have periodic limb movement during sleep and restless legs syndrome in the evening, also indicative of failure to suppress motor activity when at rest.